Molecular aspects of Arabidopsis nonhost resistance to *Phakopsora pachyrhizi*

(Molekulare Aspekte der Nichtwirt-Resistenz von Arabidopsis gegen *Phakopsora pachyrhizi*)

Von der Fakultät für Mathematik, Informatik und Naturwissenschaften
der RWTH Aachen University zur Erlangung des akademischen Grades
einer Doktorin der Naturwissenschaften genehmigte Dissertation

vorgelegt von
Diplom-Biologin Ruth Campe
aus Siegburg

Berichter: Juniorprofessorin Dr. rer. nat. Katharina Göllner
Universitätsprofessor Dr. rer. nat. Uwe Conrath

Tag der mündlichen Prüfung: 05.09.2014

Et kütt wie et kütt.

Un et hätt noch emmer joot jejange.

Parts of this dissertation have already been published. Thus, wording in this dissertation and the published articles in part can be identical.

Teile dieser Dissertation wurden bereits veröffentlicht. Deshalb können Wortwahl und Formulierungen in dieser Dissertation mit denen der Publikationen teilweise identisch sein.

Campe, R., Loehrer, M., Conrath, U., Goellner, K. (2014). *Phakopsora pachyrhizi* induces marker genes to necrotrophs in *Arabidopsis thaliana*. Physiological and Molecular Plant Pathology (2014), doi: 10.1016/j.pmpp.2014.04.005

CONTENT

CONTENT **4**
SUMMARY **9**
ZUSAMMENFASSUNG **10**
1 INTRODUCTION **11**
1.1 The plant immune system **11**
1.1.1 Basal resistance/PAMP-triggered immunity 11
1.1.2 *R*-gene-mediated resistance/effector-triggered immunity 12
1.1.3 Damage-associated molecular patterns 13
1.1.4 Systemic acquired resistance and induced systemic resistance 13
1.1.5 The role of phytohormones in plant disease resistance 14
1.1.6 Nonhost resistance 15
1.2 Soybean rust – a major threat to an important crop **17**
1.2.1 Significance and distribution of *P. pachyrhizi* 17
1.2.2 Life cycle and host range of *P. pachyrhizi* 18
1.2.3 NHR of Arabidopsis to *P. pachyrhizi* 18
1.3 The ABC transporter PEN3 ..... **19**
1.4 Aim of the study **22**
2 MATERIALS AND METHODS **23**
2.1 Material **23**
2.1.1 *Arabidopsis thaliana* accessions and mutants 23
2.1.2 Bacteria 23
2.1.3 Oligonucleotides 24
2.1.4 Enzymes 25
2.1.5 Vectors 26
2.1.6 Antibodies 27
2.1.7 Internet resources, stock centers, databases and software 27
2.2 Methods **29**
2.2.1 Plant material and cultivation 29
2.2.2 Fungal material and cultivation 29
2.2.3 Preparation and application of germination fluid 30
2.2.4 Inoculation of Arabidopsis 30
2.2.5 DNA extraction 31
2.2.6 RNA extraction 31
2.2.7 cDNA synthesis 32
2.2.8 Polymerase chain reaction (PCR) 32
2.2.9 Agarose gel electrophoresis 33
2.2.10 Quantification of nucleic acids 33
2.2.11 Sequencing 34
2.2.12 Genotyping Arabidopsis T-DNA mutants 34

2.2.13 Crossing Arabidopsis mutants ... 34
2.2.14 Cloning ... 35
2.2.15 Preparation of chemically competent *E. coli* ... 36
2.2.16 Transformation of chemically competent *E. coli* ... 36
2.2.17 Plasmid preparation ... 36
2.2.18 Preparation of electrocompetent *A. tumefaciens* ... 36
2.2.19 Transformation of electrocompetent *A. tumefaciens* ... 37
2.2.20 Heterologous production and purification of proteins ... 37
2.2.21 Quantification of proteins ... 39
2.2.22 Arabidopsis protein microarrays ... 39
2.2.23 Preparation of microsomal fractions from Arabidopsis leaves ... 40
2.2.24 Pull-down of PEN3 from microsomal fractions ... 41
2.2.25 CaM overlay assay ... 41
2.2.26 Visualization and analysis of proteins ... 42
2.2.27 Bimolecular fluorescence complementation ... 43
2.2.28 Histochemical staining ... 43
2.2.29 Microscopical analysis ... 44
3 RESULTS ... 46
3.1 *P. pachyrhizi* induces marker genes for necrotrophic interactions ... 46
3.1.1 Expression of defense marker genes in Arabidopsis upon infection with *P. pachyrhizi* ... 46
3.1.2 Application of germination fluid of *P. pachyrhizi* on Arabidopsis leaves leads to *PDF1.2* activation ... 48
3.1.3 Expression of additional defense-related marker genes ... 49
3.1.4 The *PDF1.2*-activating compound is likely to be of proteinaceous nature ... 50
3.2 The interactome of the ABC transporter PEN3 ... 52
3.2.1 PEN3 architecture ... 52
3.2.2 Production and purification of CyD1 ... 52
3.2.3 The α-PEN3 antibody is suitable for use with protein microarrays ... 54
3.2.4 Investigating the PEN3 interactome ... 55
3.2.5 Ca^{2+} sensors in the PEN3 interactome ... 57
3.2.6 PEN3 interacts with CaM *in vitro* ... 60
3.2.7 PEN3 interacts with CaM *in vivo* ... 64
3.2.8 CaM7 is involved in NHR to various pathogens ... 67
4 DISCUSSION ... 71
4.1 Can one consider *P. pachyrhizi* a „heminecrotroph“? ... 71
4.2 Screening for PEN3 interaction partners ... 74
4.2.1 Putative PEN3-interacting proteins identified on the 5K PMA ... 76
4.2.2 PEN3 is a novel CaM-binding protein ... 79
5 REFERENCES ... 87
6 APPENDIX ... 101
6.1 Abbreviations ... 101
6.3 Supplemental material ... 105

6.4 Vector maps 116
6.5 Acknowledgments/Danksagung 118
6.6 Curriculum vitae 120
6.7 List of publications 121
6.7.1 Primary research papers 121
6.7.2 Short publications/abstracts 121
6.7.3 Posters 121
6.7.4 Patent 122
6.8 Scholarships, grants and awards 122

List of figures

Figure 1. *PDF1.2* and *PR-1* mRNA transcript accumulation in Arabidopsis wild-type and *pen3-4* plants upon inoculation with *P. pachyrhizi*. ... 46
Figure 2. Preparation of germination fluid. ... 47
Figure 3. *P. pachyrhizi* germination fluid activates *PDF1.2* expression. ... 48
Figure 4. Activation of JA/ET and SA marker genes in Arabidopsis wild-type plants after inoculation with *P. pachyrhizi* or application of germination fluid. ... 49
Figure 5. Transcript accumulation of JA marker genes in Arabidopsis leaves after treatment with different fractions of germination fluid. ... 51
Figure 6. *In silico* analysis of ABC transporter PEN3. ... 53
Figure 7. Production and purification of the PEN3 domain CyD1. ... 54
Figure 8. Test array for the α-PEN3 antibody. ... 55
Figure 9. Arabidopsis Protein Microarrays. ... 56
Figure 10. The PEN3-Ca^{2+} signaling network. ... 59
Figure 11. Synthesis of HRP-linked CaM7 ... 60
Figure 12. Production and purification of CyD1 in *E. coli*. ... 61
Figure 13. CaM overlay assay with CyD1 ... 62
Figure 14. Pull-down of full-length PEN3 from Arabidopsis microsomes with CaM Sepharose. ... 63
Figure 15. CyD1ΔCaMBD binds to CaM. ... 64
Figure 16. CyD1 and CaM7 co-localize to the cytoplasm. ... 65
Figure 17. CyD1 interacts with CaM7 *in planta*. ... 66
Figure 18. Protein abundance in BIFC experiments. ... 67
Figure 19. Interaction types in the NHR of Arabidopsis against *P. pachyrhizi*. ... 68
Figure 20. Interaction of *pen3-4* and *cam* mutants with *P. pachyrhizi*. ... 69
Figure 21. The interaction of Arabidopsis with *Bgh*. ... 70

List of tables

Table 1. Arabidopsis accessions, transgenic lines and mutants used in this study 23
Table 2. Bacterial strains used in this study 23
Table 3. Oligonucleotides used in this study 24
Table 4. Enzymes used in this study 25
Table 5. Vectors used and created in this study 26
Table 6. Antibodies used in this study 27
Table 7. Internet resources, stock centers, databases, and software used in this study 27
Table 8. Putative PEN3-binding proteins with GO involved in cellular response to stimulus 58

Table A1. Putative PEN3-binding proteins identified on protein microarrays 105
Table A2. Detailed GO analysis of the 28 putative PEN3 binding proteins with GO involved in cellular response to stimulus 109
Table A3. The PEN3-Ca^{2+} signaling network 111

SUMMARY

Arabidopsis expresses nonhost resistance (NHR) to *Phakopsora pachyrhizi*, the causal agent of Asian soybean rust disease that threatens worldwide soybean cultivation. Nonhost resistance is durable and effective to a broad spectrum of pathogens. Understanding nonhost immunity at the molecular level would likely provide knowledge one could use to make susceptible hosts immune to a given disease. The ABC transporter PEN3 is required for Arabidopsis NHR to several nonadapted pathogens, including *P. pachyrhizi*. However, PEN3's molecular function is poorly understood. An *in vitro* binding screen with protein microarrays delivered 28 proteins which bound to PEN3 and based on their GO annotation were found to be associated with the biotic and abiotic plant stress response. Nine of the proteins represented cellular Ca^{2+} sensors, including calmodulin (CaM) and several CaM-like proteins. The PEN3-CaM interaction was confirmed *in vitro* by a CaM overlay assay and pull-down of PEN3 with CaM Sepharose and *in vivo* by bimolecular fluorescence complementation. Furthermore, the *cam7* mutant was shown to be compromised in NHR against *P. pachyrhizi* and the nonadapted powdery mildew fungus *Blumeria graminis* f. sp. *hordei*. This study thus provides a novel link between Ca^{2+} signaling and Arabidopsis NHR. Furthermore, I investigated changes in mRNA transcript accumulation in Arabidopsis upon treatment with *P. pachyrhizi* uredospores and germination fluid. This approach revealed *P. pachyrhizi* induces marker genes for defense to necrotroph pathogens, asking whether one can consider the ostensible biotroph a "heminecrotroph" pathogen.

ZUSAMMENFASSUNG

Arabidopsis ist für *Phakopsora pachyrhizi*, den Erreger des Asiatischen Sojabohnenrosts, der den weltweiten Sojaanbau bedroht, eine sogenannte "Nichtwirt-Pflanze". „Nichtwirt-Resistenz" verleiht der Pflanze einen beständigen Schutz gegen vermeintlich alle Varianten eines bestimmten Pathogens. Das molekulare Verständnis der Nichtwirt-Resistenz könnte es möglich machen, diese sehr beständige Form der pflanzlichen Immunität auf Wirt-Pflanzen zu übertragen und diese gegen ihre hauptsächlichen Krankheitserreger immun zu machen. Der ABC-Transporter PEN3 ist ein wichtiger Bestandteil der Nichtwirt-Resistenz von Arabidopsis gegen verschiedene, nichtangepasste Pathogene (z.B. *P. pachyrhizi*). Über die molekulare Funktion von PEN3 bei der Nichtwirt-Resistenz ist allerdings bislang nur wenig bekannt. In einem *in vitro*-Bindungsassay wurden 28 Proteine identifiziert, die mit PEN3 wechselwirken und -aufgrund ihrer Annotation- an der zellulären Antwort auf abiotischen und biotischen Stress beteiligt zu sein scheinen. Neun dieser Proteine sind Ca^{2+}-Sensoren, z.B. Calmodulin (CaM) und CaM-ähnliche Proteine. Die Interaktion von PEN3 mit CaM konnte mit einem CaM-Overlay-Assay und anhand der Präzipitation von PEN3 mit CaM-Sepharose *in vitro* und mit bimolekularer Fluoreszenzkomplementierung *in vivo* bestätigt werden. Da die Nichtwirt-Resistenz gegen die phytopathogenen Pilze *P. pachyrhizi* und *Blumeria graminis* f. sp. *hordei* in der *cam7* Mutante von Arabidopsis abgeschwächt ist, konnte eine direkte Verbindung der Nichtwirt-Resistenz von Arabidopsis mit Ca^{2+}-vermittelten Signalwegen neu aufgezeigt werden. Zusätzlich wurde die Aktivierung von ausgesuchten Arabidopsis-Genen nach Behandlung mit Sporen oder mit Keimwasser von *P. pachyrhizi* untersucht. Bei diesem Ansatz war bemerkenswert, dass sowohl mit Sporen als auch mit Keimwasser in Arabidopsis Markergene induziert wurden, die üblicherweise mit der Abwehr von nekrotrophen Krankheitserregern in Verbindung gebracht werden. Deshalb stellt sich die Frage, ob man den vermeintlich biotrophen Pilz *P. pachyrhizi* nicht eher als „heminekrotrophen" Organismus betrachten sollte.

1 INTRODUCTION

1.1 The plant immune system

Most plants cannot move to escape biotic or abiotic challenges. Biotic stresses are provoked by a battery of potential pests: Fungi, oomycetes, bacteria, insects, nematodes, and viruses try to exploit the plant using a remarkable variety of strategies. Plants, in turn, need to perceive and recognize the invader and activate appropriate defense responses. Thereto, the plant is equipped with several branches of defense reactions that together form the plant immune system.

1.1.1 Basal resistance/PAMP-triggered immunity

A first active plant response to pathogen attack is based on the recognition of conserved microbe- or pathogen-associated molecular patterns (MAMPS or PAMPs) by pattern recognition receptors (PRRs; (Jones & Dangl, 2006; Boller & Felix, 2009)). MAMPs/PAMPs are defined as mostly invariant epitopes within molecules that are fundamental to the pathogen's fitness, widely distributed among different microbes, absent in the host and recognized by a wide array of potential hosts (Schwessinger and Zipfel, 2008). Flagellin and lipopolysaccharides are prime examples for bacterial MAMPs/PAMPs, whereas those of fungi often derive from membrane and cell wall components, such as β-glucan, ergosterol or chitin (Felix et al., 1999; Zipfel et al., 2004; Newman et al., 2007; Boller, 1995; Nürnberger et al., 2004). Within seconds to minutes, recognition of MAMPs/PAMPs by PRRs leads to diverse cellular responses, including ion fluxes across the plasma membrane (most notably seen by an increase in cytosolic Ca^{2+} levels with a concomitant efflux of K^{+}), production of reactive oxygen species (ROS), activation of mitogen-activated protein kinase (MAPK) cascades and associated changes in protein phosphorylation. These early responses result in extensive transcriptional changes, stomatal closure and local cell wall reinforcement (Boller and Felix, 2009).

Many PRRs are receptor kinases such as the *Arabidopsis thaliana* (hereafter referred to as Arabidopsis) leucine-rich-repeat (LRR) receptor-like kinases (RLK) FLAGELLIN SENSING 2 (FLS2) and EF-TU RECEPTOR (EFR), that detect bacterial flagellin (or its elicitor-active epitope flg22) and the N-terminal peptide elf18 from the bacterial elongation factor Tu, respectively (Gómez-Gómez and Boller, 2000; Chinchilla et al., 2006; Kunze et al., 2004; Zipfel et al., 2006). Upon ligand binding both FLS2 and EFR bind to the LRR-RLK BRI1-ASSOCIATED RECEPTOR KINASE1 (BAK1) to form a kinase signaling complex that by reciprocal phosphorylation initiates downstream defense responses (Chinchilla et al., 2007; Roux et al., 2011; Schwessinger et al., 2011). A PRR for detecting fungal pathogens is the LysM receptor kinase CHITIN ELICITOR RECEPTOR KINASE1 (CERK1; (Miya et al., 2007; Wan et al., 2008)). The first layer of defense,

consisting of MAMP/PAMP recognition by PRRs and the translation of the stimulus into downstream cellular defense responses can result in so-called PAMP-triggered immunity (PTI) that can halt further colonization (Jones and Dangl, 2006).

1.1.2 *R*-gene-mediated resistance/effector-triggered immunity

Successful pathogens evolved to overcome PTI by delivering effectors that contribute to virulence, resulting in effector-triggered susceptibility (ETS; (Jones and Dangl, 2006)). Effectors were defined as all pathogen proteins and small molecules that alter host cell structure and function. These alterations either facilitate infection (virulence factors and toxins), or trigger defense responses (avirulence factors and elicitors), or both (Huitema et al., 2004). Effectors can function in the apoplast or inside a plant cell. Gram-negative bacteria deliver their effectors inside the host cell by their specialized type III secretion system (T3SS; (Cornelis and Van Gijsegem, 2000)). Several T3SS effectors were demonstrated to suppress PAMP-induced basal defenses, including the *Pseudomonas syringae* effectors AvrRpm1 and AvrRpt2 that both target Arabidopsis RIN4, a regulator of PAMP signaling (Kim et al., 2005). Recently, a tyrosine phosphatase secreted by *P. syringae*, HopAO1, was shown to target the PRR EFR and reduce its phosphorylation, thereby preventing subsequent immune responses (Macho et al., 2014). In contrast to bacteria, the mechanisms by which fungi and oomycetes shuttle their effectors across the cell wall and plant plasma membrane are not fully resolved. Many fungal and oomycete effectors are secreted by haustoria (Catanzariti et al., 2006; Kemen et al., 2005; Whisson et al., 2007), specialized structures that form within infected plant cells and remain encased by a modified plant cell membrane (Hahn and Mendgen, 2001; Panstruga, 2003), or via the eukaryotic secretory pathway by exo- and endocytosis (Panstruga and Dodds, 2009; Kuhn and Panstruga, 2014).

The next level of defenses in plants involves recognition of effectors by specific disease resistance (R)-genes that mostly encode intracellular nucleotide-binding (NB)-LRR proteins. If an effector is recognized by a corresponding NB-LRR protein, effector-triggered immunity (ETI) ensues, a faster and stronger version of PTI that often passes the threshold for induction of hypersensitive cell death (HR; (Jones and Dangl, 2006). Pathogen effectors can be recognized either directly (Kay and Bonas, 2009; Elmore et al., 2011) as in case of binding of the *Hyaloperonospora arabidopsidis* effector ATR1 to the Arabidopsis NB-LRR RPP1 (Krasileva et al., 2010), or indirectly as argued in the so-called “guard hypothesis”(Dangl and Jones, 2001). One prominent example for indirect effector recognition is the activation of the peripheral plasma membrane NB-LRR protein RPM1 by AvrRpm1 through interaction with RIN4 (Belkhadir and Nimchuk, 2004).

Whereas MAMPs/PAMPs are considered to be conserved throughout classes of microbes, effectors are species-, race-, or strain-specific. The absence or presence of an effector together with the absence or presence of the corresponding *R*-gene decide about compatibility or incompatibility of a given plant-pathogen interaction, as described in the "gene-for-gene resistance" concept by Flor (1971). Therefore, depending on the attacked host, an effector can serve as a virulence (vir) or avirulence (avr) factor. This then leads to a continuous selective pressure on both the pathogen and the plant resulting in a co-evolutionary arms race for disease or susceptibility (Jones and Dangl, 2006).

Although the separation between MAMPs/PAMPs and effectors, between PRRs and R proteins, and between PTI and ETI was shown true for many examples of plant-pathogen interaction, it was recently argued that at least in some cases PTI and ETI share downstream signaling components. Hence, there is a continuum between PTI and ETI mediated by an integrated signaling network (Tsuda and Katagiri, 2010; Thomma et al., 2011).

1.1.3 Damage-associated molecular patterns

Detection of an attacking pathogen can also be evoked by damage-associated molecular patterns (DAMPs), plant-derived signals that are released by lytic enzymes produced by the pathogen (or plant) to breach the structural barriers of plant tissue (Boller and Felix, 2009). Classical examples of DAMPs are plant cell wall fragments released by microbial enzymes such as polygalacturonases or cutinases. Cutin monomers as well as oligogalacturonides act as endogenous elicitors to trigger immune responses (Schweizer et al., 1996; Kauss et al., 1999; D'Ovidio et al., 2004). Furthermore, several peptides were found to be released from endogenous precursors and to elicit defense upon pathogen attack. They include the 18-amino-acid peptide systemin from tomato (Pearce et al., 1991; Felix and Boller, 1995), the 23-amino-acid peptide PEP1 from Arabidopsis (Huffaker et al., 2006; Huffaker and Ryan, 2007; Ross et al., 2014) and the eight-amino-acid peptide GmPep914 from soybean (Yamaguchi et al., 2011).

1.1.4 Systemic acquired resistance and induced systemic resistance

In addition to the above strategies plants seem to have sort of a "disease memory", which becomes evident by the existence of additional types of resistance, namely "systemic acquired resistance" (SAR) and "induced systemic resistance" (ISR). SAR describes the phenomenon of an acquired broad-spectrum resistance in uninoculated (systemic) tissue upon localized primary infection by a necrotizing pathogen (Ryals et al., 1996; Conrath, 2006). The first event associated with SAR is the systemic distribution of one (or more) yet unknown signal(s) throughout the plant. However, a variety of small metabolites has been suggested to be involved in long-distance signaling during SAR, including (methyl) salicylic acid (SA), pipecolic acid, glycerol-3-

phosphate, azelaic acid, lipid-derives signals and terpenoids (Métraux et al., 1990; Malamy et al., 1990; Nandi et al., 2004; Park et al., 2007; Chanda et al., 2011; Návarová et al., 2012; Shah et al., 2014). The signal causes systemic accumulation of SA that, in turn, directly activates SAR genes and also transfers the tissue to a "primed" state of defense, which is characterized by an enhanced capacity to activate defense responses upon further pathogen attack (Conrath, 2006, 2011). The faster and/or more robust activation of defense results in the establishment of SAR associated with a decrease in symptom development.

Another type of induced resistance is ISR, elicited by nonpathogenic growth-promoting bacteria. Root colonization by these rhizobacteria leads to a broad-spectrum systemic resistance in the aerial parts of the plant. In contrast to SAR, ISR is independent of SA accumulation, but requires responsiveness to jasmonic acid (JA) and ethylene (ET; (Pieterse et al., 1996, 1998; van Wees et al., 1999; Conrath, 2006)).

1.1.5 The role of phytohormones in plant disease resistance

Phytohormones are small molecules that are essential for the regulation of plant growth, development, and survival. They act as signaling molecules already at very low concentrations. Classical phytohormones are abscisic acid, auxins, cytokinins, ET, and gibberellins, but small signaling molecules such as brassinosteroids, JA and SA are recognized as phytohormones as well (Pieterse et al., 2009). Evidence for the key role of phytohormones in plant immunity was provided through studies with Arabidopsis and tobacco, in which various mutants and transgenic lines impaired in hormone biosynthesis, perception, or signaling were demonstrated to exhibit altered resistance to pathogens (Pieterse et al., 2009). Particularly well established is the importance of SA, JA, and ET as primary signals in the regulation of plant defense (Loake and Grant, 2007; Pozo et al., 2004; van Loon et al., 2006).

Upon pathogen attack, the quantity, composition and timing of the phytohormonal blend produced by the plant greatly depends on the lifestyle and infection strategy of the invader. Plant pathogens are often roughly divided into biotrophic pathogens, which feed on living plant tissue and require a living host to reproduce, and necrotrophs, which kill the host tissue and feed on the remains. Pathogens, which switch from a biotrophic lifestyle in the early stages of infection to a necrotrophic lifestyle in the later stages, are referred to as hemibiotrophs (Glazebrook, 2005). SA is known to be involved in defense signaling against biotroph and hemibiotroph pathogens whereas JA, together with ET, mediates defense against necrotrophs. JA alone activates responses to wounding and herbivory (Glazebrook, 2005; Grant and Jones, 2009). SA- and JA- mediated defense pathways have been demonstrated to cross-communicate in both an antagonistic and synergistic manner, thereby providing the plant with the flexibility

to fine-tune its overall defense response (Schenk et al., 2000; Mur et al., 2006; van Wees et al., 2000; Felton and Korth, 2000; Feys and Parker, 2000).

1.1.6 Nonhost resistance

Although pathogens continuously evolve elaborate strategies to circumvent the plant's defenses, it is generally appreciated that the majority of plants are immune to the majority of microbes with pathogenic potential. This type of immunity is referred to as "nonhost resistance" (NHR), and defined as the capacity of an entire plant species to resist infection by all isolates of a given microbe species (Heath, 2000). NHR, therefore, contrasts with host resistance, which is expressed by plant genotypes within an otherwise susceptible host species. NHR it is the most common form of disease resistance and is characterized by high durability and broad-spectrum activity (Mysore and Ryu, 2004).

Much effort has been put into understanding NHR. With increasing information it became evident that NHR relies on both preformed and inducible mechanisms and that there is huge overlap between host and nonhost resistance responses (Mysore and Ryu, 2004; Schulze-Lefert and Panstruga, 2011). Preformed defenses do not only include structural barriers such as the plant cell wall but also peptides, proteins and secondary metabolites that act as potential deterrents against microbes (Broekaert et al., 1995; Heath, 2000). Evidence for preformed passive barriers being insufficient for establishing broad-spectrum NHR, is given by the fact that certain elicitors such as chitin induce responses in both host and nonhost plants (Heath, 2000; Eckardt, 2008). Typical induced reactions against non-adapted pathogens include the HR, induction of pathogenesis-related (PR) genes, ROS production, cell-wall cross-linking, and callose deposition (Mysore and Ryu, 2004). These responses also are a part of ETI and PTI and many examples suggest that both PRR- and NB-LRR-triggered immunity contribute to NHR. Schulze-Lefert and Panstruga (2011) hypothesized that the contribution of PRR-triggered immunity to NHR increases with phylogenetic divergence time between a host and nonhost species, whereas the relative contribution of NB-LRRs decreases simultaneously. One explanation for this could be that effectors from a given pathogen species fail to effectively suppress PRR-triggered immunity in nonhost plants because their corresponding host cellular targets have diverged to an extent that impedes manipulation by the effector repertoire (Schulze-Lefert and Panstruga, 2011). Also several plant hormones, including SA, JA and ET can play crucial roles in NHR (Mysore and Ryu, 2004). Mutant studies showed that Arabidopsis resistance against different non-adapted rust species can depend on functional SA or JA signaling (Mellersh and Heath, 2003; Loehrer et al., 2008).

Often, NHR against fungal pathogens is associated with the penetration process. In a screening for Arabidopsis mutants with increased penetration by the nonhost fungal pathogen *Blumeria graminis* f. sp. *hordei* (*Bgh*), which causes powdery mildew in barley, three penetration (*pen*) mutants were identified (Collins et al., 2003; Lipka et al., 2005; Stein et al., 2006). PEN1 is a SNARE-domain containing and plasma membrane-resident syntaxin that becomes recruited into plasma membrane microdomains beneath fungal entry sites and supposedly plays a role in vesicle trafficking (Assaad et al., 2004; Bhat et al., 2005). PEN2 is a S-glycosyl-hydrolase (or myrosinase) associated with the periphery of peroxisomes, that accumulate at incipient *Bgh* entry sites (Lipka et al., 2005). PEN3 is a plasma membrane-localized ATP-binding cassette (ABC) transporter, which, just like PEN1 and PEN2, accumulates at the site of pathogen attack (Stein et al., 2006). Interaction studies of several pathogens with *pen* single and double mutants suggested that PEN1 functions independently of PEN2 and PEN3, whereas PEN2- and PEN3-mediated defenses seem to be interconnected (Lipka et al., 2005; Stein et al., 2006). It has been hypothesized that PEN2 converts a nontoxic substrate to a toxic product, which is then exported to the apoplast by PEN3 to poison invading hypha (Stein et al., 2006). Further details on PEN3's function and possible role in NHR will be described in chapter 1.3.

Although single and double *pen* mutants have lost the first layer of pre-invasion resistance and thus allow higher penetration rates of *Bgh*, subsequent post-invasion resistance is still sufficient to stop, or significantly reduce, fungal proliferation (Lipka et al., 2005). The second layer of post-invasion NHR is mediated by ENHANCED DISEASE SUSCEPTIBILITY1 (EDS1), SENESCENCE-ASSOCIATED GENE101 (SAG101) and PHYTOALEXIN-DEFICIENT4 (PAD4), components identified in R protein–triggered and basal immune responses (Feys et al., 2005; Lipka et al., 2005). On single mutants *eds1*, *pad4* and *sag101* fungal entry rates are not enhanced. Remarkably, by depletion of components of both pre- and post-invasion resistance in the *pen2 pad4 sag101* mutant, nonhost resistance against the powdery mildew fungi *Bgh* and *Erysiphe pisi* can be broken (Lipka et al., 2005). However, other fungal pathogens such as the rust fungus *Phakopsora pachyrhizi* are unable to sporulate on triple mutant *pen2 pad4 sag101* (Langenbach et al., 2013), indicating additional components involved in Arabidopsis NHR to this pathogen.

Taken together, rather than being a specific type of defense, NHR depends on the cooperation of different defense branches that are also involved in the battle against adapted pathogens. In line with this, perception of a single pathogen-induced stimulus can simultaneously induce several layers of defense, as shown by rapid transcriptional activation of *EDS1*, *PAD4*, and *SAG101* as well as *PEN1*, *PEN2*, and *PEN3* upon FLS2-mediated flagellin perception (Zipfel et al., 2004). This multi-layered composition of NHR contributes to its robustness.

1.2 Soybean rust – a major threat to an important crop

Plant rusts are caused by basidiomycetes of the order Uredinales and have been most notorious for their destructiveness on grain crops, especially wheat, oats and barley; But they also attack vegetables including bean and asparagus, field crops like cotton and soybean, and they also can cause tremendous tissue loss on trees such as pine, apple and coffee (Agrios, 2005). Rust fungi mostly spread from plant to plant by windblown spores that attack leaves and stems and infections usually appear as numerous rusty, orange, yellow or white-colored spots. Rust fungi are obligate biotrophs and usually specialized parasites that attack only certain genera or varieties of plants. There are more than 5,000 species of rust. Some famous examples are cereal rusts caused by *Puccinia* species, tree-infecting rusts such as *Hemileia* and *Cronartium* and legume rusts caused by *Uromyces* and *Phakopsora* (Agrios, 2005).

1.2.1 Significance and distribution of *P. pachyrhizi*

Two different species of fungi can cause Asian soybean rust (ASR) on plants, named *Phakopsora pachyrhizi* and *P. meibomiae* which is the less aggressive species (Goellner et al., 2010). *P. pachyrhizi* was first recorded in 1902 by Hennings in Japan, and designated *Uredo sojae* Henn (Hennings, 1903). In 1914, Hans and Paul Sydow assigned the current name *Phakopsora pachyrhizi* Syd. & P. Syd (Sydow and Sydow, 1914). Soybean (*Glycine max* (L.) Merr), with over 100 million hectares acreage and a production of about 240 million metric tons of beans per year (FAOSTAT, 2012), is the economically most important crop species affected by ASR. The distribution of soybean cultivation from Asia to all other regions with appropriate climate was followed by the spread of ASR from the East to the West. Today, *P. pachyrhizi* is present in all major soybean growing regions in Asia, Australia, Africa, South America, where until 2001 only the less aggressive *P. meibomiae* was found, and the continental USA, where the pathogen was first reported in 2004 (Vakili and Bromfield, 1976; Bromfield, 1984; Killgore et al., 1994; Stokstad, 2004; Schneider et al., 2005; Levy, 2005; Bonde et al., 2006). ASR-infected soybean plants develop chlorotic leaf areas resulting in tan or brown polygonal lesions and premature yellowing and abscission of leaves may occur, especially when lesion density is high (Bromfield, 1984). Hence, the pathogen can defoliate soybean fields within a few days and yield losses up to 80 % have been reported in Asian countries (Miles et al., 2003). As soybean varieties with resistance to all isolates of the pathogen are not yet available, ASR can currently only be controlled by extensive fungicide treatment (Miles et al., 2007).

1.2.2 Life cycle and host range of *P. pachyrhizi*

P. pachyrhizi spreads from plant to plant by wind-blown asexual uredospores. On the leaf surface uredospores germinate with a single germ tube. Its tip swells to form a globose appressorium, which usually is located over anticlinal cell walls of the host plant, the center of epidermal cells or, rarely, over stomata (Tremblay, 2009). Penetration of the leaves occurs directly through the cuticle. This is an unusual feature for rust fungi, which usually penetrate leaves via stomata (Koch et al., 1983). After about 12 hours post inoculation (hpi) a funnel-shaped structure, referred to as appressorial cone, forms within the appressorium and, by elongation develops into the penetration hypha. Upon penetration, the epidermal cells collapse (Keogh et al., 1980). After penetration, the hypha traverses the epidermal cell and reaches the intercellular space at about 20 hpi. By formation of a first septum the penetration hypha is separated from the primary hypha which continues intercellular growth by branching into secondary hyphae (Koch et al., 1983). The formation of the first haustoria can be observed at 24–48 hpi. Thereafter, intense colonization of the mesophyll tissue occurs and the intercellular spaces of the leaves become filled with fungal mycelium resulting in macroscopically visible necrotic lesions of host cells at about six days post inoculation (dpi). First uredia and uredospores are formed and released at 8 dpi to complete the life cycle of *P. pachyrhizi* (Koch et al., 1983).

In contrast to other rusts that are usually specialized to infect only a limited number of plant species, *P. pachyrhizi* has an extremely wide host range. In the field the fungus sporulates on 31 species of 17 genera of leguminous plants and on several other plant species after non-natural inoculation (Rytter, 1984; Ono et al., 1992).

1.2.3 NHR of Arabidopsis to *P. pachyrhizi*

Although Arabidopsis is a nonhost for *P. pachyrhizi*, the first steps of fungal development seem not to be different from those on a host plant. The uredospore germinates, forms an appressorium and attempts to penetrate an epidermal cell. In Arabidopsis wild-type plants *P. pachyrhizi* infection can be arrested either before penetration by formation of an effective papilla or in the penetrated epidermal cell, which dies just like in the soybean host. Further proliferation of a fungal hypha into the mesophyll tissue is rarely observed (Loehrer et al., 2008).

Several Arabidopsis mutants were identified, that allow more frequent mesophyll invasion by *P. pachyrhizi* when compared to the wild type. The penetration mutants *pen1*, *pen2*, and *pen3*, known to be compromised in NHR against *Bgh*, also are more susceptible to *P. pachyrhizi*, as obvious by a more frequent growth of fungal hyphae in the mesophyll tissue (Loehrer et al., 2008). In *pen2* the formation of haustoria was observed in few cases (Langenbach et al., 2013)

whereas in *pen3* mesophyll invasion by fungal hyphae is often associated with death of adjacent mesophyll cells (Loehrer et al., 2008, also see Figures 19 and 20).

SA signal transduction mutants SA-DEFICIENT (*sid2*) and ENHANCED DISEASE SUSCEPTIBILITY (*eds1*) also are slightly compromised in NHR to *P. pachyrhizi*, whereas the response to *P. pachyrhizi* infection of the JA RESPONSE (*jar1*) mutant, which is compromised in JA signaling, does not differ from the wild type. However, double mutants *pen3 jar1* and *pen3 sid2* are more susceptible than the *pen3-1* single mutant, suggesting that JAR1 and SID2 act synergistically with PEN3 in controlling ASR development in Arabidopsis (Loehrer et al., 2008).

As for NHR against *Bgh*, post-invasion resistance is still intact in the various *pen* mutants but can be broken in the triple mutant *pen2 pad4 sag101* in which *P. pachyrhizi* frequently develops haustoria (Langenbach et al., 2013). Another component identified to be involved in post-invasion mesophyll resistance against *P. pachyrhizi* is the UDP-glycosyltransferase BRIGHT TRICHOMES 1 (BRT1). *BRT1* expression is induced in *pen2,* but not in the wild type upon ASR infection. In line with this, the number of invasion sites with haustoria formation is strongly enhanced in the double mutant *pen2 brt1* relative to *pen2*, and even exceeded the one observed in the infected *pen2 pad4 sag101* mutant (Langenbach et al., 2013). BRT1 is involved in the phenylpropanoid pathway but its function in plant immunity still needs to be elucidated (Langenbach et al., 2013). However, in none of the Arabidopsis mutants tested, *P. pachyrhizi* is able to sporulate, indicating additional components that contribute to the multi-layered NHR.

Interestingly, the early interaction of *P. pachyrhizi* with Arabidopsis is associated with the induction of plant defensin *PDF1.2*, a marker gene for JA-mediated defenses against necrotrophs. In contrast, *PR-1*, a common marker for SA-mediated defenses against biotrophs, is only induced at later times in *pen* mutants, suggesting that *P. pachyrhizi* is not recognized as a biotroph until invasion of the mesophyll (Loehrer et al., 2008). The authors hypothesized that *P. pachyrhizi* mimics aspects of a necrotrophic pathogen, to circumvent or even suppress appropriate defenses to biotrophs. This might provide the fungus with a head start facilitating its entry into the plant and the establishment of a biotrophic interaction with the host.

1.3 The ABC transporter PEN3

As outlined above, PEN3 is a key component of Arabidopsis NHR. PEN3, which is also referred to as PDR8 or ABCG36, is a membrane-localized ABC transporter of the pleiotropic drug resistance (PDR) family (Stein et al., 2006). ABC transporters are present in all living organisms and characterized by having one or two cytosolically orientated ABCs (or nucleotide-binding folds) linked to multiple (usually six) hydrophobic transmembrane-spanning (TMS) domains. The ABC

domains are highly conserved and contain an ATP-binding site consisting of a Walker A and a Walker B box and, between the two boxes, a consensus sequence specific for ABC transporters known as the 'ABC signature' (Walker and Hudspeth, 1996; van den Brûle and Smart, 2002; also see Figure 6). In eukaryotes these structures are arranged in a modular fashion. ABC transporters with only one ABC-TMS or TMS-ABC module are designated "half-size" transporters, whereas proteins with multiple modules are referred to as "full-size" transporters. PDRs belong to the full-size transporter class and exhibit a unique reverse configuration of two ABC-TMS modules (van den Brûle and Smart, 2002). Furthermore, the PDR subfamily is special in that it is only found in fungi and plants (Crouzet et al., 2006). In Arabidopsis, 15 genes coding for PDRs were identified (Sánchez-Fernández et al., 2001; Martinoia et al., 2002; van den Brûle and Smart, 2002; Crouzet et al., 2006). The closest homologs of PDR8 are PDR1 and PDR7. While *PDR1* and *7* are mostly expressed in roots, *PDR8* is expressed in all organs and represents by far the most abundant PDR in leaves, reaching levels of housekeeping genes (van den Brûle and Smart, 2002; Crouzet et al., 2006).

Besides its compromised NHR to *Bgh* and *P. pachyrhizi* (Stein et al., 2006; Loehrer et al., 2008) *pen3* additionally displays enhanced susceptibility to the inappropriate biotroph pea powdery mildew (*Erysiphe pisi*), the hemibiotroph oomycete *Phytophtora infestans* and the necrotroph *Plectosphaerella cucumerina* (Stein et al., 2006; Kobae et al., 2006). Contradictory results were reported with respect to the role of PEN3 in resistance to bacteria. While Kobae et al. (2006) reported *pen3* would exhibit elevated basal defense against *Pseudomonas syringae* pv. tomato (*Pst*) DC3000, *pen3* was shown to have compromised resistance to this pathogen by Xin et al. (2013). Additional findings revealed that *PEN3* expression is activated by flagellin treatment (Zipfel et al., 2004) and PEN3 being required for flg22-induced focal deposition of callose (Bednarek et al., 2009; Clay et al., 2009) thus supporting the latter finding. Remarkably, *pen3* mutants are resistant to the adapted powdery mildew *E. cichoracearum*. This resistance depends on SA and correlates with chlorotic patches. Consistently, SA pathway genes are hyperinduced in *pen3* when compared to the wild type (Stein et al., 2006).

Using green fluorescent protein (GFP) fusion constructs PEN3 was shown to be equally distributed over the plasma membrane under resting conditions. Upon attack by *Bgh* and *E. cichoracearum* PEN3-GFP accumulates at the penetration site (Stein et al., 2006). Furthermore, Meyer et al. (2009) showed PEN3-GFP incorporation into extracellular encasements surrounding haustoria of *Golovinomyces orontii*. Recruitment of PEN3 to sites of pathogen detection was demonstrated to be triggered by perception of the PAMPs flg22 and chitin and dependent on the respective PRRs FLS2 and CERK1 (Underwood and Somerville, 2013). This suggests that PRRs can provide spatial information at the plasma membrane. Additionally, the process by

which PEN3 is targeted to the host-pathogen interface is independent of protein synthesis, suggesting that existing PEN3 is redirected to sites of pathogen detection by an unknown trafficking pathway (Underwood and Somerville, 2013).

ABC transporters have been implicated in the active movement of a variety of substrates across cellular membranes (Higgins, 1992). PEN3 was proposed to contribute to heavy metal resistance by pumping Cd^{2+} over the plasma membrane of root epidermal cells (Kim et al., 2007). Furthermore, it has been implicated in the efflux of the auxin precursor indole-3-butyric acid, which is involved in plant development (Strader and Bartel, 2009). Given that PEN3 is also a key component plant immunity, this ABC protein is likely to transport a very broad range of substrates (Strader and Bartel, 2009).

Additionally, PEN3 together with PEN2, is involved in glucosinolate-dependent callose deposition that can restrict bacterial growth (Clay et al., 2009). Glucosinolates are 1-thio-β-D-glucosides, that are synthesized and stored by cruciferous plants, including Arabidopsis, and are converted by endogenous S-glycosyl-hydrolases into compounds that function as potential antimicrobials and insect deterrents (Tierens et al., 2001; Halkier and Gershenzon, 2006). Flg22/FLS2-induced PAMP signaling leads to ET-dependent activation of several transcription factors, that in turn induce genes involved in biosynthesis of indole glucosinolates (IGS), such as 4-methoxy-indol-3-ylmethylglucosinolate (Clay et al., 2009). PEN2 was demonstrated to be involved in IGS breakdown, generating hydrolytic products such as isothiocyanates, which act as defense compounds and signaling molecules for flg22-induced callose deposition (Bednarek et al., 2009; Clay et al., 2009). Both, *pen2* and *pen3* exhibit a loss of the callose response to flg22 and accumulate high amounts of 4-methoxy-indol-3-ylmethylglucosinolate, indicating that also PEN3 is involved in IGS breakdown or transport of breakdown products. The glucosinolate-dependent callose deposition mediated by PEN2 and PEN3 contributes to growth suppression of *Pst* DC3000 (Clay et al., 2009). This is in line with *Pst* DC3000 actively suppressing pathogen-activated callose deposition (Hauck et al., 2003).

Besides induction of *PEN3* gene expression, PEN3-mediated callose deposition and focal accumulation of the PEN3 protein, flg22 perception also leads to enhanced phosphorylation of PEN3 (Benschop et al., 2007), suggesting PEN3 regulation at the posttranslational level. Enhanced PEN3 phosphorylation was also observed upon treatment with the fungal elicitor xylanase, the phytohormone abscisic acid and the rapid alkalinization factor RALF, which is known to be involved in root development (Benschop et al., 2007; Kline et al., 2010; Haruta et al., 2014). In Arabidopsis seedlings RALF treatment leads to a rapid increase in cytoplasmic Ca^{2+} (Haruta et al., 2008), suggesting that PAMP-induced phosphorylation of PEN3 also might be regulated by Ca^{2+}-mediated signaling. In agreement with this the calcium-dependent protein kinase CPK10

was demonstrated to phosphorylate a PEN3 peptide *in vitro*, which contains the identified phosphorylation sites (Curran et al., 2011).

1.4 Aim of the study

This study is to investigate molecular aspects of the NHR of Arabidopsis against *P. pachyrhizi* and to disclose the molecular function of PEN3. Therefore, a screen for PEN3-interacting proteins was performed using Arabidopsis protein microarrays delivering a list of putative PEN3 interaction partners that also might be involved in Arabidopsis NHR. Furthermore, to elucidate fungal strategies to circumvent NHR, a gene expression analysis of Arabidopsis leaves was done upon treatment with *P. pachyrhizi* spores and germination fluid. This led to the challenging question of whether the ostensible biotroph *P. pachyrhizi* should rather be considered a "heminecrotroph".

2 MATERIALS AND METHODS

2.1 Material

All chemicals used in this study were purchased from Applichem, Carl Roth GmbH, Merck or Sigma Aldrich unless indicated otherwise. For all molecular biological work in this study distilled water (dH_2O) was further purified to ddH_2O using a Sartorius arium® lab water system.

2.1.1 *Arabidopsis thaliana* accessions and mutants

Table 1. Arabidopsis accessions, transgenic lines and mutants used in this study

Accession			**NASC stock Nr.**
Col-0			N70000
Transgenic lines	**Accession**		**Source**
PDF1.2::GUS	Col-0		Corné Pieterse, Utrecht University, Netherlands
Mutants	**Accession**	**Mutation**	**Stock Nr.**
cam1	Col-0	T-DNA	Sail_256_G09
cam2	Col-0	T-DNA	Salk_66990
cam3	Col-0	T-DNA	Salk_001357
cam5	Col-0	T-DNA	Salk_007371
cam6	Col-0	T-DNA	Salk_033803
cam7	Col-0	T-DNA	Salk_074336C
pen3-4	Col-0	T-DNA	Salk_000578

2.1.2 Bacteria

Table 2. Bacterial strains used in this study

Strain	**Genotype**	**Antibiotic resistance**
Escherichia coli DH5α	F- endA1 glnV44 thi-1 recA1 relA1 gyrA96 deoR nupG Φ80dlacZΔM15 Δ(lacZYA-argF)U169, hsdR17(rK- mK+), λ–	Na
Escherichia coli DB3.1	F- gyrA462 endA1 glnV44 Δ(sr1-recA) mcrB mrr hsdS20(rB-, mB-) ara14 galK2 lacY1 proA2 rpsL20(Smr) xyl5 Δleu mtl1	Sm
Escherichia coli BL21(DE3)	F– ompT gal dcm lon hsdSB(rB- mB-) λ(DE3 [lacI lacUV5-T7 gene 1 ind1 sam7 nin5])	Cm
Agrobacterium tumefaciens AGL-1	pTiBo542D T-DNA	Carb, Rif
Agrobacterium tumefaciens GV2260	pTiB6S3D T-DNA	Carb, Rif
Agrobacterium tumefaciens GV3101	pMP90RK (pTiC58D T-DNA)	Gent, Kan, Rif

Carb: Carbenicillin; Cm: Chloramphenicol; Gent: Gentamycin; Kan: Kanamycin; Na: Nalidixic acid; Rif: Rifampicin; Sm: Streptomycin

2.1.3 Oligonucleotides

Table 3. Oligonucleotides used in this study

Primer for cloning	Description	Sequence (5'-3')
CyD1-GW_F	Gateway®-Cloning	GGGGACAAGTTTGTACAAAAAAGCAGGCTTAATGGATTACAATCCAAATCTTC
CyD1-GW_R(-Stop)	Gateway®-Cloning	GGGGACCACTTTGTACAAGAAAGCTGGGTACGCGTTTCGCTGCATAAG
CyD1-GW_R(+Stop)	Gateway®-Cloning	GGGGACCACTTTGTACAAGAAAGCTGGGTATTACGCGTTTCGCTGCATAA
CaM7-GW_F	Gateway®-Cloning	GGGGACAAGTTTGTACAAAAAAGCAGGCTCAATGGCGGATCAGCTAACC
CaM7-GW_R(-Stop)	Gateway®-Cloning	GGGGACCACTTTGTACAAGAAAGCTGGGTACTTTGCCATCATGACTTTGAC
CaM7-GW_R(+Stop)	Gateway®-Cloning	GGGGACCACTTTGTACAAGAAAGCTGGGTATCACTTTGCCATCATGACTTT
CML37-GW_F	Gateway®-Cloning	GGGGACAAGTTTGTACAAAAAAGCAGGCTCAATGACTCTCGCTAAGAACCA
CML37-GW_R(-Stop)	Gateway®-Cloning	GGGGACCACTTTGTACAAGAAAGCTGGGTAACGCATCATCAAAACAAACT
CML37-GW_R(+Stop)	Gateway®-Cloning	GGGGACCACTTTGTACAAGAAAGCTGGGTATCAACGCATCATCAAAACAA
BamHI-CyD1_F	Cloning into pET$_\lambda$HIS	CTAGGGATCCATGGATTACAATCCAAATCTTC
XhoI-CyD1_R(-Stop)	Cloning into pET$_\lambda$HIS	ACGTCTCGAGCGCGTTTCGCTGCATAAG
BamHI-CaM7_F	Cloning into pET$_\lambda$HIS	CTAGGGATCCATGGCGGATCAGCTAACC
XhoI-CaM7_R(-Stop)	Cloning into pET$_\lambda$HIS	ACGTCTCGAGCTTTGCCATCATGACTTTGAC
Primer for genotyping	**T-DNA line**	**Sequence (5'-3')**
pen3-3_F	*pen3-4*	ACAACGTAAAAGAGCCGTCAC
pen3-3_R		AGCAGAGGTCTTTCTCGGAAC
CaM1_F	*cam1*	TCGAAGAGGCTAAAAGCTTCC
CaM1_R		CGAAGAGATGGTAGTGCGAAG
CaM2_F	*cam2*	TTTTAACCAGCAAAAACCAGC
CaM2_R		CTCTTCTCATGTCAACCTGGC
CaM3-TDNA_F	*cam3*	AGTGCAATTGGTTGTTTAGGG
CaM3-TDNA_R		TTGGCAAATCTCCAAGTCATC
CaM5-TDNA_F	*cam5*	GGTTTGGAGATTCTCATTTCATC
CaM5-TDNA_R		AAGAAGCTTTCAGGGTTTTCG
CaM6-TDNA_F	*cam6*	AAGGTAGTCCGGTTCGCTATC
CaM6-TDNA_R		CAAAACCCAACAGAAGCTGAG
CaM7-1_F	*cam7*	TTTCCGAAATACATGCGATAAC
CaM7-1_R		TGTGCAGAGATTCACGATCAC
Primer for RT-qPCR	**Locus**	**Sequence (5'-3')**
ACTIN2_F	AT3G18780	GGTAACATTGTGCTCAGTGGTGG
ACTIN2_R		GGTGCAACGACCTTAATCTTCAT
CaM1-qPCR_F	AT5G37780	ACAAAGGAAGAGAAGAAAGACGA
CaM1-qPCR_R		ACACATCGCCATCTTTGTCG
CaM2-3UTR_F	AT2G41110	TGGCTAAGTGAGGATTGAAACA
CaM2-3UTR_R		AGAACAAAGCGAAGGAACATTCT
CaM3-3UTR_F	AT3G56800	CCTTGGTCTAGTTCGCGGTT
CaM3-3UTR_R		ACCACACCACGTTTTGACCT
CaM5-qPCR_F	AT2G27030	GCAGCAAAGCGTAGTAGCAA
CaM5-qPCR_R		CGGAGCTCAGAGAATACGGC
CaM6-3UTR_F	AT5G21274	CCCTTGTTTGTTTGGTTAAGCCT

continued

Primer for RT-qPCR	Locus	Sequence (5'-3')
CaM6-3UTR_R		ACAGAATAAAATCAGATGCCCAAA
CaM7-qPCR_F	AT3G43810	ATCACCACAAAGGAGCTTGG
CaM7-qPCR_R		GTCTGCATCCACTTCGTTGA
CaM7-3UTR_F	AT3G43810	ATCCCTCGAAATCCTAAGCA
CaM7-3UTR_R		AAGGCAAAGAAGAAGCAACG
CaM7-5UTR_F	AT3G43810	GAGAAGGAACATTCACTCTCACG
CaM7-5UTR_R		TGTCTTCTTCGGATTTTCTCG
ORA59-qPCR_F	AT1G06160	AGAGTGTGGCTTGGGACATT
ORA59-qPCR_R		CCGGAGAGATTCTTCAACGA
PDF1.2-qPCR_F	AT5G44420	CGAGAAGCCAAGTGGGACAT
PDF1.2-qPCR_R		TCCATGTTTGGCTCCTTCAA
PEN3-qPCR_F	At1G59870	TGAAAGCTTCTGCTGCTCAA
PEN3-qPCR_R		CAAATGTCAAGCCCCAAAAT
PR-1-qPCR_F	AT2G14610	TCGGAGCTACGCAGAACAACT
PR-1-qPCR_R		TCTCGCTAACCCACATGTTCA
PR-2-qPCR_F	AT3G57260	TCTTGAACCCACTTGTCGGC
PR-2-qPCR_R		GGCTCTGACATCGAGCTCATC
PR-3-qPCR_F	AT3G12500	CCACGAGGAAGAAGGAGGTC
PR-3-qPCR_R		CCCATGAATATGGTCCGTCT
PR-4-qPCR_F	AT3G04720	GACCTCGTGGTCAAGCTTCT
PR-4-qPCR_R		GTTGCTGCATTGGTCCACTA
PR-5-qPCR_F	AT1G75040	TCCTTGACCGGCGAGAGTT
PR-5-qPCR_R		AGGAACAATTGCCCTACCACC

Gateway® attachment sites and restriction sites are marked in blue.

2.1.4 Enzymes

Table 4. Enzymes used in this study

Enzyme	Description	Supplier
Restriction enzyme FastDigest® BamHI	Classical cloning	Fermentas/Thermo Scientific
Restriction enzyme FastDigest® XhoI	Classical cloning	Fermentas/Thermo Scientific
T4 DNA Ligase	Classical cloning	Fermentas/Thermo Scientific
Gateway® BP Clonase® II enzyme mix	Gateway® cloning	Invitrogen/Life Technologies
Gateway® LR Clonase® II enzyme mix	Gateway® cloning	Invitrogen/Life Technologies
Proteinase K	Gateway® cloning	Invitrogen/Life Technologies
Phusion® High-Fidelity DNA Polymerase	Proofreading PCR	Finnzymes/Thermo Scientific
Taq DNA-Polymerase	Standard PCR	Self-produced
DNase I, RNase-free	cDNA synthesis	Fermentas/Thermo Scientific
RevertAid™ M-MuLV Reverse Transcriptase	cDNA synthesis	Fermentas/Thermo Scientific
PreScission Protease	Protein cleavage	Amersham Biosciences/GE
Poroszyme® Immobilized Trypsin	Protein digestion	Applied Biosystems/Life Technologies

2.1.5 Vectors

Table 5. Vectors used and created in this study

Vector	Description	Cloning method	Selection in bacteria	Source
pDONR207	Donor vector for Gateway®-based cloning	Gateway®	Gent	Invitrogen/Life Technologies
pDEST-^{GW}VYCE	BIFC (N-terminal VENUS^{C}-Terminus)	Gateway®	Kan	Gehl et al., 2009
pDEST-VYCE(R)^{GW}	BIFC (C-terminal VENUS^{C}-Terminus)	Gateway®	Kan	Gehl et al., 2009
pDEST-^{GW}VYNE	BIFC (N-terminal VENUS^{N}-Terminus)	Gateway®	Kan	Gehl et al., 2009
pDEST-VYNE(R)^{GW}	BIFC (C-terminal VENUS^{N}-Terminus)	Gateway®	Kan	Gehl et al., 2009
pET$_{\lambda}$HIS	Bacterial expression vector (C-terminal 6xHis)	Classical	Kan	Groot et al., 2006
pSITE-2NB	Plant expression vector (C-terminal eGFP)	Gateway®	Spec	Chakrabarty et al., 2007
pSITE-4NB	Plant expression vector (C-terminal mRFP)	Gateway®	Spec	Chakrabarty et al., 2007
pSITE-6C1	Plant expression vector (N-terminal tagRFP)	Gateway®	Spec	Chakrabarty et al., 2007
pYL436	Plant expression vector (C-terminal TAP-tag)	Gateway®	Spec	Liu et al., 2004
Generated Entry vectors for Gateway®-based cloning				
pDONR207-CyD1(-Stop)	Cytoplasmic domain 1 of *PEN3*		Gent	
pDONR207-CyD1(+Stop)	Cytoplasmic domain 1 of *PEN3* with Stop Codon		Gent	
pDONR207-CaM7(-Stop)	*CaM7* ORF without Stop Codon		Gent	
pDONR207-CaM7(+Stop)	*CaM7* ORF		Gent	
pDONR207-CML37(+Stop)	*CML37* ORF		Gent	
Generated Expression clones				
pETλHIS-CyD1	Expression of CyD1-His in *E. coli*		Kan	
pETλHIS-CyD1ΔCaMBD	Expression of CyD1ΔCaMBD-His in *E. coli*		Kan	
pETλHIS-CaM7	Expression of CaM7-His in *E. coli*		Kan	
pEXP-GWVYCE-CyD1	Expression of CyD1-VENUS^{C} in *N. benthamiana*		Kan	
pEXP-GWVYNE-CyD1	Expression of CyD1-VENUS^{N} in *N. benthamiana*		Kan	
pEXP-VYNE(R)GW-CyD1	Expression of CyD1-VENUS^{N} in *N. benthamiana*		Kan	
pEXP-GWVYCE-CaM7	Expression of CaM7-VENUS^{C} in *N. benthamiana*		Kan	
pEXP-VYNE(R)GW-CaM7	Expression of CaM7-VENUS^{N} in *N. benthamiana*		Kan	
pEXP-VYCE(R)GW-CML37	Expression of CML37-VENUS^{C} in *N. benthamiana*		Kan	
pSITE-2NB-CaM7	Expression of CaM7-eGFP in *N. benthamiana*		Spec	
pSITE-4NB-CyD1	Expression of CyD1-mRFP in *N. benthamiana*		Spec	
pSITE-6C1-CyD1	Expression of CyD1-tagRFP in *N. benthamiana*		Spec	
pYL436-CyD1	Expression of CyD1-TAP in *N. benthamiana*		Spec	
pYL436-CyD1ΔCaMBD	Expression of CyD1ΔCaMBD-TAP in *N. benthamiana*		Spec	

Gent: Gentamycin; Kan: Kanamycin; Spec: Spectinomycin

For vector maps see appendix 6.4.

2.1.6 Antibodies

Table 6. Antibodies used in this study

Primary antibodies	Blocking reagent (WB)	Dilution (WB)	Secondary antibody	Supplier
α-HA	5 % BSA in TBS-T	1:1000	α-rabbit	Cell Signaling
α-c-myc	5 % milk in TBS-T	1:2000	α-mouse	provided by U. Commandeur, RWTH Aachen
α-PDR8 (referred to as α-PEN3)	5 % milk in TBS-T	1:4000	α-rabbit	Agrisera
HRP-labeled antibodies				
α-His	5 % Casein solution	1:1500		Novagen/Merck
α-mouse	5 % milk in TBS-T	1:2000		Cell Signaling
α-rabbit	5 % milk in TBS-T	1:2000		Cell Signaling
Fluorophore-labeled antibodies				
α-c-myc-Cy3				Sigma Aldrich
α-rabbit-DyLight649				JacksonImmunoResearch

WB: Western Blot

2.1.7 Internet resources, stock centers, databases and software

Table 7. Internet resources, stock centers, databases, and software used in this study

Sequence information and GO annotation	
TAIR (The Arabidopsis Information Resource)	http://www.arabidopsis.org/
AmiGO	http://amigo.geneontology.org/cgi-bin/amigo/go.cgi
Genbank (National Center for Biotechnology Information, NCBI)	http://www.ncbi.nlm.nih.gov/genbank/
Acquisition of seeds	
NASC (European Arabidopsis Stock Center)	http://arabidopsis.info/
Acquisition of protein microarrays	
Arabidopsis Biological Resource Center (ABRC)	http://abrc.osu.edu/
Primer design	
Primer3	http://frodo.wi.mit.edu/
NCBI Primer Blast	http://www.ncbi.nlm.nih.gov/tools/primer-blast/
Signal	http://signal.salk.edu/tdnaprimers.2.html
Calculation of primer Tm for proofreading PCR	
NEB TM Calculator	https://www.neb.com/tools-and-resources/interactive-tools/tm-calculator
Analysis of RT-qPCR data	
ABI 7300 software	Applied Biosystems
Sequence alignment, BLAST, reverse complementation	
Basic local alignment search tool (BLAST)	http://blast.ncbi.nlm.nih.gov/Blast.cgi
Alignment Emboss Needle	https://www.ebi.ac.uk/Tools/psa/
Alignment ClustalW	www.ebi.ac.uk/Tools/msa/clustalw2/
Reverse Complement	http://www.bioinformatics.org/sms/rev_comp.html
Analysis of sequencing results	
Chromas Lite software	Technelysium
***In silico* cloning**	
Clone Manager Professional Suite version 8.0	Sci-Ed
***In silico* protein analysis**	
MEMSAT (transmembrane prediction)	http://saier-144-21.ucsd.edu/barmemsat.html
Pfam (protein families)	http://pfam.sanger.ac.uk/

continued

TMpred	http://www.ch.embnet.org/software/TMPRED_form.html
Prosite (domains, families and functional sites)	http://prosite.expasy.org/
Smart protein database	http://smart.embl-heidelberg.de/
Calmodulin target database	http://calcium.uhnres.utoronto.ca/ctdb/ctdb/home.html
Software for acquisition of agarose gels	
DeVision G version 2.0	Decon Science Tec
Software for acquisition of western blots and protein gels	
Image Lab	BioRad
Statistical analysis	
Sigma Stat 3.2	Systat Sowtware Inc.
Processing and analysis of cLSM images	
Leica Confocal Software Lite version	Leica Microsystems
Acquisition of microscopical images	
Mikroskopische Diskussion (DISKUS)	Carl H. Hilgers
Analysis of protein microarrays	
GenePix Pro 6.0	Molecular Devices
Matlab	The MathWorks

2.2 Methods

2.2.1 Plant material and cultivation

2.2.1.1 *Arabidopsis thaliana*

Arabidopsis accessions and mutants used in this study are listed in Table 1. Seeds were sown on wet soil (Einheitserde Werkverband, type VM), covered with a transparent plastic hood and stratified for two days at 4 °C in the dark. Germination was induced by transfer to a growth chamber with short day conditions (8 h photoperiod), 22 °C, 65 % relative humidity, and a photon irradiance of 120 µmol m^{-2} s^{-1}. After seed germination, the plastic hood was removed and the two-to-three week-old seedlings transplanted to fresh soil. Plants were watered twice a week and treated once per week with a nematode solution (Sauter und Stepper) against thrips.

2.2.1.2 *Glycine max*

The susceptible soybean cultivars Thunder 2703 RR (Thunder Seed, Inc., Hawley, MN) and Petrina (PZO SAAT GmbH, Schwäbisch Hall, Germany) were used for maintenance of *P. pachyrhizi* and production of fungal inoculum. To induce germination seeds were incubated on moist filter paper for two days at RT in the dark. Germinated seeds were transplanted to pots with a moist 2:1 mixture of soil (Einheitserde Werkverband, type P) and sand. Plants were cultivated in a growth chamber with long day conditions (16 h photoperiod) at 22 °C, 75 % relative humidity and a photon irradiance of 306 µmol m^{-2} s^{-1}. Plants were watered twice weekly.

2.2.1.3 *Nicotiana benthamiana*

N. benthamiana plants were grown in long day conditions (parameters see 2.2.1.2). After germination single plants were transplanted to pots with moist soil (Einheitserde Werkverband, type ED-73). For heterologous expression of proteins five-to-six week-old plants were used.

2.2.2 Fungal material and cultivation

2.2.2.1 *Phakopsora pachyrhizi*

P. pachyrhizi isolate BR05 was isolated from infected plant material in Brazil and maintained on the susceptible soybean cultivars Thunder 2703 RR and Petrina. For rust infection, two-week-old soybean plants were sprayed with a spore suspension that had been prepared by washing one infected soybean leaf in 50 ml of Tween solution (0.01 % (v/v) Tween-20 in H_2O). Inoculated plants were kept in a dark incubation chamber with 26 °C at saturated humidity for 24 h before returning them to long day growth conditions (see 2.2.1.2). Emerging uredospores could be harvested after ten days or later by brushing them off leaves.

2.2.2.2 *Blumeria graminis f. sp. hordei*

The *Bgh* isolate K1 (MPIPZ, Cologne) was maintained in a light cabinet with long-day conditions (16 h light period, 18 °C, 65 % humidity) on the susceptible barley cultivar Golden promise (obtained from the Leibniz Institute of Plant Genetics and Crop Plant Research, Gatersleben). For infection, 7-10 day-old barley plants were placed in a settling tower and inoculated by dusting the conidia from heavily infected barley plants.

2.2.3 Preparation and application of germination fluid

P. pachyrhizi uredospores were evenly spread on ddH_2O containing 50 µg/ml ampicillin and 25 µg/ml streptomycin and incubated for 24 h at 25 °C. Fungal spores and hyphae were subsequently removed with a spatula. The resulting germination fluid was collected, filtered through a Whatman 1mm paper, lyophilized and stored at -80 °C until further use. For application on Arabidopsis leaves the lyophilized germination fluid corresponding to 100 mg spores was resolved in 100 µl ddH_2O. The protein concentration of germination fluid ranged from 0.5 to 0.6 mg/ml. Approximately eight drops of a volume of 3 µl were evenly applied on leaves of three-to-four week-old Arabidopsis wild-type plants. As control solution lyophilized ddH_2O containing the respective amounts of antibiotics was used. Plants were covered with moistened plastic domes to prevent drying of the drops. For RT-qPCR analysis (2.2.8.3) one leaf of three plants each was collected and pooled at 8 h after treatment.

2.2.3.1 Fractionation of germination fluid

To obtain different fractions aliquots of germination fluid were treated as follows: for the autoclaved fraction, germination fluid was incubated at 121 °C for 30 min. For protein digestion, germination fluid was incubated with 1 % (v/v) Poroszyme Trypsin bead solution at 37 °C with gentle shaking overnight. Beads were removed by centrifugation at 4,500 x g for 1 min. For TCA precipitation (adapted from Chevallet et al. (2007)) of the protein fraction 100 µl germination fluid were mixed with 1.2 ml ddH_2O and 0.8 µl 30 % sodium lauroyl sarcosinate and incubated for 5 min at RT. The sample was subsequently mixed with 90 µl trichloroacetic acid (TCA) and incubated for 2 h on ice. The protein pellet was collected by centrifugation for 10 min at 14,000 x g and 4 °C, washed twice with ice-cold tetrahydrofurane and resolved in 50 µl ddH_2O.

2.2.4 Inoculation of Arabidopsis

2.2.4.1 *Phakopsora pachyrhizi*

Fungal inoculum was obtained from infected soybean plants (2.2.2.1). To inoculate Arabidopsis, a suspension of 1 mg spores per ml Tween solution (0.01 % (v/v) Tween-20 in H_2O) was evenly sprayed on leaves of four-to-five week-old plants. For mock treatment Tween solution without

spores was sprayed. Plants were transferred into short day conditions (for parameters see 2.2.1.1) and covered with a plastic hood for 24 hours. For microscopical analysis leaves were harvested 48 hpi and stained with trypan blue (2.2.28.1).

2.2.4.2 *Blumeria graminis f. sp. hordei*

For *Bgh* infection four-to-five week-old Arabidopsis plants were placed into a settling tower, inoculated by dusting the conidia from heavily infected barley plants and re-transferred into short day conditions until being harvested 48 hpi for aniline blue staining and microscopical analysis (2.2.28.2).

2.2.5 DNA extraction

DNA extraction was done according to Edwards et al. (1991). Per leaf sample approximately 100 mg of leaf material of Arabidopsis were harvested into 2 ml reaction tubes containing five glass beads (Ø 2 mm), frozen in liquid nitrogen and ground for 20 s at 5,000 rpm in a homogenizer (Precellys®24, Peqlab). After addition of 300 µl Edwards buffer (200 mM Tris-HCl pH 7.5, 250 mM NaCl, 25 mM EDTA, 0.5 % (w/v) SDS) samples were incubated for 10 min at 65 °C and then kept on ice for further 10 min. 200 µl of cold chloroform were added followed by a centrifugation step of 5 min at 14,000 rpm at RT. The supernatant (200 µl) was transferred into a new microcentrifuge tube and DNA was precipitated with 200 µl cold isopropanol. After centrifuging the samples for 5 min the pellet was washed with 70 % (v/v) ethanol, dried and resuspended in 100 µl ddH_2O.

2.2.6 RNA extraction

RNA was extracted from Arabidopsis leaves following a modified guanidinium thiocyanate-phenol protocol (Chomczynski and Sacchi, 1987). 50-100 mg of leaf material were harvested into 2 ml reaction tubes containing five glass beads (Ø 2 mm, Merck) and frozen in liquid nitrogen. Tissue was ground for 20 s at 5,000 rpm in a homogenizer (Precellys®24, Peqlab) and stored in liquid nitrogen until extraction in 1 ml Trizol (380 mM ammonium thiocyanate, 780 mM guanidinium thiocyanate, 59 mM sodium acetate, 5 % (v/v) glycerol, 47.5 ml/l phenol, pH 5.0). After incubation for 5 min at RT, 200 µl of chloroform were added and the samples mixed again for 15 s. After incubation for three more minutes the samples were centrifuged at 4 °C and 14,000 rpm for 15 min in a tabletop centrifuge. 500 µl of the aqueous phase were transferred into a new microcentrifuge tube, mixed with 500 µl isopropanol, incubated at RT for 10 min, and centrifuged at 4 °C and 14,000 rpm for 10 min. The resulting pellet was washed with 70 % (v/v) ethanol and centrifuged again for 5 minutes. The resulting pellet was dried for ap-

proximately 10 min and dissolved in 30 µl ddH_2O by heating the samples for 10 min at 60 °C and pipetting up and down. RNA was stored at -20 °C.

2.2.7 cDNA synthesis

All steps of cDNA synthesis were performed on ice. 1 µg of RNA was mixed with 1 µl 10x DNase Buffer (Fermentas/Thermo Scientific) and 1 µl DNase I and filled up to 10 µl with ddH_2O. Samples were then incubated at 37 °C for 30 min to digest DNA and afterwards for 15 min at 70 °C to inactivate DNase. To allow primer annealing, 1 µl random primer (50 µM stock solution) and 1 µl ddH_2O were added to each sample, followed by an incubation at 70 °C for 5 min. Then 4 µl 5x M-MuLV buffer (Fermentas/Thermo Scientific), 2 µl dNTPs (10 mM stock solution), 1 µl RevertAid™ M-MuLV Reverse Transcriptase (Fermentas/Thermo Scientific) and 1 µl ddH_2O were added to each sample. Reverse transcription of RNA was initiated by incubation of the samples at 37 °C for 60 min. With a last incubation step at 70 °C for 10 min the enzyme was inactivated and the cDNA was stored at -20 °C.

2.2.8 Polymerase chain reaction (PCR)

2.2.8.1 Standard PCR

Standard PCR was used for genotyping of Arabidopsis T-DNA insertion lines and confirmation of positive clones from bacterial transformation events. Gene-specific primers were designed using the Primer 3 online primer design tool and tested *in silico* for off targets using Primer Blast at NCBI. All primers used in this study were obtained from Invitrogen/Life Technologies and are listed in Table 3. 22.5 µl of PCR Supermix (22 mM Tris-HCl pH 8.4, 1.65 mM $MgCl_2$, 55 mM KCl, 220 µM of each dATP, dGTP, dTTP and dCTP, 20 µl/ml self-made Taq-polymerase and 1/10 volume of 10x loading dye solution; in ddH_2O), 1.25 µl forward primer and 1.25 µl reverse primer (10 µM stock solution corresponding to 0.5 µM final concentration of each primer) were mixed with appropriate amount of template. For genotyping 2 µl of plant DNA were used as template whereas single bacterial colonies were picked with a pipette tip and mixed with the PCR reaction mix for verification of positive clones. The PCR reaction was performed in a PeqStar Cycler (Peqlab) under the following default conditions: 3 min (94 °C), 35 cycles [30 s (94 °C), 30 s (55 °C), 1 min (72 °C)], 10 min (72 °C), 10 min (16 °C). The annealing temperature and elongation time were adjusted according to primer melting temperatures (T_m) and amplicon length, respectively. 10 µl PCR product were analyzed by gel electrophoresis.

2.2.8.2 Proofreading PCR

Proofreading PCR was performed to obtain PCR products suitable for cloning. Primers used in proofreading PCR were designed as described above and obtained from the same manufacturer.

The required recognition sites (for restriction enzyme cloning) or attB sites (for Gateway® cloning) were added to the primers' 5' end (see Table 3). The PCR reaction was performed using the Phusion® High-Fidelity DNA Polymerase (Finnzymes/Thermo Scientific) according to the manufacturer's guidelines. Primer annealing temperatures were calculated using the Finnzyme T_m-Calculator. PCR products were analyzed by gel electrophoresis and purified using the Zymoclean™ Gel DNA Recovery Kit (Zymo Research) according to the manufacturer's instructions.

2.2.8.3 RT-qPCR

RT-qPCR was used to determine the amount of gene specific mRNA. Primers used for RT-qPCR were designed using the Primer 3 online primer design tool following standard criteria (Udvardi et al., 2008). Primers were tested prior to analysis to determine their specificity and efficiency. Efficiency was calculated from the slope of a cDNA dilution series using the Finnzymes PCR efficiency calculator. For the RT-qPCR reaction a master mix of 5 µl SYBR® Green qPCR Mix (Life Technologies), 2.7 µl ddH_2O, and 0.15 µl of each primer (end concentration 150 nM) per reaction was prepared and pipetted in 96-well plates (Sarstedt). 2 µl of 1:10 diluted cDNA were added to each well and for each reaction at least two technical replicates were done. The PCR reaction was conducted in an ABI7300 Real-time PCR system under the following conditions: 2 min (50 °C), 10 min (95 °C), 40 cycles [15 s (95 °C), 1 min (60 °C)]. To detect unspecific PCR products or primer dimer formation a dissociation stage enabling the determination of PCR product melting temperatures was integrated in the RT-PCR program. According to the mathematic model of Pfaffl (2001) every gene specific transcript level was normalized to the supposedly constitutively expressed housekeeping gene *ACTIN2* using the $2^{-\Delta\Delta Ct}$ method.

2.2.9 Agarose gel electrophoresis

PCR products and digested plasmids were separated by gel electrophoresis in gels with 0.8–2 % (w/v) agarose, depending on the size of the DNA fragments. Agarose was dissolved in 1x TAE buffer (30 mM Tris-HCl, 0.1142 % acetic acid, 1 mM EDTA pH 8.0) and ethidium bromide (EtBr) was added to a concentration of 0.2 µg/ml before pouring the gel. Gel electrophoresis was conducted with constant voltage (80-150 V) in 1x TAE buffer. Fluorescent EtBr-staining was visualized under UV light (366 nm) in a DEVISION DBOX (Decon DC Science Tec) and compared to a DNA ladder (Generuler 1 kb, Fermentas/Thermo Scientific) to estimate the fragment sizes.

2.2.10 Quantification of nucleic acids

Nucleic acids were diluted 1:100 in ddH_2O and quantified spectrophotometrically using a Beckman DU7500 (Beckman Coulter Inc.) diode-array photometer by measuring the absorbance at 260 and 280 nm. An absorbance of 1 at 260 nm equals a concentration of 50 µg/ml DNA or

40 µg/ml of RNA, such that the concentration could be calculated with either of the following formulas:

Concentration DNA $(\mu g * \mu l^{-1}) = (A260nm * 50\mu g * \text{dilution factor}) * (\mu l * 1000)^{-1}$

Concentration RNA $(\mu g * \mu l^{-1}) = (A260nm * 40\mu g * \text{dilution factor}) * (\mu l * 1000)^{-1}$

The ratio of the absorbance at 260 and 280 nm ($A_{260/280}$) can further be used to estimate the purity of the extracted nucleic acids. For pure DNA, $A_{260/280}$ is ~1.8 whereas for pure RNA $A_{260/280}$ is ~2.

2.2.11 Sequencing

Plasmids to be sequenced were mixed with 20 pmol of primer and sent to Seqlab (Sequence Laboratories Göttingen GmbH, Germany). The resulting sequence files were analyzed using the Chromas Lite software and the online alignment tool Emboss Needle.

2.2.12 Genotyping Arabidopsis T-DNA mutants

Arabidopsis T-DNA knockout lines were cultivated as described in 2.2.1.1. Three-to-four week-old plants were used for verification of the genotype by extracting DNA (2.2.5) and subsequent PCR analysis (2.2.8.1). Primers for genotyping PCRs were generated using the SiGnAL online tool, which automatically designs gene specific primers located left and right of the insertion site of a given T-DNA line. For genomic PCR a combination of forward (_F) and reverse (_R) primer was used, whereas the T-DNA left border primers Lbb1-3 (Salk lines) or Lb1 (Sail lines) were used in combination with the reverse primer to confirm the presence of the insert. All primers used for genotyping are listed in Table 3. Additionally, the absence or reduction of mRNA of the respective gene was confirmed by RT-qPCR (2.2.8.3).

2.2.13 Crossing Arabidopsis mutants

After approximately four weeks under short day conditions (2.2.1.1) Arabidopsis mutants were transferred to long day conditions to stimulate inflorescence development. First, any siliques, open flowers or open buds were removed with a forceps. Then, also the sepals, petals and immature anthers were removed to expose the stigma. The stigma of the mother plant was pollinated with anthers from a mature flower of the genotype to be crossed. Pollinated stigmas were protected with a plastic bag to maintain high humidity for two days. Successfully pollinated stigmas develop into a mature silique and set seeds. Plants of the resulting F_1 generation were genotyped (2.2.12) and double heterozygous plants were proceeded to the next generation. In the F_2 generation double homozygous plants could be identified.

2.2.14 Cloning

2.2.14.1 Restriction enzyme cloning

For cloning of *CyD1* and *CaM7* into the bacterial expression vector pET$_\lambda$HIS, both genes were amplified by proofreading PCR (2.2.8.2) from Arabidopsis wild-type cDNA (2.2.7) using gene-specific primers containing recognition sites for the restriction enzymes BamHI or XhoI (Table 3). PCR products were purified via gel electrophoresis (2.2.9) and the Zymoclean™ Gel DNA Recovery Kit (Zymo Research). The purified PCR products and the vector pET$_\lambda$HIS were digested using the fast digest restriction enzymes BamHI and XhoI (Fermentas/Thermo Scientific) according to the manufacturer's instructions. Before ligation using the T4 DNA Ligase (Fermentas/Thermo Scientific) the digested PCR products and vector backbone were once again purified. 10 µl of the ligation reaction were transformed into competent *E. coli* BL21 cells (2.2.16).

2.2.14.2 Gateway® cloning

For cloning of *CyD1*, *CaM7* and *CML37* into different plant expression vectors, the Gateway® cloning technology (Invitrogen/Life Technologies) was applied. The Gateway® technology is a universal cloning method based on the site-specific recombination properties of bacteriophage lambda (Landy, 1989). Site-specific attachment (*att*) sites were fused to the 5'end of the gene specific primers (Table 3) to mediate the transfer into the Gateway® vector pDONR207. The resulting entry vectors were used to recombine the target genes into the following destination vectors: pYL436 for protein expression and purification; pDEST-^{GW}VYCE, pDEST-VYCE(R)^{GW}, pDEST-^{GW}VYNE and pDEST-VYCE(R)^{GW} for BIFC experiments (2.2.27) and pSITE1637, 1643 and 1644 for cellular localization. All vectors generated in this study are listed in Table 5.

2.2.14.3 Generation of entry clones (BP reaction)

For the BP reaction 250 ng of a Gateway®-compatible PCR product were mixed with 250 ng of pDONR207 donor vector. The volume was filled up to 9 µl with 1x TE buffer (10 mM Tris pH 8.0, 1 mM EDTA) and 1 µl Gateway® BP Clonase® II enzyme mix (Invitrogen/Life Technologies) was added. The BP reaction was incubated overnight at RT. For protein digestion 1 µl of Proteinase K was added and the mixture incubated at 37 °C for 10 min. 5 µl of the entry vector were transformed into competent *E. coli* DH5α.

2.2.14.4 Generation of expression clones (LR reaction)

For the LR reaction 150 ng of a Gateway®-compatible entry vector were mixed with 150 ng of destination vector. The volume was filled up to 9 µl with 1x TE buffer and 1 µl Gateway® LR Clonase® II enzyme mix (Invitrogen/Life Technologies) was added. The LR reaction was incubated overnight at RT. For protein digestion 1 µl of Proteinase K was added and the mixture was

incubated at 37 °C for 10 min. 5 µl of the entry vector were transformed into competent *E. coli* DH5α.

2.2.15 Preparation of chemically competent *E. coli*

100 ml lysogeny broth (LB, 1 % tryptone, 0.5 % yeast extract, 1 % NaCl) were inoculated with *E. coli* and incubated with shaking (210 rpm) at 37 °C overnight. 100 ml LB medium were inoculated with 1 ml of the overnight culture and incubated with shaking at 37 °C until OD_{600} reached 0.3 to 0.5. The culture was transferred into 50 ml reaction tubes and kept on ice for 15 min, followed by a centrifugation step of 10 min at 4 °C and 3,000 rpm. The supernatant was discarded and the pellet resuspended in 10 ml TFB I buffer (30 mM potassium acetate (KAc), 50 mM $MnCl_2$, 100 mM RbCl, 10 mM $CaCl_2$, 15 % (v/v) glycerol, in H_2O, pH 5.8 with HCl). Cells were kept on ice for 10 min and centrifuged again for 10 min. The supernatant was discarded and the pellet resuspended in 1 ml TFB II buffer (10 mM MOPS, 10 mM RbCl, 75 mM $CaCl_2$, 15 % (v/v) glycerol, in H_2O, pH 7.0 with HCl). Competent cells were frozen in 50 µl aliquots at -80 °C.

2.2.16 Transformation of chemically competent *E. coli*

50 µl competent *E. coli* were mixed with 5-10 µl DNA and incubated on ice for 10 min. After a heat shock for 60 sec at 42 °C samples were chilled on ice for another 10 min. Bacteria were incubated at 37 °C for 30 min after adding 1 ml LB medium. Cells were pelleted for 1 min at 5,000 rpm, 900 µl of the supernatant were discarded and the pellet resuspended in the remaining 100 µl of medium. Bacteria were plated on LB-agar with appropriate antibiotics and incubated for one day at 37 °C. Resulting colonies were tested for successful transformation of the candidate gene by PCR (see 2.2.8.1).

2.2.17 Plasmid preparation

Plasmids were prepared from a 2 ml LB overnight culture of transformed *E. coli* using the ZR Plasmid Miniprep-Classic Kit (Zymo Research) or Invisorb® Spin Plasmid Mini Two Kit (Stratec molecular) according to the manufacturers' instructions.

2.2.18 Preparation of electrocompetent *A. tumefaciens*

2 ml yeast extract broth (YEB, 0.5 % beef extract, 0.1 % yeast extract, 0.5 % tryptone, 0.5 % peptone, 0.5 % sucrose) with appropriate antibiotics were inoculated with Agrobacterium strains AGL-1, GV3101, or GV2260 and incubated with shaking overnight at 28 °C. Bacteria were diluted 1:100 in fresh YEB with antibiotics and incubated at 28 °C until the OD_{600} reached 1 to 1.5. The culture was transferred to pre-chilled 50 ml reaction tubes and kept on ice for 10 min, followed by a centrifugation step of 5 min at 3,500 rpm and 4 °C. The pelleted cells were resuspended in

10 ml prechilled ddH_2O and kept on ice for further 10 min. Centrifugation was repeated and the pellet was resuspended in 500 µl 10 % (v/v) glycerol. Cells were stored in 50 µl aliquots at -80 °C.

2.2.19 Transformation of electrocompetent *A. tumefaciens*

1 µg of expression vector was added to 50 µl electrocompetent agrobacteria and transferred to a pre-chilled electroporation cuvette. Upon electroporation (2.20 kV for 5 ms) in a micropulser (MicroPulser Electroporator, Bio-Rad) 1 ml YEB medium was immediately added and agrobacteria were transferred to a fresh microcentrifuge tube. Bacteria were incubated at 28 °C for 2 h. Following centrifugation for 1 min at 7,000 rpm the cells were resuspended in 100 µl ddH_2O and plated on YEB-agar containing the appropriate antibiotics. Plates were incubated for two to three days at 28 °C. In terms of successful transformation of the candidate gene, colonies were tested by PCR (see 2.2.8.1). Positively tested colonies were transferred on new plates and incubated for two more days at 28 °C. A liquid culture of 2 ml YEB medium with appropriate antibiotics was inoculated with bacterial cells from the plates, incubated for one day at 28 °C with shaking and stored at -80 °C after adding 20 % (v/v) glycerol.

2.2.20 Heterologous production and purification of proteins

2.2.20.1 Production of proteins in *N. benthamiana*

Agrobacterium strain AGL-1 harboring the plant expression vector pYL436-CyD1 and strain GV2260 carrying p19 were cultured for 14-16 h at 26 °C with shaking. The bacteria were pelleted at 3,000 x g for 20 min, resuspended in infiltration medium (10 mM MES, 10 mM $MgCl_2$, 200 µM acetosyringone), adjusted to an OD_{600} of 0.4 and incubated at RT for approximately 2 h. *Agrobacterium* strain GV2260 was resuspended in infiltration media to an OD_{600} of 0.8. Equal volumes of CyD1-TAP and p19 cultures were mixed and infiltrated into *N. benthamiana* plants using a 1 ml needleless syringe. Three to four days after infiltration, the leaves were collected and stored at -80 °C.

2.2.20.2 Total protein extraction

To rapidly test for the protein abundance in transiently transformed *N. benthamiana* leaves, ground material of one leaf disc of approximately 1 cm^2 was resuspended in 150 µl protein extraction buffer (50 mM Tris-HCl pH 8, 1 mM EDTA, 0.1 % (v/v) 2-mercaptoethanol, 30 µg/ml PMSF). The extract was centrifuged twice at 12,000 x g for 30 min at 4 °C. 50 µl of the resulting protein extract were mixed with NuPAGE® LDS sample buffer and reducing agent (both Life Technologies), heated to 95 °C for 5 min and analyzed via SDS-PAGE (2.2.26.1) and western blotting analysis (2.2.26.3).

2.2.20.3 Purification of proteins from *N. benthamiana*

15 g of plant tissue was ground finely in liquid nitrogen and mixed with 30 ml extraction buffer (100 mM Tris-HCl pH 7.5, 150 mM NaCl, 5 mM EDTA, 10 mM 2-mercaptoethanol, 10 % glycerol, 0.1 % Triton X-100, 1x Roche Complete protease inhibitors, 1 mM PMSF) and approximately 1 g of 0.5 mm glass beads in a 50 ml tube. The mixture was processed by beating in a paint shaker five times for 1 min each with 1 min on ice in between. Lysates were centrifuged twice for 20 min at 14,000 x g. The supernatant was aliquot into 1 ml fractions and incubated each with 40 µl of a 1:1 IgG Sepharose 6 Fast Flow beads: buffer preparation for 2 h with rotation at 4 °C. Beads were collected by centrifugation for 1 min at 3,000 x g, washed three times in washing buffer (extraction buffer with 350 mM NaCl) and once in cleavage buffer (100 mM Tris-HCl pH 7.5, 150 mM NaCl, 1 mM EDTA, 1 mM DTT, 0.1 % Triton X-100). After removal of the buffer beads were mixed with 30 µl cleavage buffer containing 10 µl/ml of PreScission protease (Amersham Biosciences/GE) and incubated overnight with rotation at 4°C. The supernatant was mixed with 30 µl equilibrated GST-Agarose (Clontech/TaKaRa) and incubated for 1 h with rotation at 4 °C to capture the protease. Protease-bound beads were subsequently discarded and the supernatant mixed with glycerol to a final concentration of 20 % and stored at -80 °C.

2.2.20.4 Production of proteins in *E. coli*

3 ml LB medium with 25 µg/ml kanamycin was inoculated with *E. coli* BL21 pET$_\lambda$HIS-*CyD1* or -*CaM7* and incubated overnight at 37 °C with shaking (210 rpm). 250 ml fresh LB medium were inoculated with 2.5 ml of the overnight culture. Bacteria were grown to an OD_{600} of 0.6. IPTG was added to a final concentration of 1 mM, the cultures were incubated for further 3 h at 37 °C and then pelleted by centrifugation for 15 min at 4,000 rpm and 4 °C.

2.2.20.5 Purification of proteins from *E.coli* under native conditions

CaM7-6xHis was purified from *E. coli* under native conditions by affinity chromatography. Bacterial pellets (2.2.20.4) were resuspended in 10 ml lysis buffer (25 mM HEPES pH 7.5, 300 mM NaCl, 10 % glycerin, 5 mM imidazol), mixed with lysozyme and incubated for 30 min at 4 °C with gentle shaking. Lysates were sonicated for 2 min and centrifuged for 50 min at 4,000 rpm and 4 °C. The supernatant was applied on a pre-equilibrated Ni-NTA Superflow column (Qiagen). The column was extensively washed with wash buffer (25 mM HEPES pH 7.5, 300 mM NaCl, 10 % glycerin, 10 mM imidazol) and the protein eluted from the column by applying 5 ml elution buffer (25 mM HEPES pH 7.5, 300 mM NaCl, 10 % glycerin, 300 mM imidazol). Eluted fractions were directly tested for protein abundance by adding a 10 µl aliquot to 90 µl Bradford reagent (2.2.21). Protein containing fractions were pooled and submitted to a buffer exchange against

PBS using a PD-10 desalting column (GE). The protein concentration was determined by a Bradford assay (2.2.21).

2.2.20.6 Purification of proteins from *E. coli* under denaturing conditions

CyD1-6xHis was purified from *E. coli* under denaturing conditions by affinity chromatography. Bacterial pellets (2.2.20.4) were resuspended in 10 ml denaturing buffer (100 mM NaH_2PO_4, 10 mM Tris-HCl, 8 M urea pH 8.0) and incubated for 1 h at RT with gentle shaking. Lysate was centrifuged for 30 min at 10,000 x g at RT and the supernatant applied on a pre-equilibrated Ni-NTA column. The column was washed twice with 4 ml wash buffer C (100 mM NaH_2PO_4, 10 mM Tris-HCl, 8 M urea pH 6.3) and eluted by successively adding 2 ml elution buffer D (100 mM NaH_2PO_4, 10 mM Tris-HCl, 8 M urea pH 5.9) and 2 ml elution buffer E (100 mM NaH_2PO_4, 10 mM Tris-HCl, 8 M urea pH 4.5). Eluted fractions were directly tested for protein abundance by adding a 10 µl aliquot to 90 µl Bradford reagent (2.2.21). The protein containing fractions were pooled.

2.2.21 Quantification of proteins

The protein concentration in solutions was determined by a Bradford assay (Bradford, 1976). Therefore, 5 µl protein solution were mixed with 995 µl 1 x Quick Start™ Bradford 1x Dye Reagent (Bio-Rad) and incubated at RT for 10 min. The OD_{595} was measured in a DU700 spectrophotometer (Beckman Coulter Inc.). Protein concentration was calculated using a standard curve of bovine serum albumin (BSA) in the respective buffer.

2.2.22 Arabidopsis protein microarrays

2.2.22.1 Printing the test array

To test whether the α-PEN3 antibody was suitable for use on protein microarrays (PMAs), a test array was designed containing 20 % glycerol and 1 % BSA as negative controls, purified CyD1 protein and the antibody in a 1:1000 dilution. All probes were printed six timed in a row onto FAST slides (Schleicher & Schuell, Keene, NH, USA) with a quill-pin contact microarray printer, (Micro Grid Pro, BioRobotics). The test array was air-dried and stored at -80 °C.

2.2.22.2 Probing protein microarrays

PMAs were blocked in TBS-T (20 mM Tris, 137 mM NaCl, 0.1 % Tween-20) with 1 % BSA for 1 h, drained and placed in a humid chamber. 500 µl of purified CyD1 or cleavage buffer, both mixed with 1 % BSA and 5 mM $MgCl_2$ were applied on the slides and incubated for 1.5 h. Slides were washed once in washing buffer (PBS (137 mM NaCl, 2.7 mM KCl, 10 mM Na_2HPO_4, 1.76 mM KH_2PO_4) 5 mM $MgCl_2$, 0.05 % Triton X-100, 5 % glycerol, 1 % BSA), incubated with 500 µl

α-PEN3 (1:8,000, Agrisera) for 30 min, washed once and incubated with 500 µl α-rabbit-DyLight649 (1:10,000, JacksonImmunoResearch) for 30 min and washed once again. Slides were dipped in water, spun-dried and scanned at 650 nm in a ScanArray Express scanner (Perkin Elmer). Three replicates for the array probing with CyD1 and two replicates for the negative controls were performed.

For the immunoassay of the 10K PMA the slide was incubated with α-c-myc-Cy3 (1:10,000, Sigma Aldrich) instead of the primary and secondary antibodies.

2.2.22.3 Bioinformatic analysis of the protein microarrays

Array images were processed using GenePix® Pro 7 Acquisition and Analysis Software (Molecular Devices) as described in Moreau et al. (2013). To analyze candidates with significantly stronger binding signals vs. control signals a cross-array normalization method was implemented in Matlab followed by a statistical testing method. All microarrays (probe and control) datasets were normalized using a linear regression model as follows: 1) The background median intensity was subtracted from signal median intensity; 2) Linear regression coefficients for each probe and control PMAs pairs were calculated: $\{\hat{a}, \hat{b}\} = \text{argmin}_{i\in\{1..N\}}\{(y_P(i) - ay_C(i) - b)^2\}$, where N is the number of proteins printed on the microarray; 3) "Between arrays" normalization was performed using a linear transformation of probe datasets (using the estimated regression coefficients) and scaling of control datasets: $\boldsymbol{y}_P{}'(j) = \left(\boldsymbol{y}_P(j) - \hat{b}(j)\right)/\left(\hat{a}(j) * mean\left(\boldsymbol{y}_C(j)\right)\right)$, $\boldsymbol{y}_C{}'(j) = \boldsymbol{y}_C(j)/mean(\boldsymbol{y}_C(j))$, $j = 1..M$, the number of (probe, control) pair datasets. To select probe binding candidates a one-side t-test was used: $= {(\overline{\boldsymbol{y}}_P - \overline{\boldsymbol{y}}_C)}/{s_{\overline{\boldsymbol{y}}_P - \overline{\boldsymbol{y}}_C}}$, where $s_{\overline{\boldsymbol{y}}_P - \overline{\boldsymbol{y}}_C}$ is the standard error of the difference between the means, using pooled variance and a 5 % significance level due to the small sample set. The type II errors were controlled by applying an false discovery rate method described in Storey (2002). Results were summarized in files containing the Arabidopsis identifiers, gene description, position on the array and the pValues and qValues resulting from the testing procedures.

2.2.23 Preparation of microsomal fractions from Arabidopsis leaves

Arabidopsis microsomes were prepared as described in Qi and Katagiri (2009) with minor modifications. All steps were performed at 4 °C. 5 g of fresh leaf material from 5-to-6 week-old Arabidopsis plants were cut into pieces and ground in 25 ml grinding buffer (50 mM HEPES-KOH pH 7.5, 10 mM EDTA, 330 mM sucrose, 0.6 % PVPP, 1 mM DTT, 1 mM PMSF, 1 µg/ml leupeptin, 1 µg/ml pepstatin, 1 µg/ml E-64). The homogenate was filtered through double-layered miracloth and centrifuged for 10 min at 18,000 x g. The supernatant was further centrifuged for 1 h at

100,000 x g and the resulting microsome pellet was resuspended in 4 ml resuspension buffer (20 mM HEPES-KOH pH 7.5, 1 mM EDTA, 330 mM sucrose, 1 mM PMSF, 1 µg/ml leupeptin, 1 µg/ml pepstatin, 1 µg/ml E-64). To solubilize the proteins 10 % (w/v) S-DOC was added to a final concentration of 0.05 %. The solution was incubated for 1 h with rotation, centrifuged for 30 min at 100,000 x g and the resulting supernatant containing the microsomal fraction was collected.

2.2.24 Pull-down of PEN3 from microsomal fractions

For each treatment 40 µl Calmodulin Sepharose 4B (GE) were added to 1 ml microsomal protein solution. A different combination of 5 mM $CaCl_2$ and/or 7 mM EDTA or EGTA (final concentration) was added to each sample. The solution was incubated with rotation for 4 h at 4 °C. After centrifugation for 1 min at 7,000 rpm the beads were washed four times with CaM Washing buffer (50 mM Tris-HCl pH 7.5, 150 mM NaCl) containing the respective amount of $CaCl_2$ and/or EDTA or EGTA for each sample. After the last centrifugation step the supernatant was discarded, the beads resolved in 50 µl NuPAGE® LDS sample buffer and reducing agent and loaded on a NuPAGE® 4-12 % Bis-Tris Protein gel (all reagents Life Technologies, 2.2.26.1). After immunoblotting (2.2.26.3) PEN3 was detected using the α-AtPDR8 (referred to as α-PEN3) antibody (Agrisera).

2.2.25 CaM overlay assay

2.2.25.1 Synthesis of HRP-labeled CaM7

100 µl of the CaM7 protein solution (~8 µg/µl, see 2.2.20.5) were reduced with 50 µl of 1 mM TCEP by incubation for 2 h at RT. TCEP was subsequently removed by using a PD-10 desalting column (GE). 1 mg maleimide-activated HRP (Thermo Scientific) was resolved in 500 µl PBS, mixed with the CaM7 protein and incubated at RT overnight. The CaM7-HRP conjugate was mixed with glycerol to a final concentration of 20 % and successful linkage was confirmed by SDS-PAGE (2.2.26.1) and subsequent Coomassie staining (2.2.26.2).

2.2.25.2 Overlay assay

Purified CyD1 (2.2.20.6) was loaded four times on the same SDS-PAGE: once for Coomassie staining (2.2.26.2) and three times for immunoblotting on nitrocellulose (2.2.26.3). One part was used for detection with an α-His antibody (Novagen/Merck) and two for the overlay assay in presence or absence of $CaCl_2$. For the overlay assay the membrane was rinsed in TBS-T and blocked overnight in 7 % milk powder in TBS-T. After washing three times in TBS-T the membrane was cut into two parts and equilibrated in overlay buffer (50 mM imidazole pH 7.5, 150 mM NaCl) with 1 mM $CaCl_2$ or 5 mM EGTA. Membranes were then incubated for 1 h in over-

lay buffer with 0.1 % gelatine and 20 µl/ml CaM7-HRP conjugate (approximate concentration of 5 µg/µl) and 1 mM $CaCl_2$ or 5 mM EGTA. After washing five times for 5 min in wash buffer 1 (TBS-T, 50 mM imidazole pH 7.5, 1 mM $CaCl_2$ or 5 mM EGTA), five times for 5 min in wash buffer 2 (20 mM Tris-HCl pH 7.5, 0.5 % Tween-20, 50 mM imidazole pH 7.5, 0.5 M KCl, 1 mM $CaCl_2$ or 5 mM EGTA) and five times for 5 min with wash buffer 3 (20 mM Tris-HCl pH 7.5, 0.1 % Tween-20, 0.5 M KCl, 1 mM $CaCl_2$ or 5 mM EGTA) chemiluminescence was detected using the Clarity Western ECL Substrate (BioRad).

2.2.26 Visualization and analysis of proteins

2.2.26.1 SDS-PAGE

Proteins were separated by TRIS-glycine sodium dodecyl sulfate polyacrylamide gel electrophoresis (SDS-PAGE, Laemmli, 1970). Depending on the protein mass, pre-cast NuPAGE® 4-12 % Bis-Tris Protein gels and the Novex®NuPAGE® SDS-PAGE Gel system (both Life Technologies) or self-cast 12 % Bis-Tris gels and the Mini-PROTEAN® system (Bio-Rad) were used. To cast a 12 % running gel (12.5 % (v/v) acrylamide mix (29:1 acrylamide:bisacrylamide), 375 mM TRIS pH 8.8, 0.1 % (v/v) SDS, 0.1 % (v/v) APS, 0.04 % (v/v) TEMED, in water) was layered with a 4 % stacking gel (5 % (v/v) acrylamide mix (29:1 acrylamide:bisacrylamide), 126 mM TRIS pH 6.8, 0.1 % (v/v) SDS, 0.1 % (v/v) APS, 0.1 % (v/v) TEMED, in water). Samples (beads or typically 10 µg of protein) were dissolved in 50 µl NuPAGE® LDS sample buffer with reducing agent, loaded on the gel and run in 1 x MES buffer (50 mM MES, 50 mM Tris, 1 mM EDTA, 0.5% (w/v) SDS) at constant voltage (150-200 V). The PiNK Prestained Protein Marker (Nippon genetics) was used to estimate the molecular mass of the separated proteins. Gels were either stained with Coomassie blue (2.2.26.2) or used for immunoblotting (2.2.26.3).

2.2.26.2 Coomassie staining

Gels were stained in Coomassie solution (Page Blue™ Protein Staining Solution, Fermentas/Thermo Scientific) overnight with gentle shaking and destained in ddH_2O. Gels were photographed in a ChemiDOC™ MP System (BioRad).

2.2.26.3 Protein transfer and immunodetection

Proteins were transferred onto Roti-NC nitrocellulose membranes (Carl Roth) in TRIS-glycine blotting buffer (25 mM TRIS, 250 mM glycine, 0.1 % SDS, in ddH_2O) using the Mini Trans-Blot Cell wet-blotting system (Bio-Rad). Transfer was conducted for 1 h at 250 mA.

If the α-PEN3, α-HA or α-c-myc antibodies were used, membranes were blocked in 5 % milk powder or BSA in TBS-T (see Table 6). Membranes were then washed three times for 5 min with TBS-T and incubated with the primary antibody (diluted in milk or BSA solution) overnight with

gentle shaking. The next day membranes were again washed three times with TBS-T and then incubated with the HRP-labeled secondary antibody (diluted in milk solution) for 1 h. After three more washing steps in TBS-T and a last washing in TBS, chemiluminescence was detected using the Clarity Western ECL Substrate (BioRad) in a ChemiDOC™ MP System (BioRad). Pictures were analyzed using the Bio-Rad Image Lab software.

If the α-His antibody was used the membranes were first washed twice with TBS-TT (TBS-T with 0.2 % Triton X-100) and once in TBS for 10 min before blocking for 1 h in 5 % casein blocking solution (Novagen/Merck). The three washing steps were repeated and the membrane incubated with the HRP-labeled α-His antibody diluted in casein solution for 1 h with gentle shaking. Following three more washing steps chemiluminescence was detected as described above.

To confirm equal loading of protein samples, membranes were finally stained with Ponceau S solution (Sigma Aldrich) for a few minutes and washed several times in water.

2.2.27 Bimolecular fluorescence complementation

Bimolecular fluorescence complementation (BIFC) is a method for the visualization of interaction between proteins in living cells. It is based on the use of nonfluorescent fragments of a fluorophore that only reconstitute their fluorescent property when brought together by interactions between proteins covalently linked to each fragment (Hu et al., 2002). In this study I used the Gateway®-compatible vectors pDEST-^{GW}VYCE, pDEST-VYCE(R)^{GW}, pDEST-^{GW}VYNE and pDEST-VYCE(R)^{GW} to fuse candidate genes to fragments of the fluorophore Venus. Agrobacteria carrying split-Venus fusion constructs were grown and infiltrated into *N. benthamiana* leaves as described in 2.2.20.1. Different combinations of N- and C-terminal tagged fusions with Venus^{C} or Venus^{N} were tested for each candidate. Leave sections were harvested three days after infiltration and analyzed by confocal laser scanning microscopy (2.2.29.3).

2.2.28 Histochemical staining

2.2.28.1 Trypan Blue staining

For microscopic analysis of the interaction between Arabidopsis and *P. pachyrhizi* leaves were stained with trypan blue. Cellular accumulation of trypan blue indicates the collapse of the stained cell (Keogh et al., 1980). Leaves were covered with trypan blue staining solution (10 % (v/v) lactic acid, 10 % (v/v) glycerol, 10 % (v/v) dH_2O, 70 % (v/v) ethanol, 0.025 % (w/v) trypan blue) and incubated for 1 min at 80 °C. After incubation for 10 min at RT the staining solution was replaced by 2.5 g/ml chloral hydrate. Leaves were kept in chloral hydrate for at least five days, before they were mounted on glass slides in 50 % (v/v) glycerol and analyzed by brightfield microscopy (2.2.29.1).

2.2.28.2 Aniline blue staining

The interaction between Arabidopsis and *Bgh* was assessed by staining callose depositions with aniline blue. Leaves were destained in 2.5 g/ml chloral hydrate for at least five days. 12-24 h prior to microscopic analysis the destaining solution was replaced by aniline blue staining solution (0.01 % aniline blue in 150 mM KH_2PO_4 pH 7.5). Leaves were then mounted on glass slides in 50 % (v/v) glycerol and analyzed immediately by brightfield and fluorescence microscopy (2.2.29.1 and 2.2.29.2).

2.2.28.3 ß-glucuronidase (GUS) staining

Arabidopsis leaves were vacuum-infiltrated with GUS staining solution (0.1 M PBS pH 7.0, 10 mM EDTA, 5 mM of each potassium ferrocyanide (II) and (III), 1 mM x-Gluc) and incubated overnight at 37 °C. Leaves were then destained with 2.5 g/ml chloral hydrate for at least five days. GUS staining was documented by brightfield microscopy using the Keyence BZ-9000 E microscope (Keyence GmbH, Neu-Isenburg, Germany).

2.2.29 Microscopical analysis

2.2.29.1 Brightfield microscopy

For brightfield microscopy a Leica DMR microscope was used. Photos were taken with a digital JVC KYF 750 camera and edited with the acquisition software DISKUS. 100 interaction sites were examined on each leaf. Statistical evaluation of microscopic results was done with help of the Sigma Stat 3.1 software.

2.2.29.2 Fluorescence microscopy

Fluorescence of aniline blue stained callose-containing appositions was observed in a Leica TCS SP fluorescence microscope with an epifluorescent filter (A-513804, 340–380 nm excitation, and 425 nm emission, Leica). Photos were taken with a digital JVC KYF 750 camera.

2.2.29.3 Confocal laser scanning microscopy

Confocal laser scanning microscopy (cLSM) was applied for BIFC experiments and for analysis of the subcellular localization of CyD1-RFP and CaM7-GFP fusions. Sections of infiltrated *N. benthamiana* leaves (2.2.20.1) were mounted on glass slides in 50 % glycerol (v/v) and analyzed using a Leica TCS SP Spectral Confocal Microscope. Venus- and GFP-fluorescence was excited with the 488 nm excitation line of an argon-krypton laser whereas RFP was excited at 568 nm. Emission was monitored at 510-525 nm for GFP, 515-535 nm for Venus, 580-610 nm for RFP and 650-700 nm for chlorophyll autofluorescence, respectively. A 20 fold magnification objective (Leica HCX PL FLUOTAR) was chosen for micrograph production. A series of optical sections

was acquired by scanning multiple positions along the orthogonal axis (z-stack). Images were processed with Leica confocal software LCS lite to produce 2D projections from z-stack series.

3 RESULTS

3.1 *P. pachyrhizi* induces marker genes for necrotrophic interactions

3.1.1 Expression of defense marker genes in Arabidopsis upon infection with *P. pachyrhizi*

In a previous study Loehrer et al. (2008) investigated the expression profile of the marker genes *PDF1.2* and *PR-1* in Arabidopsis leaves at 24, 48 and 72 hpi with *P. pachyrhizi*. They reported that *PDF1.2* expression was strongly induced at 24 hpi in wild-type plants and penetration mutants *pen1-1*, *pen2-1* and *pen3-1*. Over the next two days the abundance of *PDF1.2* transcripts decreased to basal levels. In contrast, upon infection with *P. pachyrhizi PR-1* expression was not induced in wild-type plants at any of the time points tested. *PR-1* mRNA transcripts were detected at 24 hpi only in *pen3-1* and the *pen1-1 pen2-1* double mutant in which they further accumulated at later times. The late accumulation of *PR-1* transcripts correlated with impaired postinvasion resistance of these genotypes (Loehrer et al., 2008). The authors speculated that *P. pachyrhizi* would mimic a necrotrophic attacker in the early stages of plant invasion to circumvent, or even inhibit, effective plant defense.

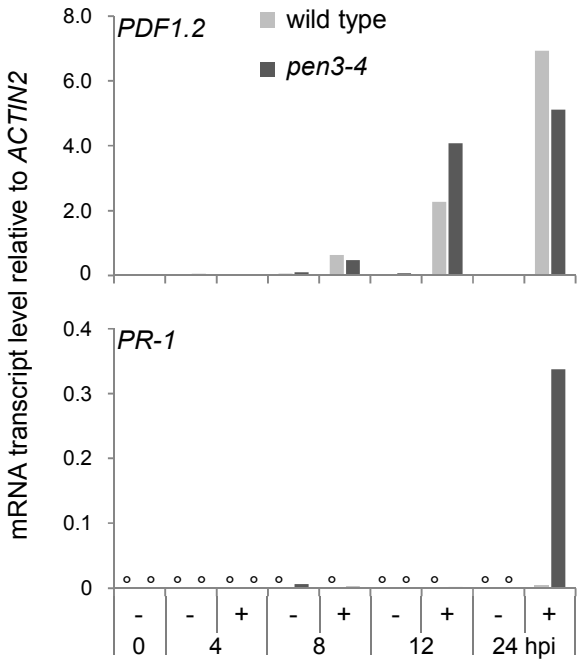

Figure 1. *PDF1.2* and *PR-1* mRNA transcript accumulation in Arabidopsis wild-type and *pen3-4* plants upon inoculation with *P. pachyrhizi*. Leaves of four-to-five week-old Arabidopsis plants were control treated (-) or inoculated with *P. pachyrhizi* uredospores (+). At 0, 4, 8, 12 and 24 hpi three leaves from three plants were harvested and pooled and total RNA was extracted from the leaves. mRNA transcript abundance was analyzed by RT-qPCR with *ACTIN2* as the normalization standard. Values are from one representative experiment. Three independent experiments were performed with similar results. ° not detected

At the time points of investigation, however, penetration and potential colonization of the plant probably have already occurred (Loehrer et al., 2008). To determine whether expression of defense markers was already induced prior to penetration and colonization by *P. pachyrhizi*, abundance of *PDF1.2* and *PR-1* transcript was measured in Arabidopsis wild type and the *pen3-4* mutant at earlier time points. *PDF1.2* transcripts were detected as early as 8 hpi in both genotypes (Figure 1). At this time most *P. pachyrhizi* uredospores had germinated, formed an appressorium, and penetrated the epidermal cell under the conditions applied (not shown). *PDF1.2* was strongly induced by 12 hpi in both the wild type and *pen3-4* mutant with stronger induction in *pen3-4*. Enhanced *PDF1.2* activation in *pen3-4* correlated with increased proliferation of the fungus in the mutant mesophyll (Figure 20). At 24 hpi *PDF1.2* transcripts further accumulated in both genotypes, but less in the mutant. This was accompanied by strong induction of *PR-1* expression in *pen3-4*. In the wild type, *PR-1* transcript accumulation was not detected at any time assayed (Figure 1).

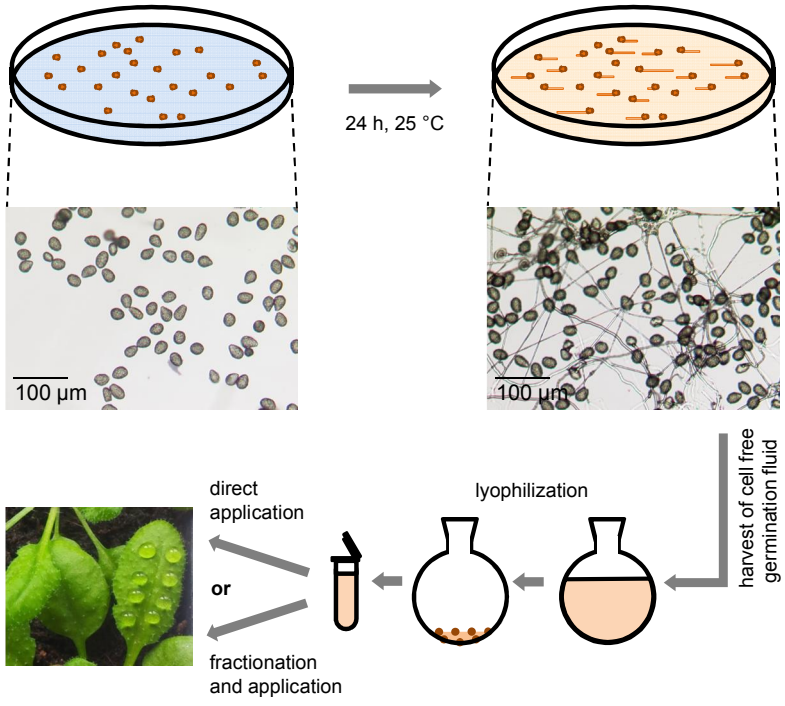

Figure 2. Preparation of germination fluid. *P. pachyrhizi* uredospores were spread on ddH_2O water supplied with 50 µg/ml ampicillin and 25 µg/ml streptavidin and incubated for 24 h at 25 °C. Formation of germ tubes and browning of germination fluid were clearly visible. The germination fluid was harvested, filtered and freeze dried before resuspension in a smaller volume of water and either directly applied or fractionated before its application to Arabidopsis leaves. Modified from Campe et al. (2014).

3.1.2 Application of germination fluid of *P. pachyrhizi* on Arabidopsis leaves leads to *PDF1.2* activation

To determine whether the induction of *PDF1.2* by *P. pachyrhizi* would depend on the presence of the fungus and/or the process of epidermal cell penetration, or whether it was rather triggered by one or more soluble fungal elicitors, a cell-free germination fluid of *P. pachyrhizi* uredospores was prepared. For this, spores were dispersed and incubated on a water surface leading to development of long germ tubes and presumably also to germination-induced secretion of fungal compounds into the aqueous phase, which was subsequently collected as outlined in Figure 2.

Drops of germination fluid were applied on leaves of Arabidopsis wild-type plants. Eight hours later *PDF1.2* expression was detected to be notably induced (Figure 3A). The level of *PDF1.2* transcript abundance at this time was similar to the one seen in plants upon treatment with spores (Figure 1). Application of germination fluid to leaves of *PDF1.2::GUS* transgenic plants resulted in a clear blue staining of leaf tissue at eight hours after treatment (Figure 3B). These findings revealed that the activation of the *PDF1.2* marker gene for defense against necrotrophs neither required the presence of fungus nor fungal penetration or death of the attacked epidermal cell. Rather, *PDF1.2* accumulation was likely induced by one or more compounds secreted during spore germination. These results support the hypothesis that *P. pachyrhizi* mimics a necrotroph to actively circumvent the plant's defense against biotrophs.

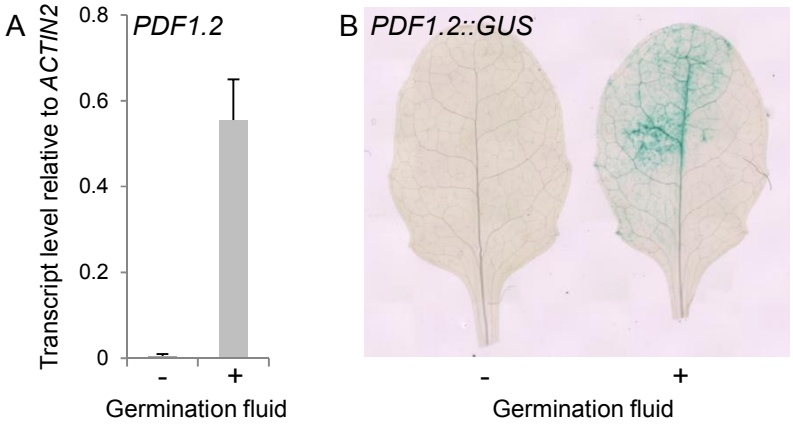

Figure 3. *P. pachyrhizi* germination fluid activates *PDF1.2* expression. Leaves of three-to-four week-old wild-type (A) and *PDF1.2::GUS* transgenic plants (B) were treated with control solution (-) or germination fluid (+) and harvested at eight hours after treatment. A. Total RNA was extracted from individual leaves of three plants. Transcript abundance was analyzed by RT-qPCR with *ACTIN2* as the standard. Values represent means ± SD of three independent experiments. B. *PDF1.2::GUS* leaves were incubated overnight in GUS staining solution and subsequently destained for five days with chloral hydrate. GUS staining was documented by brightfield microscopy using the Keyence BZ-9000 E microscope. The experiment shown in Figure 3B was performed once.

3.1.3 Expression of additional defense-related marker genes

Next, I tested whether transcript accumulation induced by germination fluid was exclusive for *PDF1.2* or whether it comprised additional genes of the JA/ET-dependent defense pathway, which is supposed to regulate plant defenses against necrotroph attackers (Glazebrook, 2005). To address this question, expression of *ORA59* and *PR-4* was measured in Arabidopsis wild-type plants eight hours upon inoculation with *P. pachyrhizi* spores or treatment with germination fluid. *ORA59* is known to be rapidly induced by JA treatment in young Arabidopsis seedlings and identified as a crucial regulator of several defense-related genes, including *PDF1.2* (Pré et al., 2008; Van der Does et al., 2013). Also *PR-3* and *PR-4* are known to be induced in a JA-dependent manner (Thomma et al., 1998).

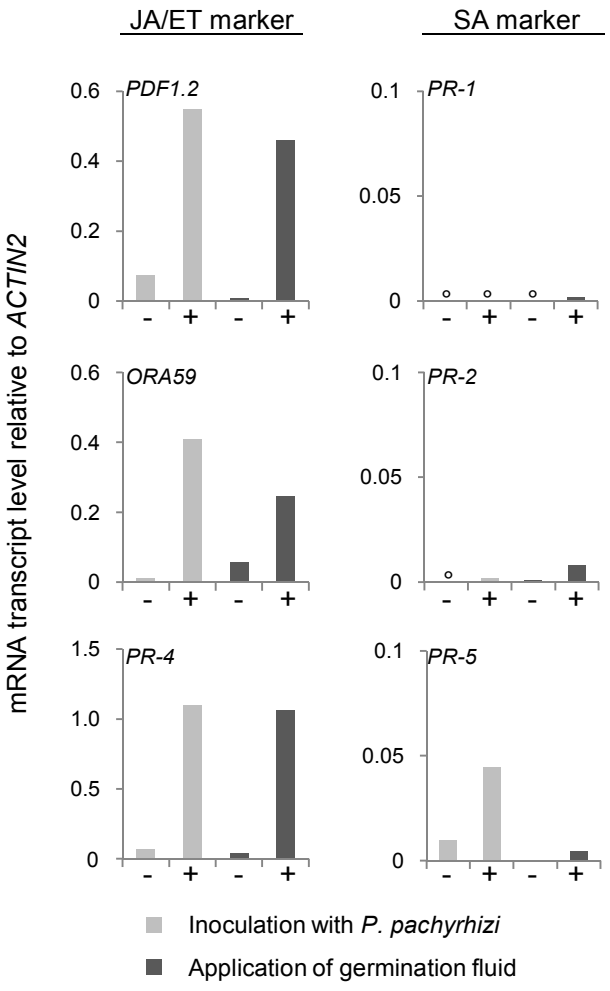

Figure 4. Activation of JA/ET and SA marker genes in Arabidopsis wild-type plants after inoculation with *P. pachyrhizi* or application of germination fluid. Leaves of four-to-five week-old Arabidopsis plants were inoculated with uredospores (+), treated with germination fluid (+) or control solution (-) and harvested eight hours after the treatment. Total RNA was extracted from a pool of three individual leaves of three plants. Transcript abundance was analyzed by RT-qPCR. *ACTIN2* was used for normalization. Values represent results of one representative experiment. For each gene, three independent experiments were performed with similar results. ° not detected

Expression of both *ORA59* and *PR-4* was notably induced in Arabidopsis leaves 8 hpi with *P. pachyrhizi* uredospores or application of germination fluid when compared to mock-treated plants (Figure 4). In addition, *PR-3* and *ANAC055*, the latter encoding for a NAC transcription factor that supposedly regulates JA-induced expression of defense genes (Bu et al., 2008), showed enhanced transcript accumulation upon both treatments (data not shown). Consequently, gene expression induced by *P. pachyrhizi* germination fluid was not exclusive for *PDF1.2* but rather comprised other JA-responsive genes as well. In contrast to the above mentioned JA-responsive genes, *PR-1*, *PR-2* and *PR-5* require SA signaling for activation (Thomma et al., 1998) and are believed to be important for the defense against biotrophic pathogens. Upon treatment with *P. pachyrhizi* spores or germination fluid these genes showed no or only marginal induction in Arabidopsis wild type leaves (Figure 4), indicating that SA-mediated defense either was not induced or even suppressed at early stages of *P. pachyrhizi* infection.

3.1.4 The *PDF1.2*-activating compound is likely to be of proteinaceous nature

To determine the biochemical nature of the *PDF1.2*-inducing compound, differentially treated fractions of germination fluid were applied to leaves of Arabidopsis wild-type plants. Autoclaved or trypsinized germination fluid had lost its capacity to induce *PDF1.2* expression (Figure 5). Trypsin is a serine protease that cleaves peptide chains mainly at the carboxyl site of lysine and arginine. These findings indicated that the *PDF1.2*-inducing compound was a peptide, protein, or protein-containing compound such as a glyco- or lipoprotein. Consistent with this conclusion, the SLS/TCA-precipitated protein fraction exhibited *PDF1.2*-eliciting capacity, whereas a precipitated and subsequently trypsinized protein fraction did not activate *PDF1.2* (Figure 5). Furthermore, upon plant treatment with the differentially treated fractions of germination fluid *PR-4* and *ORA59* exhibited the same expression pattern as *PDF1.2* (Figure 5). Taken together, the *PDF1.2*-eliciting compound was presumably a protein or peptide and possibly an actively secreted elicitor of *P. pachyrhizi*.

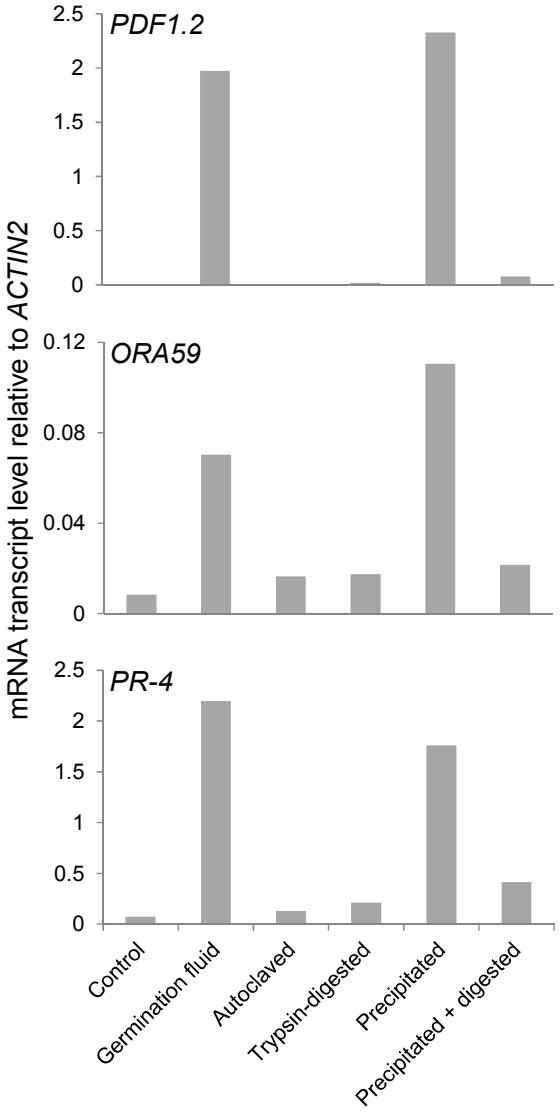

Figure 5. Transcript accumulation of JA marker genes in Arabidopsis leaves after treatment with different fractions of germination fluid. Leaves of three-to-four week-old wild-type plants were treated with control solution or untreated, autoclaved, or trypsinized germination fluid, or the untreated or digested protein precipitate. Total RNA was extracted from individual leaves of three plants, harvested, and pooled at eight hours after treatment. mRNA transcript abundance was analyzed by RT-qPCR with *ACTIN2* expression normalizing all data. Values represent the results of one representative experiment. Three independent experiments were performed with similar results.

3.2 The interactome of the ABC transporter PEN3

ABC transporter PEN3 was found to be important for Arabidopsis NHR against various pathogens (Lipka et al., 2005; Stein et al., 2006). However, only little is known about PEN3's molecular function(s) that contribute to the establishment of NHR. To address this issue I performed a protein-protein interaction screen to find PEN3-binding partners involved in NHR. In the last decade high density protein microarrays (PMAs) have evolved as powerful tools for studying thousands of proteins simultaneously (Popescu et al., 2007b). Therefore, an *in vitro* protein binding approach using Arabidopsis PMAs was chosen for the PEN3 interactome study.

3.2.1 PEN3 architecture

PEN3 belongs to the superfamily of full-size ABC transporters with two modules each consisting of a cytosolically orientated ATP-binding domain and a membrane spanning region (van den Brûle and Smart, 2002). Its large size and subcellular localization as an integral membrane protein made PEN3 not suitable for heterologous expression and subsequent protein-protein interaction studies. Other protein-protein interaction studies have succeeded using truncated versions of integral membrane proteins, e.g. the intracellular domain of FLS2 for co-immunoprecipitation experiments (Sun et al., 2012). To identify suitable domains for expression, an *in silico* analysis of PEN3 was done. For the prediction of PEN3's transmembrane domains the TMPred and MEMSAT databases were used. Twelve to 13 membrane-spanning helices were predicted and it remained unclear whether the C-terminus is located to the cytosol or apoplast. The PEN3 sequence was further subjected to the Pfam, Prosite and SMART online tools to identify specific domains, families and functional sites. All databases used for *in silico* analysis are given in Table 7. Figure 6 presents an overview of the PEN3 architecture and PEN3's predicted domains. The N-terminal cytoplasmic domain 1 (referred to as CyD1) was chosen for subsequent molecular biological experiments. CyD1 consists of the first 539 amino acids of PEN3 and thereby comprises approximately one third of the protein. It contains the three known phosphorylation sites (Benschop et al., 2007; Kline et al., 2010; Haruta et al., 2014) and the first ATP-binding cassette with the Walker A and B motifs.

3.2.2 Production and purification of CyD1

To produce CyD1 protein for probing the PMAs, I used transient expression in *N. benthamiana*. The first 1617 bps of the *PEN3* coding sequence were cloned into plant expression vector pYL436 for fusion to the tandem affinity purification (TAP) tag. The TAP tag consists of a 9x myc tag, a 6x His tag, a PreScission protease cleavage site and a 2x IgG-binding domain.

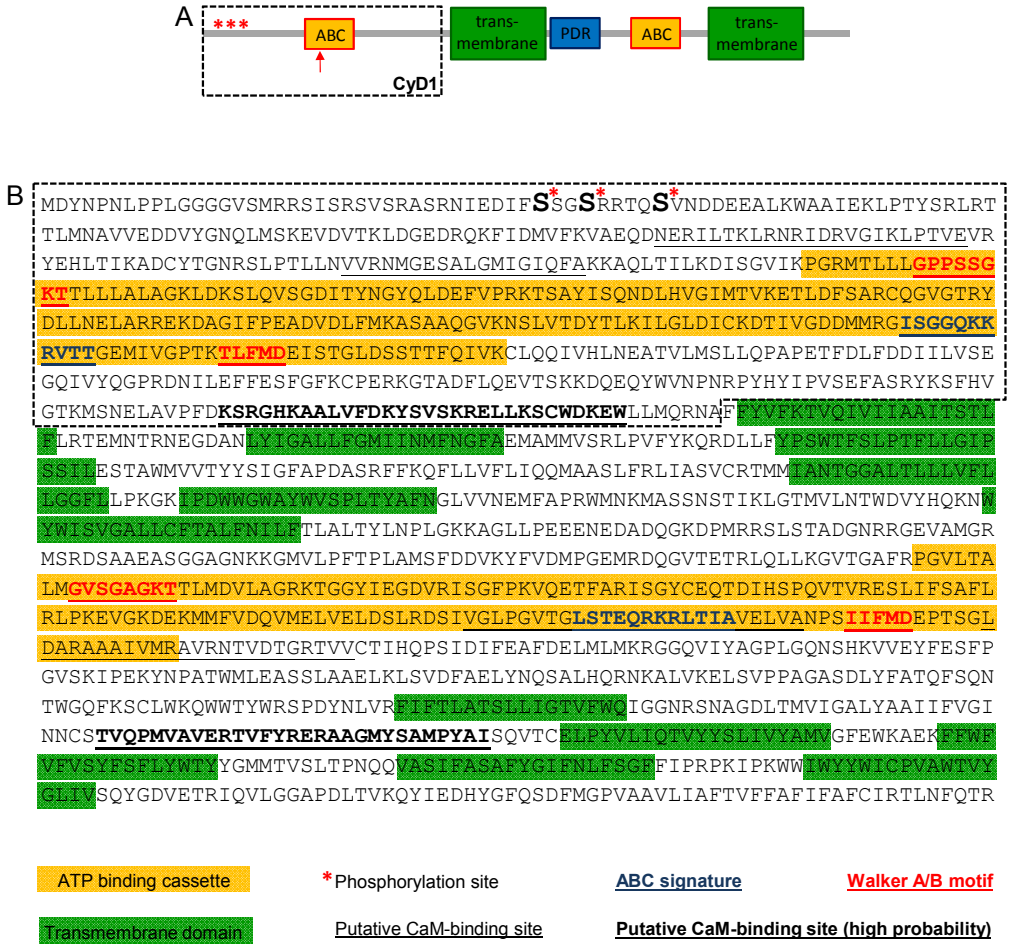

Figure 6. *In silico* analysis of ABC transporter PEN3. A. Schematic representation of the PEN3 architecture as predicted by the Pfam protein family database. Asterisks mark the known phosphorylation sites (Benschop et al., 2007), the arrow indicates the location of the epitope of the α-PEN3 antibody. ABC: ATP-binding cassette, PDR: pleiotropic drug resistance conserved domain, CyD1: cytoplasmic domain 1. B. The PEN3 protein sequence with domains and functional sites integrated from the TMpred, MEMSAT, Pfam, Prosite, SMART and Calmodulin target databases, Benschop et al. (2007) and van den Brûle & Smart (2002).

To obtain best possible protein yield, I first tested different *Agrobacterium* strains for their transformation efficiency and whether co-expression of a viral-encoded suppressor of gene silencing, the p19 protein of tomato bushy stunt virus (Voinnet et al., 2003), would enhance CyD1 expression. In plants co-expressing p19 a strong CyD1 signal was detected by western blotting and subsequent immunodetection three days after infiltration (Figure 7A). The molecular mass of CyD1 comprises approximately 60 kDa, the mass of the CyD1-TAP fusion construct approximately 95 kDa. There was hardly any signal detected for CyD1 in plants not co-expressing p19. Furthermore, there was no major difference in the transformation efficiency of the two *Agrobacterium* strains tested. For the following experiments the strain AGL-1 was used. In untransformed *N. benthamiana* plants no CyD1 signal was detected (Figure 7A).

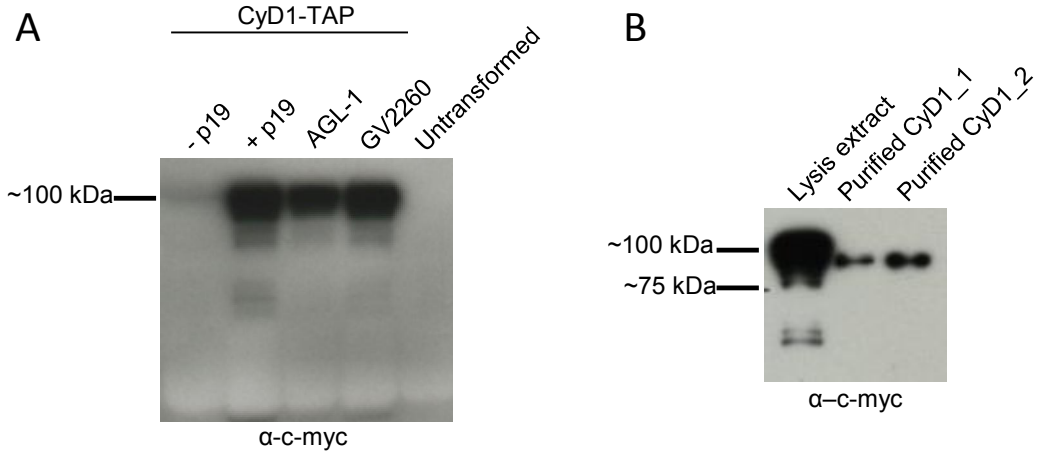

Figure 7. Production and purification of the PEN3 domain CyD1. A. Agrobacteria carrying plant expression vector pYL436-CyD1 were infiltrated into *N. benthamiana* leaves. Plant leaves were harvested three days after infiltration. Total protein was extracted and analyzed by SDS-PAGE, western blotting, and immunodetection with the α-c-myc antibody. Co-expression of the p19 protein (+p19) greatly enhanced CyD1 protein abundance, whereas it made essentially no difference for CyD1 expression to use *Agrobacterium* strains AGL-1 or GV2260. B. CyD1 was purified from *N. benthamiana* lysis extract using IgG Sepharose and released from the resin by cleavage with the PreScission protease (purified CyD1_1). The sample "purified CyD1_2" shows the purified CyD1 peptide after protease removal. Exposure time was 10 s.

Figure 7B shows the results of different steps of the CyD1 purification procedure. CyD1 was purified by affinity chromatography via the IgG-binding domain and cleaved from the IgG Sepharose using PreScission protease. The GST-tagged protease was removed from the protein solution with glutathione-agarose before further use. A large portion of the expressed protein was lost during purification (Figure 7B). Seven purifications were pooled for probing PMAs. The final purified CyD1 extract contained approximately 40 µg/ml protein.

3.2.3 The α-PEN3 antibody is suitable for use with protein microarrays

To test the suitability of the α-PEN3 antibody for CyD1 detection on the PMAs, a test array was designed and printed onto FAST® slides, containing two negative controls (glycerol and BSA), two different concentrations of the purified CyD1 peptide and the antibody itself at 1:1,000 dilution. The array was blocked, incubated with the α-PEN3 (1:8,000) and then with α-rabbit-DyLight649 (1:10,000) antibody and scanned at 650 nm. None of the negative controls delivered a signal with the α-PEN3 antibody (Figure 8). In contrast, each of the printed spots of CyD1 peptide produced a clear fluorescence signal. The signal was stronger for spots with a higher concentration of CyD1, indicating that the fluorescence intensity at least in a certain range was proportional to protein abundance. Only a weak signal was detected for the printed α-PEN3 antibody. However, the antibody might be less exposed to the secondary antibody when printed onto the slides. Taken together, these results clearly confirmed the suitability of the α-PEN3 antibody for use with PMAs.

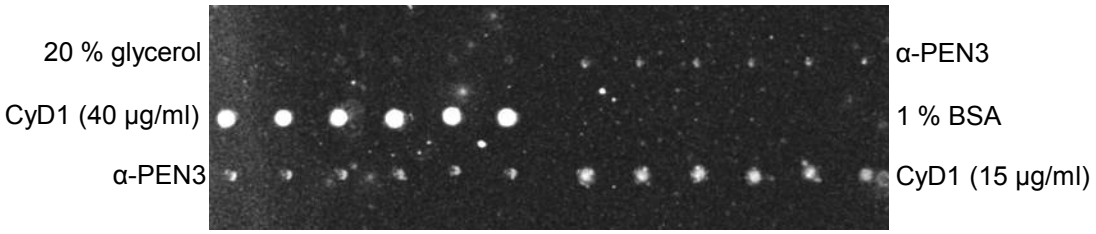

Figure 8. Test array for the α-PEN3 antibody. Two negative controls (20 % glycerol and 1 % BSA), two positive controls (the α-PEN3 antibody diluted 1:1,000) and two concentrations of purified CyD1 (15 µg/ml and 40 µg/ml) were printed onto FAST® slides using a quill-pin contact microarray printer, Micro Grid Pro (BioRobotics). The array was blocked in 1 % BSA in TBS-T, incubated with the α-PEN3 antibody (1:8,000) and subsequently the α-rabbit-DyLight649 (1:10,000) and scanned in a ScanArray Express scanner at a wavelength of 650 nm. CyD1 was detected by α-PEN3 in a concentration-dependent manner whereas no signal was observed for the negative controls.

3.2.4 Investigating the PEN3 interactome

To acquire new information on PEN3's function a screening for PEN3-protein interaction partners was conducted using Arabidopsis PMAs. Two different types of Arabidopsis PMAs were used in this study: The AtPMA-5000 (Popescu et al., 2009) also referred to as 5K PMA with an expression collection of 5,000 Arabidopsis ORFs, mainly consisting of known signaling components such as kinases and transcription factors and the ATPROTEINCHIP 2 or 10K PMA, containing an expression collection of 10,000 additional Arabidopsis ORFs. All proteins were purified using the abovementioned TAP tag and printed on the arrays in duplicated spots (Popescu et al., 2007a). The AtPMA-5000 chips were provided by Sorina Popescu, whereas the 10K PMAs were obtained from the Arabidopsis Biological Resource Center (ABRC).

First, an immunoassay was performed with a 10K PMA to assess the abundance of individual proteins on the array. An immunoassay of the 5K PMA was already available. For this, the array was first blocked in 1 % (w/v) BSA in TBS-T, incubated with a 1:10,000 dilution of α-c-myc-Cy3 antibody and scanned at 543 nm (Figure 9A). The immunoassay revealed a broad range of protein concentrations on the array. Knowledge about protein abundance of individual spots might help to assess the probability of a certain protein-protein interaction found on the array.

CyD1 was used for probing the arrays. Since both CyD1 and the target proteins on the array contained the same detection marker (myc-tag), protein-protein interactions were recorded using the specific α-PEN3 and a secondary fluorophore-labeled α-rabbit antibody. Figure 9B shows a scheme of array probing and controls. For both, the 5K and 10K PMAs three replicates for probing with CyD1 and two negative controls were performed. For all replicates the same batch of purified CyD1 was used.

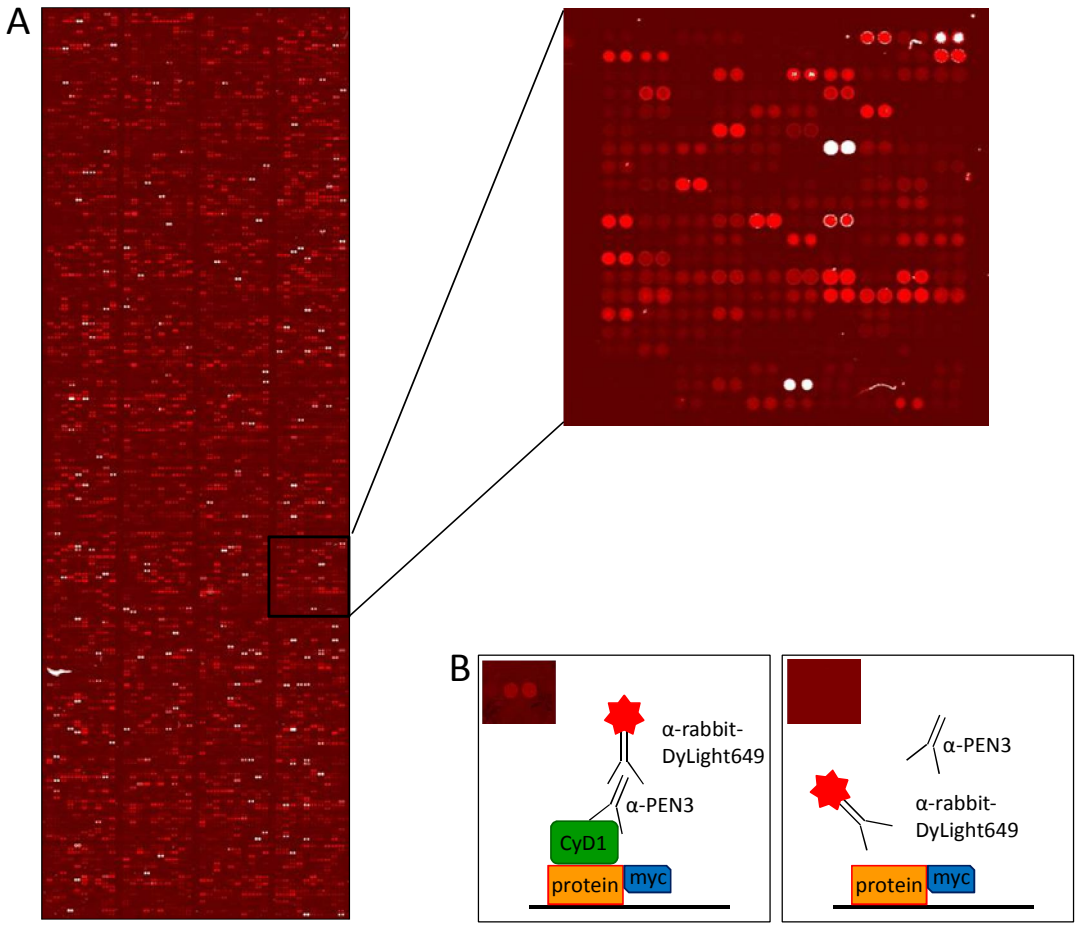

Figure 9. Arabidopsis Protein Microarrays. A. Immunoassay of a 10K PMA. Protein abundance was detected using a fluorophore-labeled α-c-myc-Cy3 antibody and scanning at 543 nm in a ScanArray Express scanner. B. Schematic representation of the PMA probing and negative controls. If CyD1 binds to a target protein the interaction is subsequently detected by the α-PEN3 and α-rabbit-DyLight649 antibodies. This leads to a prominent signal when compared to the negative control, where no antibody binding occurred.

The resulting PMA scan images then were aligned to the respective protein grid, containing information about the position and identity of every single protein spot. Alignment of the grid is an essential step of array analysis, since the signal of badly aligned spots will be mixed with the background signal, leading to a loss of signal intensity and thereby loss of identifying positive interactions. Therefore, every spot was controlled to adopt the position and size of the corresponding grid using the GenePix Pro 6.0 software. Subsequently, data were analyzed by normalizing all microarrays (probes and controls) using a linear regression model, resulting in pValues. Further, a false discovery rate was applied resulting in qValues, which served to select candidates.

After normalization and statistical testing the 5K PMAs revealed 175 putative PEN3-interacting proteins with a qValue < 0.05. These proteins are listed in Table A1. In contrast, due to high unspecific binding of the α-PEN3 antibody to the negative controls, the statistical testing

of the 10K PMAs did not indicate any target with a qValue < 0.05. However, there were many targets with pValue < 0.05. These were not included in the putative candidate list; this work rather focuses on the results from the 5K PMAs.

To filter out those proteins, whose interaction with PEN3 might have a physiological impact on NHR, the 175 putative PEN3-interacting proteins were further processed regarding their gene ontologies. First, all transcription factors were removed, since they were presumably localized in the nucleus and not very likely to interact with PEN3. In a second step, using the AmiGO gene ontology database proteins involved in the cellular response to stimulus (GO:0051716) were selected providing a list of 28 candidate proteins (Table 8). These 28 putative targets were further analyzed by retrieving detailed gene ontologies from The Arabidopsis Information Resource (TAIR). This detailed list is given in Table A2. Strikingly, nine of the 28 proteins were Ca^{2+} sensors, including Calmodulin (CaM) 3 and CaM7 and several Calmodulin-like (CML) proteins. CaM is the major Ca^{2+} sensor in all eukaryotic cells and known to be involved in the regulation of diverse cellular functions including pathogen defense (Trewavas and Malhó, 1998; Kim et al., 2002a). Furthermore, the putative PEN3-interacting proteins include CML9 that was recently shown to be involved in innate immunity (Leba et al., 2012), CML38 which was annotated to respond to fungi, chitin and defense-related hormones, PUB23 which was demonstrated to be a negative regulator of PTI (Trujillo et al., 2008), and phospholipase SOBER1 that is important for the regulation of the HR (Kirik and Mudgett, 2009). Among others these all are interesting candidates that might determine or at least influence PEN3's molecular function. This work, however, focuses on the group of Ca^{2+}-binding proteins.

3.2.5 Ca^{2+} sensors in the PEN3 interactome

Ca^{2+} fluxes are among the plant cell's first responses upon an extracellular stimulus (Vadassery and Oelmüller, 2009). Several Ca^{2+} sensors were identified as putative PEN3-interacting proteins, suggesting a role for PEN3 in early Ca^{2+} signaling. Using the BAR Arabidopsis interactome viewer (Geisler-Lee et al., 2007) that among others contains previous results from Arabidopsis PMA experiments a network was built to understand the connections of PEN3 to further targets of its Ca^{2+}-binding interaction partners. The PEN3-Ca^{2+} signaling network was organized and visualized using Cytoscape (Figure 10) and displays PEN3, its nine Ca^{2+}-binding targets and their so far known interaction partners. The size of the node is proportional to the proteins' connectivity. The major hub in the network is CaM7, which has 195 interaction partners. Also CAL4/TCH3, CML8, and CML9 are highly interactive proteins. Within the network, CaM6, HSP90, and MPK4 and 6 are outstanding connected proteins. Interestingly, the latter three have been reported to be involved in plant immune responses (Kanzaki et al., 2003; Takahashi et al., 2003;

Hubert et al., 2003; Petersen et al., 2000; Gao et al., 2008; Menke et al., 2004; Beckers et al., 2009).

HSP90 is connected to PEN3 through CaM7, MPK4 through CaM3, and MPK6 through CML38. To get a better understanding of the Ca^{2+}-mediated signaling network connected to PEN3, all members of the network were compared to expression datasets related to PEN3's function. Humphry et al., (2010) presented a conserved regulon, which contained PEN3 and was functional in antifungal plant defense. According to their data, six genes of the PEN3-Ca^{2+} signaling network were co-regulated with PEN3, including its direct interactors CAL4/TCH3 and AT2G46600. Furthermore, 14 genes of the PEN3-Ca^{2+} signaling network were shown to be induced upon infection with *P. pachyrhizi* (C. Langenbach, unpublished data). Those included genes encoding CML37, CML38 and CPK10, a calcium-dependent protein kinase shown to phosphorylate a PEN3 peptide *in vitro* (Curran et al., 2011). CPK10 was connected to PEN3 through CML9. All members of the PEN3-Ca^{2+} signaling network and the expression analysis are given in Table A3.

Table 8. Putative PEN3-binding proteins with GO involved in cellular response to stimulus

Locus	Description	Response to stimulus	Ca^{2+} sensor	Kinase activity
AT3G56800	Calmodulin 3	x	x	
AT3G43810	Calmodulin 7	x	x	
AT2G41100	Calmodulin-like 4, ATCAL4, TCH3	x	x	
AT4G14640	Calmodulin-like 8	x	x	
AT3G51920	Calmodulin-like 9	x	x	
AT5G42380	Calmodulin-like 37	x	x	
AT1G76650	Calmodulin-like 38	x	x	
AT5G24270	Calcineurin B-like protein SOS3/CBL4	x	x	
AT2G46600	Calcium-binding EF-hand family protein	x	x	
AT2G18170	MPK7	x		x
AT3G59790	MPK10	x		x
AT5G19010	MPK16	x		x
AT5G67080	MAPKKK19	x		x
AT5G58350	WNK family of protein kinases (WNK4)	x		x
AT1G75460	ATP-dependent protease La (LON) domain protein	x		
AT2G24540	ATTENUATED FAR-RED RESPONSE (AFR)	x		
AT4G24210	F-Box protein SLY1	x		
AT1G80440	Kelch repeat F-Box 20 (KMD1)	x		
AT3G59940	Kelch repeat F-Box 50 (KMD4)	x		
AT5G47420	Tryptophan RNA-binding attenuator protein-like	x		
AT2G35930	PLANT U-BOX 23 (PUB23)	x		
AT5G58700	Phosphatidylinositol-specific phospholipase C4 (PLC4)	x		
AT3G57290	EUKARYOTIC TRANSLATION INITIATION FACTOR 3E (EIF3E)	x		
AT2G25490	EIN3-BINDING F BOX PROTEIN 1 (EBF1)	x		
AT4G03190	F box protein belonging to the TIR1 subfamily (GRH1)	x		
AT5G21040	F-Box protein 2 (FBX2)	x		
AT4G04800	Methionine sulfoxide reductase B3 (MSRB3)	x		
AT4G22300	SUPPRESSOR OF AVRBST-ELICITED RESISTANCE 1 (SOBER1)	x		
Total	28			

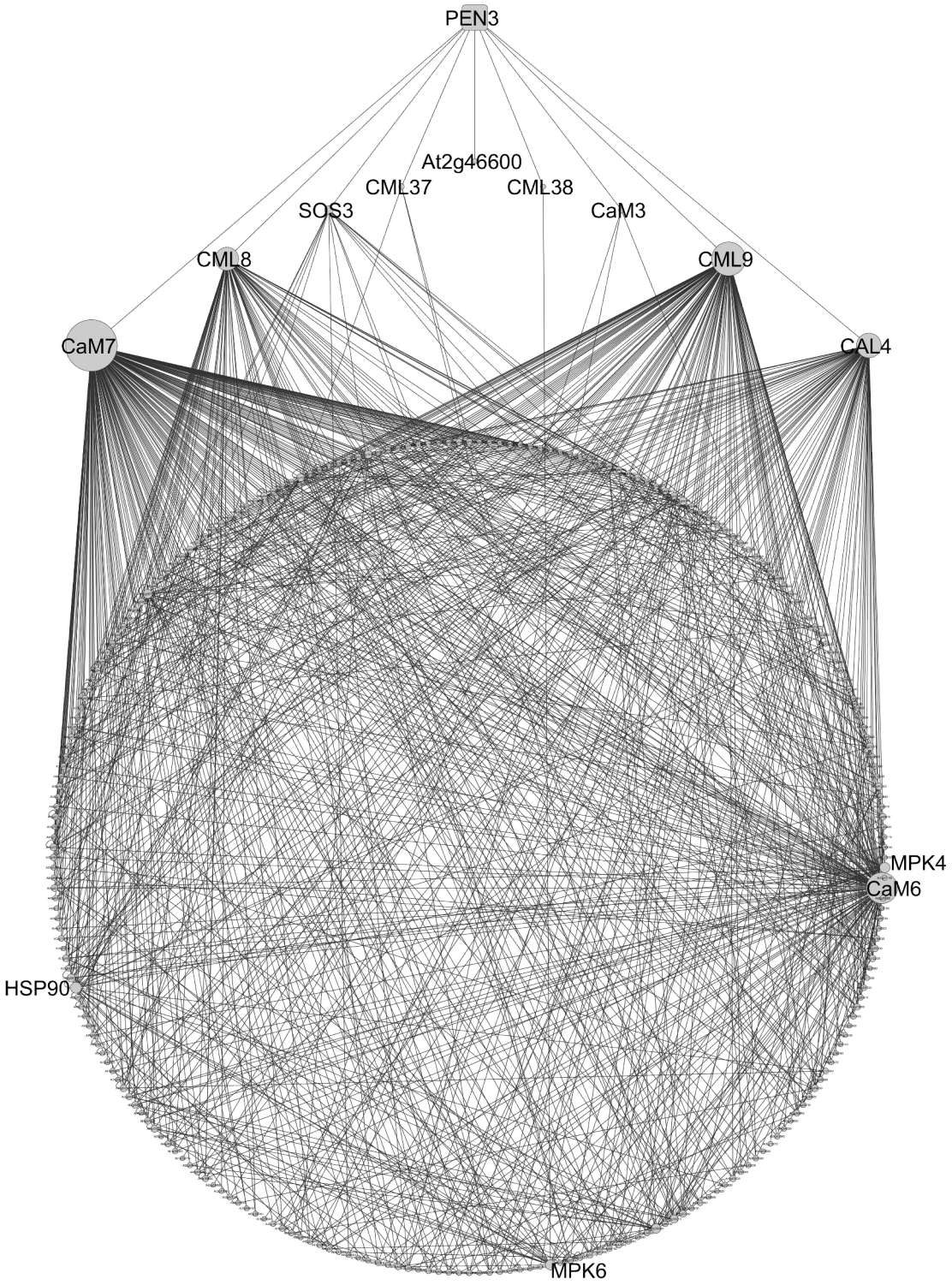

Figure 10. The PEN3-Ca^{2+} signaling network. The network shows PEN3, nine of its putative Ca^{2+}-binding target proteins and their so-far known 256 interaction partners retrieved from the BAR Arabidopsis interactome viewer represented as nodes. The size of the node is proportional to the proteins degree of connectivity. The network was designed using Cytoscape 3.0.2.

3.2.6 PEN3 interacts with CaM *in vitro*

3.2.6.1 CaM overlay assay

To confirm the interaction of PEN3 with CaM, a CaM overlay assay was performed. Both, the isoforms CaM3 and CaM7 interacted with CyD1 on the PMA. The analysis was done with CaM7 since this Ca^{2+} sensor is, like PEN3, associated with the plasma membrane (Alexandersson et al., 2004) and known to be SA-responsive (Cheng et al., 2009) and, thus, likely involved in the defense against biotrophic pathogens such as *P. pachyrhizi*.

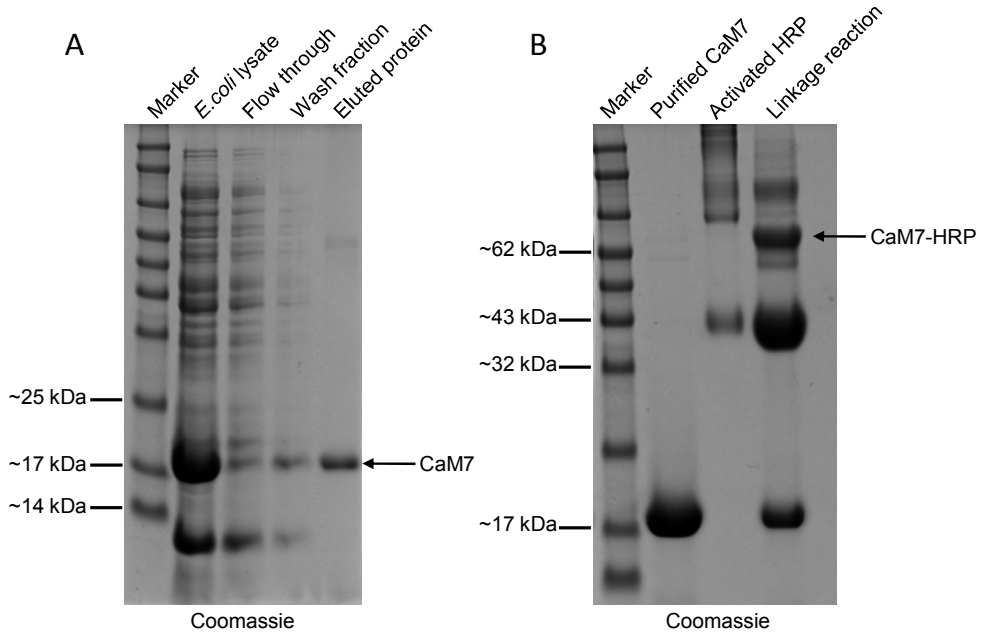

Figure 11. Synthesis of HRP-linked CaM7. A. Expression and purification of CaM7 from *E. coli*. CaM7 was cloned into the bacterial expression vector pETλHIS and transformed into *E. coli* BL21 cells. Expression was induced by addition of IPTG. CaM7 was purified via the His-tag using a Ni-NTA column. B. The purified CaM7 was coupled to maleimide-activated HRP (Pierce). Molecular masses according to Nippon Genetics.

Both CaM7 and CyD1 were cloned from Arabidopsis cDNA into the bacterial expression vector pETλHIS for C-terminal fusion with a 6 x His-tag and transformed into the *E. coli* expression strain BL21. CaM7 expression caused appearance of a prominent 19 kDa band in the bacterial lysate (Figure 11A). CaM7 was purified under native conditions via the His-tag using a Ni-NTA column, resulting in a discrete CaM7 band in the eluted fraction. CaM7 purity was determined to be > 95 % using the BioRad Image Lab software. The purified CaM7 was then reduced using the strong reducing agent TCEP for the linkage to maleimide-activated HRP. Maleimide is used for the conjugation to sulfhydryl groups, such as reduced cysteines. CaM contains one cysteine and can thus be covalently linked to one maleimide-activated HRP molecule. The activated HRP has an apparent molecular mass of 44 kDa (Figure 11B). SDS-PAGE and Coomassie staining revealed

that the purchased HRP solution was impure, leading to several additional products in the linkage reaction. Nevertheless, CaM7 could be coupled to HRP, resulting in a protein band of approximately 63 kDa.

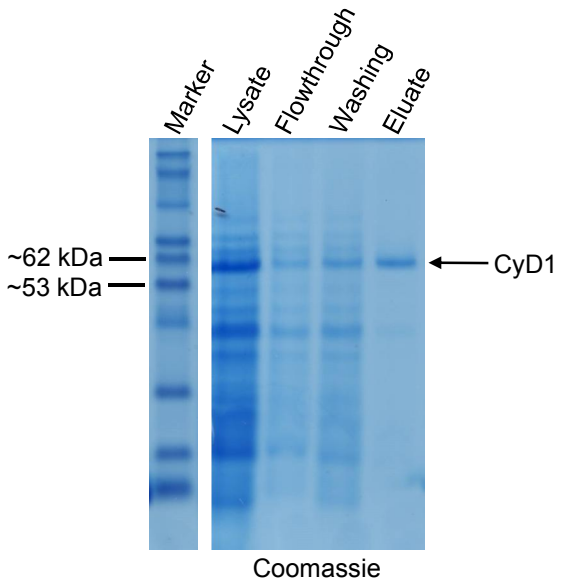

Figure 12. Production and purification of CyD1 in *E. coli*. CyD1 was cloned into bacterial expression vector pETλHIS and transformed into *E. coli* BL21 cells. Expression was induced by adding IPTG. CyD1 was purified under denaturing conditions via the His-tag using a Ni-NTA column. Molecular masses according to Nippon Genetics.

Upon expression in *E. coli* BL21 CyD1 could not be purified under native conditions, probably due to its size and formation of inclusion bodies. Thus, a denaturing protocol was applied leading to a discrete CyD1 band in the eluted fractions (Figure 12).

For the overlay assay, CyD1 was subjected four times to a same SDS-PAGE. To prove that the signal detected by CaM7-HRP is truly CyD1, protein was stained with Coomassie blue and detected on a membrane after western blotting analysis using an α-His antibody (Figure 13). The overlay assay was performed in the presence of 1 mM $CaCl_2$ or 5 mM EGTA during the entire experiment. CyD1 was detected by CaM7-HRP in the presence of $CaCl_2$ but not in the presence of EGTA (Figure 13). This experiment provided first proof that the truncated PEN3 domain CyD1 interacts with CaM and that this interaction might be Ca^{2+}-dependent.

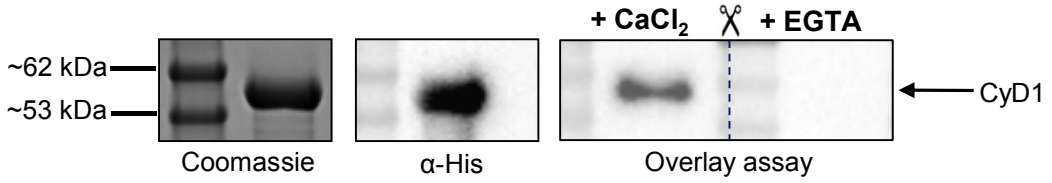

Figure 13. CaM overlay assay with CyD1. The truncated PEN3 version CyD1(-6x His) was expressed in *E. coli*, purified by affinity chromatography using Ni-NTA and subjected to SDS-PAGE, western blotting with an α-His antibody for immunodetection and a CaM overlay assay using CaM7-HRP in presence of 1 mM $CaCl_2$ or 5 mM EGTA. Exposure time: 10 s (α-His antibody) and 60 s (overlay assay).

3.2.6.2 Pull-down of PEN3 from Arabidopsis microsomes using CaM Sepharose

Next, I investigated whether full-length PEN3 also interacts with CaM using a pull-down approach with CaM Sepharose. In a protein lysate prepared from Arabidopsis leaves PEN3 could hardly be detected (Figure 14A). Therefore, a microsomal fraction from Arabidopsis leaves was prepared and solubilized using 0.05 % (final concentration) S-DOC, leading to the enrichment of PEN3 and a strong signal of approximately 160 kDa in the wild type which was absent in the *pen3-4* mutant (Figure 14A). The solubilized microsomes were used for the pull-down of PEN3 using CaM Sepharose. Without adding any further reagents PEN3 was precipitated by CaM (Figure 14B). Yet, the binding was strongly enhanced by adding $CaCl_2$ to the reaction. In contrast, addition of EDTA or EGTA diminished PEN3 binding to CaM. Supplying both, $CaCl_2$ and EDTA reduced the amount of precipitated PEN3 when compared to the non-treated sample with a stronger effect when double the amount of EDTA was added. No PEN3 was pulled-down with IgG Sepharose as a negative control (Figure 14B). Together, these results revealed that not only CyD1 but also full-length PEN3 interacts with CaM and that the presence of Ca^{2+} is not essential but beneficial to the PEN3-CaM interaction.

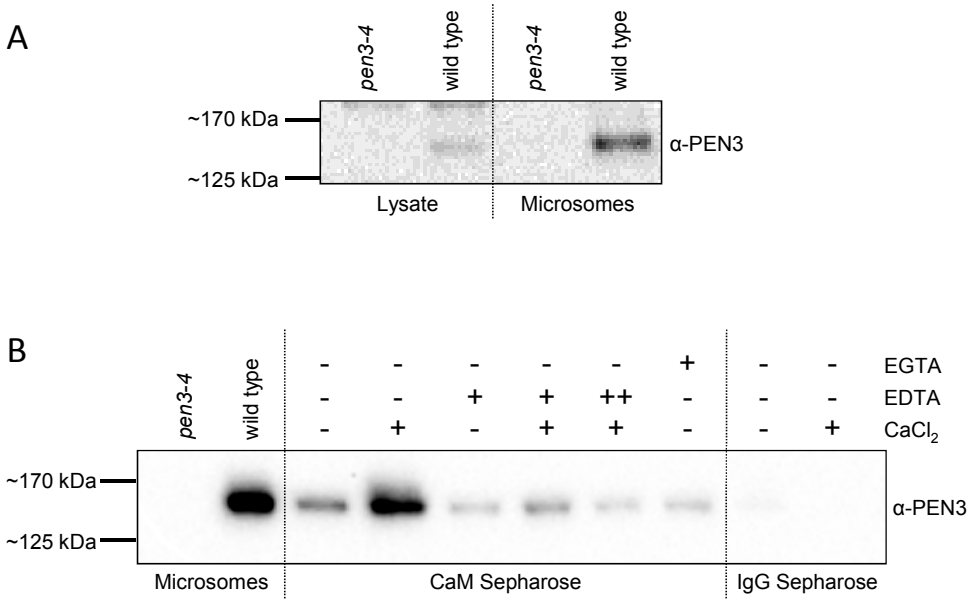

Figure 14. Pull-down of full-length PEN3 from Arabidopsis microsomes with CaM Sepharose. A. Enrichment of PEN3 by extraction of the microsomal fraction. Microsomes were extracted from leaves of Arabidopsis wild-type or *pen3-4* mutant plants via differential ultracentrifugation steps in a high-sucrose buffer and solubilized using 0.05 % (final concentration) S-DOC. Exposure time was 1 min. B. Solubilized microsomal fractions were incubated with CaM Sepharose 4B (or IgG Sepharose as negative control) and different combinations of 5 mM $CaCl_2$ and/or 7 mM EDTA/EGTA. PEN3 was detected by western blotting and immunodetection using an α-PEN3 antibody. Exposure time was 30 s.

3.2.6.3 A truncated CyD1 version binds to CaM

To identify the part of PEN3 important for CaM binding, the PEN3 protein sequence was analyzed in the Calmodulin target database. Putative CaM-binding domains (CaMBD) are annotated in Figure 6B. The PEN3 domain CyD1 contains three putative CaMBDs, two with a lower probability in the N-terminal part and one with high probability at the C-terminus of CyD1. To test whether the latter domain is crucial for CaM-binding a truncated CyD1 version without the respective domain was cloned, referred to as CyD1ΔCaMBD. The *CyD1ΔCaMBD* construct was cloned into both pET$_\lambda$HIS and pYL436 for expression in *E. coli* and *N. benthamiana*, respectively. The protein that was expressed in *N. benthamiana* was purified under native conditions via the His-tag using a Ni-NTA column and used for a pull-down using CaM Sepharose. Just like CyD1, CyD1ΔCaMBD could be pulled-down by CaM. The addition of $CaCl_2$ only slightly enhanced their interaction (Figure 15A). For the overlay assay CyD1ΔCaMBD was expressed in *E. coli* and purified under denaturing conditions. In presence of $CaCl_2$ CyD1ΔCaMBD was detected by CaM7-HRP, just as demonstrated before for the entire CyD1. CaM-binding to both CyD1 and CyD1ΔCaMBD was diminished when adding EGTA (Figure 15B). Both results disclose that this CaMBD was not crucial for the PEN3-CaM interaction. The other CaMBDs, predicted with a lower

probability, might be important for the interaction. This possibility needs to be tested in future experiments.

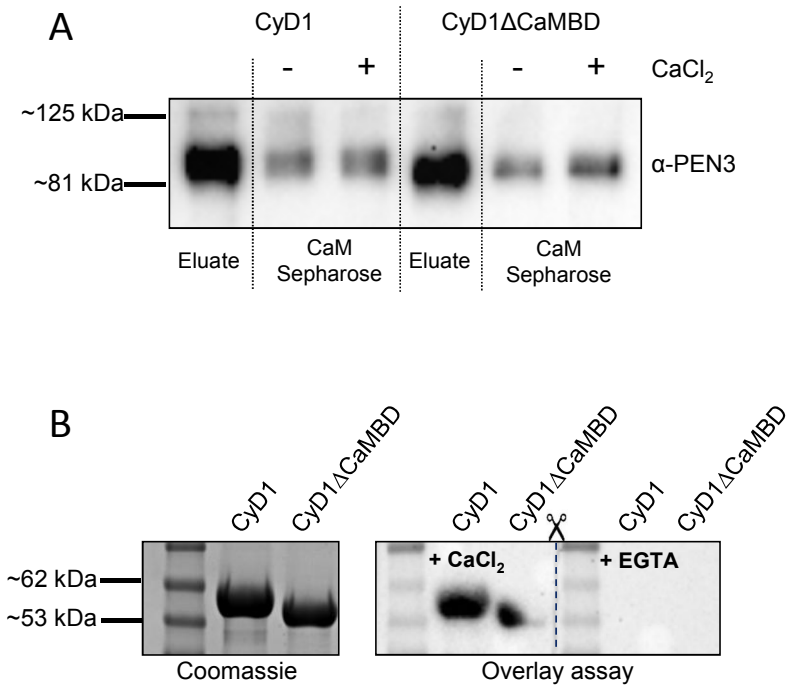

Figure 15. CyD1ΔCaMBD binds to CaM. A. Pull-down of CyD1 and CyD1ΔCaMBD with CaM Sepharose 4B (GE). CyD1 and CyD1ΔCaMBD were expressed in *E. coli* strain BL21 and purified under native conditions via the His-tag using Ni-NTA. Eluates were incubated with CaM Sepharose in the presence or absence of 5 mM $CaCl_2$. The Sepharose was loaded onto an SDS-PAGE and precipitated proteins detected by western blot analysis and immunodetection using the α-PEN3 antibody. Exposure time was 6 min. B. CaM overlay assay with CyD1 and CyD1ΔCaMBD. Both peptides were expressed in *E. coli* strain BL21 and purified under denaturing conditions via the His-tag using Ni-NTA and tested by SDS-PAGE and a CaM overlay assay in presence of 1 mM $CaCl_2$ or 5 mM EGTA. Exposure time was 5 min.

3.2.7 PEN3 interacts with CaM *in vivo*

After identifying PEN3-CaM complex formation *in vitro*, it was interesting to know whether the association between the two proteins would also occur *in planta*. To address this question a bi-molecular fluorescence complementation (BIFC) approach was performed.

For their interaction *in planta*, protein partners must be localized, at least transiently, to a same cellular compartment. Hence, I first determined the subcellular localization of CyD1 and CaM7 by infiltrating Agrobacteria carrying fluorescent fusion constructs of both these polypeptides into *N. benthamiana* and subsequently performing cLSM. CaM7 was fused to green fluorescent protein variant eGFP and found to localize to the cytoplasm and the nucleus (Figure 16). The CyD1 domain was also detected in the cytoplasm when fused to different versions of red fluorescent protein (RFP). Co-localization of both polypeptides became obvious upon merging the individual green and red cLSM images. The cytosol-located polypeptides appeared as a per-

fect yellow overlap, whereas the nucleus appeared green due to the absence of CyD1-RFP (Figure 16).

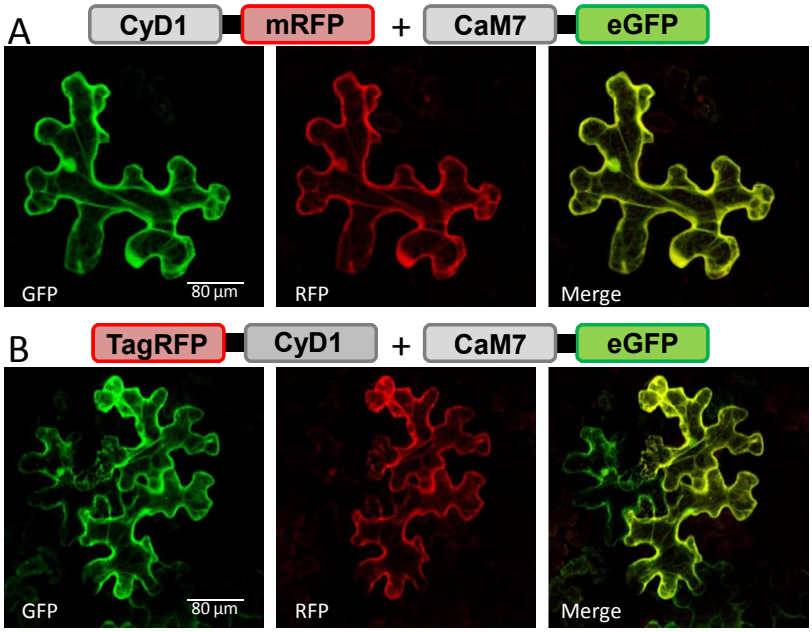

Figure 16. CyD1 and CaM7 co-localize to the cytoplasm. Agrobacteria carrying different combinations of RFP- or GFP-fusion proteins were mixed in equivalent optical densities and infiltrated into *N. benthamiana* leaves. Localization was analyzed three days after infiltration by confocal Laser Scanning Microscopy (cLSM). Invidual cLSM pictures represent the GFP and RFP signals and the merged pictures (Merge).

For the BIFC experiments CyD1 and CaM7 were cloned into Gateway-compatible vectors pDEST-^{GW}VYCE, pDEST-VYCE(R)^{GW}, pDEST-^{GW}VYNE, pDEST-VYNE(R)^{GW} for fusion to the C- or N-terminal part of the fluorophore Venus, transformed into Agrobacteria and co-infiltrated in different combinations into *N. benthamiana* leaves. All combinations of N- and C-terminally tagged Venus^{C}- or Venus^{N}-fusion constructs of CyD1 and CaM7 caused a strong fluorescence in *N. benthamiana* epidermal cells (Figure 17A and B). Co-infiltration of Venus^{C}- and Venus^{N}-CyD1 fusion constructs did not lead to any fluorescence and served as a negative control (Figure 17C). Since CaM was demonstrated to form noncovalent dimers (Lafitte et al., 1999) we used co-infiltration of Venus^{C}- and Venus^{N}-CaM7 fusion constructs as a positive control (Figure 17D). In this case fluorescence was not only detected in the cytosol but also in the nucleus, verifying dimer formation in both these compartments. Furthermore, I analyzed the PEN3 interaction with CML37, and also detected a strong BIFC signal (Figure 17E).

Protein abundance for all single fusion constructs was verified by western blotting analysis (Figure 18). In all co-infiltrations both binding partners strongly accumulated, as shown by detection of Venus^{N}- and Venus^{C}- fusions with the α-c-myc and α-HA antibody, respectively.

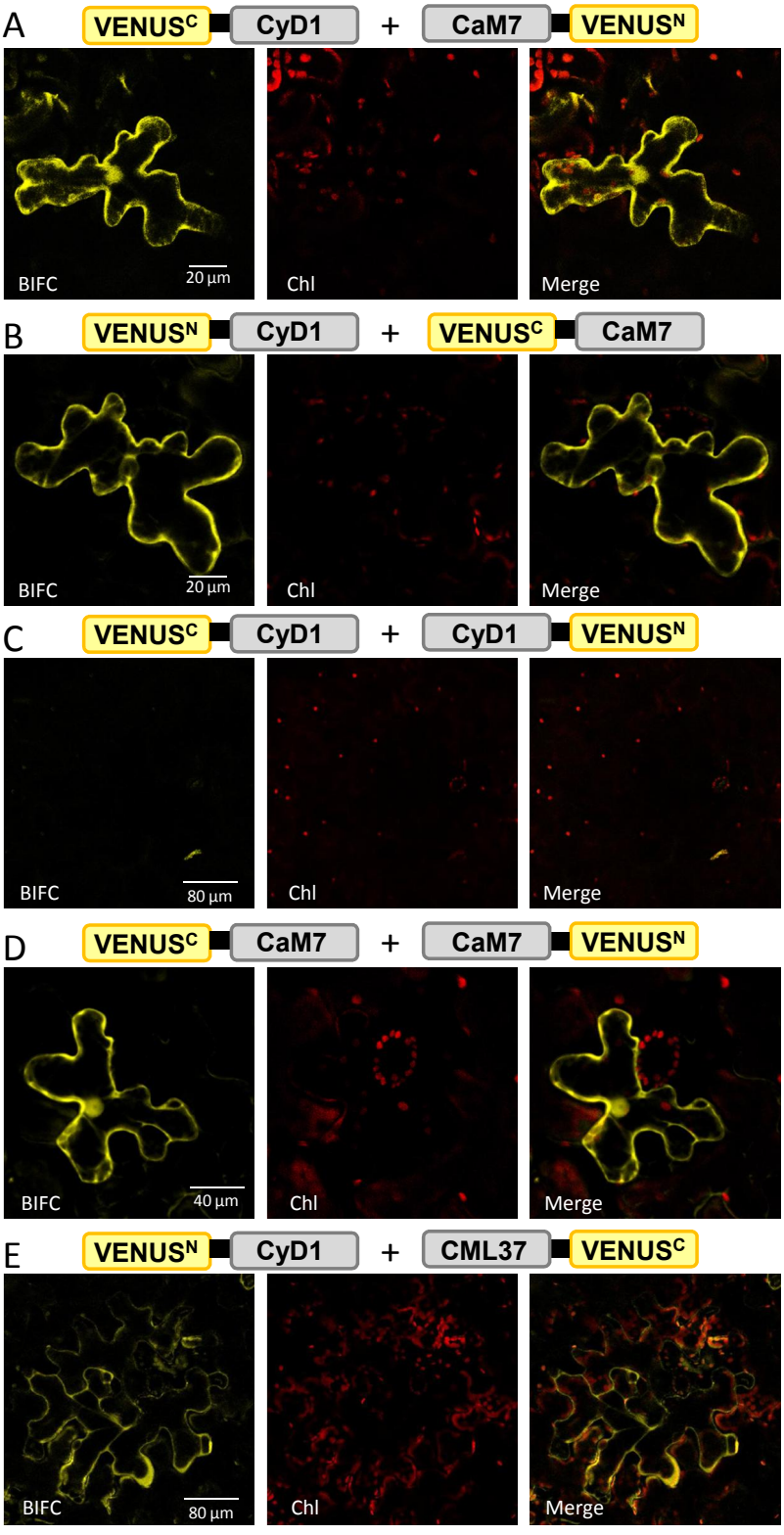

Figure 17. CyD1 interacts with CaM7 *in planta*. Bimolecular fluorescence complementation (BIFC) using the Venus fluorophore. Agrobacteria carrying different combinations of Venus^{C}- or Venus^{N}-fusion proteins were mixed in equivalent optical densities and infiltrated into *N. benthamiana* leaves. Protein-protein interactions were analyzed three days after infiltration by confocal Laser Scanning Microscopy (cLSM). The single cLSM pictures represent the BIFC signal (BIFC), the chlorophyll autofluorescence (Chl) and the merged pictures (Merge).

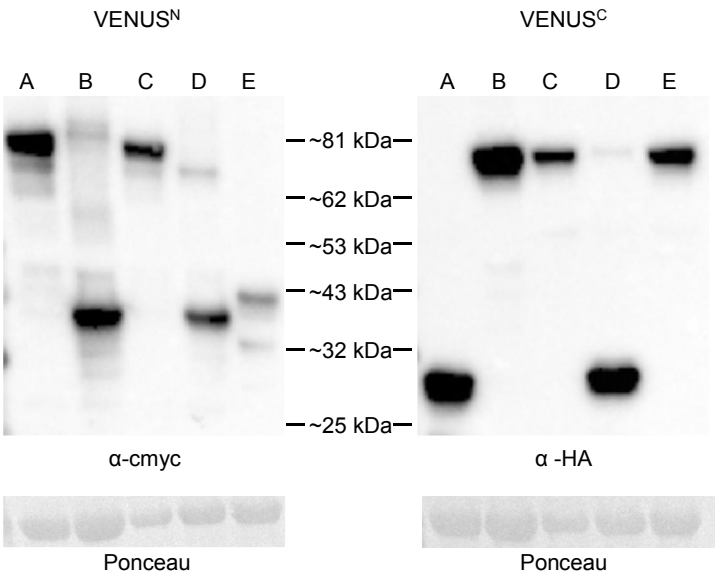

Figure 18. Protein abundance in BIFC experiments. The protein abundance of each co-infiltrated Venus^{C}- or Venus^{N}-fusion protein was verified by western blotting analysis. Venus^{N}-fusions were detected using an α-c-myc antibody, Venus^{C}-fusions by using an α-HA antibody. Letters A- E correspond to Figure 17. Chemiluminescence was detected using the Clarity Western ECL Substrate (BioRad). Exposure time: 10 s.

3.2.8 CaM7 is involved in NHR to various pathogens

3.2.8.1 The *cam7* mutant has enhanced susceptibility to *P. pachyrhizi*

To evaluate the possible impact of the PEN3-CaM interaction on NHR, I analyzed the Arabidopsis wild type, *pen3-4* and several *cam* mutants for interaction with *P. pachyrhizi*. To do so, Arabidopsis plants were inoculated with *P. pachyrhizi* uredospores, harvested at 48 hpi and stained with trypan blue which stains dead or dying cells. Interaction sites were assigned to different interaction categories to quantitatively assess the degree of resistance or susceptibility. The plant can inhibit the penetration attempt of the fungus by forming an effective papilla (Figure 19) contributing to pre-penetration resistance. In contrast, upon successful penetration by the fungus the attacked epidermal cell usually undergoes cell death as indicated by trypan blue staining of the cell. The fungus might then invade the mesophyll tissue which becomes obvious by the appearance of fungal hyphae in between mesophyll cells which in some cases is accompanied by cell death in the mesophyll (Figure 20).

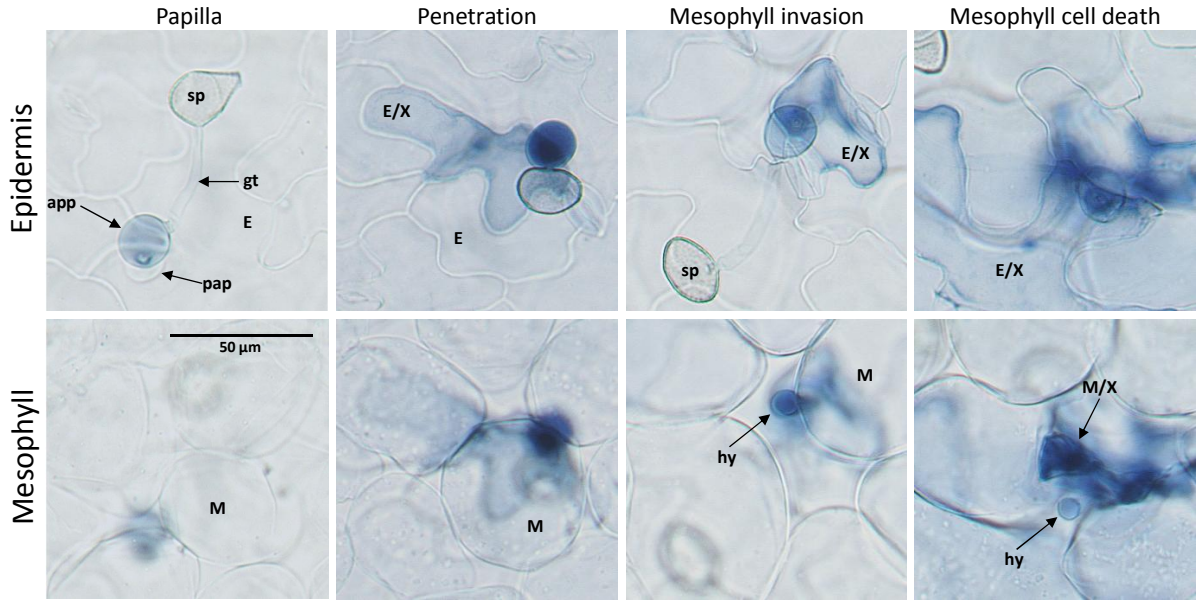

Figure 19. Interaction types in the NHR of Arabidopsis against *P. pachyrhizi*. Three-to-four week-old Arabidopsis plants were inoculated with uredospores of *P. pachyrhizi* and harvested at 48 hpi. Leaves were stained with trypan blue and subsequently destained with chloral hydrate. Destained leaves were analyzed by light microscopy using a Leica DMR microscope. Photos were taken with a digital Jvc KYF 750 camera and edited with the acquisition software DISKUS. App appressorium, E epidermal cell, E/X trypan blue stained epidermal cell, gt germ tube, hy hyphe, M mesophyll cell, M/X collapsed and trypan blue stained mesophyll cell, pap papilla, sp uredospore. Magnification 200 fold. Scale bar is representative for all photos.

Consistent with a previous report (Loehrer et al., 2008), I observed epidermal resistance with no further mesophyll invasion in about 85 % of the interaction sites in the wild type, whereas fungal hyphae were observed in ~90 % of the interaction sites in *pen3-4* (Figure 20A). Approximately 40 % of the invasion events in *pen3-4* were accompanied by death of the adjacent mesophyll cell, which was obvious by collapse and trypan blue staining. Only in very few cases (< 5 %) the penetration attempt was successfully inhibited by formation of an effective papilla.

T-DNA insertion lines of all seven Arabidopsis CaM isoforms were genotyped to assess their interaction with *P. pachyrhizi*. Only for *cam4* no homozygous plants were obtained. Of mutants *cam1*, *2*, *3*, *5*, *6*, and *7*, only *cam7* was slightly more susceptible to *P. pachyrhizi* (Figure 20B). When compared to wild-type plants *cam7* mutant showed an increase of approximately 10 % of fungal hyphae proliferation into the mesophyll (Figure 20A and B).

Furthermore, a *pen3-4 cam7* double mutant was generated and analyzed in terms of resistance to *P. pachyrhizi*. Due to the limited amount of double homozygous plants, only one biological replicate was performed so far and compared to *pen3-4* plants from several replicates. While the total frequency of mesophyll invasion with or without mesophyll cell death barely differed between different plants and replicates, the amount of interaction sites with cell death varied from 16 to 63 % between the inoculation replicates in *pen3-4*, thus causing a high standard devi-

ation (Figure 20A). When compared to the mean from all replicates, the response to *P. pachyrhizi* of double mutant *pen3-4 cam7* did not differ significantly from that of single mutant *pen3-4*. However, upon comparison of respective single experiments in which both the *pen3-4* and *pen3-4 cam7* mutants were inoculated, the double mutant exhibited twice the frequency of mesophyll cell death than the single mutant (data not shown). Therefore, these experiments need to be repeated to determine whether the additional knockout of *CaM7* truly increases mesophyll cell death frequency in the *pen3-4* genetic background.

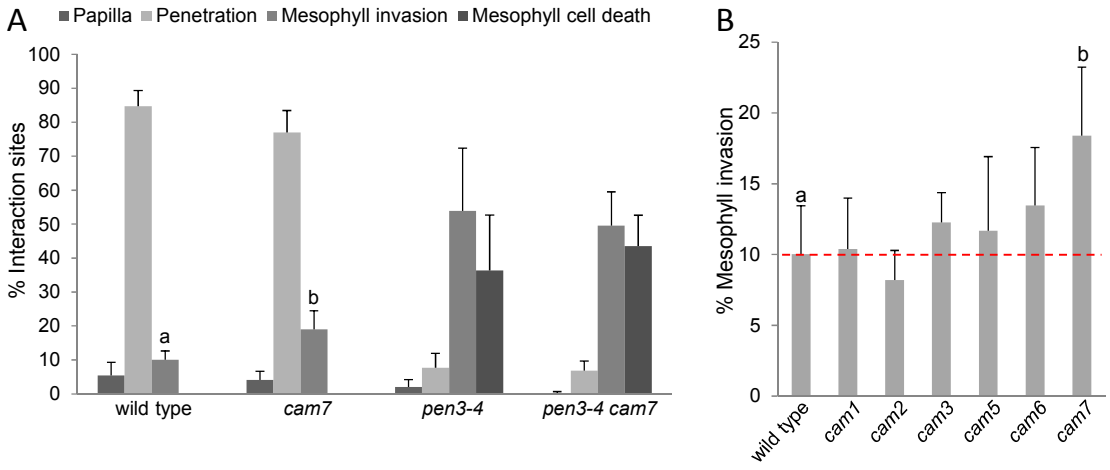

Figure 20. Interaction of *pen3-4* and *cam* mutants with *P. pachyrhizi*. A. Quantitative microscopical analysis of the interaction of wild type, *cam7*, *pen3-4* and the *pen3-4 cam7* double mutant with *P. pachyrhizi*. B. Percentage of fungal mesophyll invasion of several *cam* mutants compared to the wild type. All plants were inoculated with *P. pachyrhizi* uredospores, harvested at 48 hpi and stained with trypan blue for microscopical analysis. On each evaluated leaf 100 interaction sites were evaluated and assigned to different interaction categories. Wild type (Col-0) (B), n=36 leaves from nine biological replicates; Wild type (Col-0) (A) and *pen3-4*, n=16 leaves from four biological replicates; *cam1, cam2, cam5, cam6, cam7*, n=12 leaves from three biological replicates; *pen3-4/cam7*, n=5 leaves from one biological replicate. Letters on top of columns indicate significant differences between genotypes in terms of frequency of mesophyll invasion as determined by t-test ($p<0.001$; SigmaStat32).

3.2.8.2 *Bgh* penetrates *cam7* at a higher rate

To test whether the impaired NHR of *cam7* was exclusive for *P. pachyrhizi* or also seen with other fungal pathogens, I analyzed the interaction of *cam7* with the powdery mildew *Bgh*. Three-to-four week-old plants were dust-inoculated with *Bgh* spores, harvested at 48 hpi and subjected to aniline blue staining. The interaction was analyzed by simultaneous fluorescence and brightfield microscopy. The fluorophore sirofluor is an impurity product in commercial aniline blue that interacts with callose and thus stains callose appositions. Every interaction site was assigned to one of the following categories: successful resistance reaction by formation of an effective papilla or successful penetration of the epidermal cell and formation of a haustorium by the fungus.

Both the papilla and haustorial encasement seemed to contain callose because they were stained with aniline blue (Figure 21A).

The interaction of *cam7* with *Bgh* was analyzed and compared to the wild type and to the more susceptible *pen3-4* mutant. *Bgh* penetrated the wild type at approximately 15 % interaction sites (Figure 21B). The *pen3-4* mutant was successfully invaded in almost half of the fungal penetration attempts. *cam7* exhibited intermediate resistance with a statistically relevant increase of approximately 15 % penetration events when compared to the wild type. These results support the assumption that CaM7 plays an important role in the NHR against not only to *P. pachyrhizi* but several non-adapted fungal pathogens.

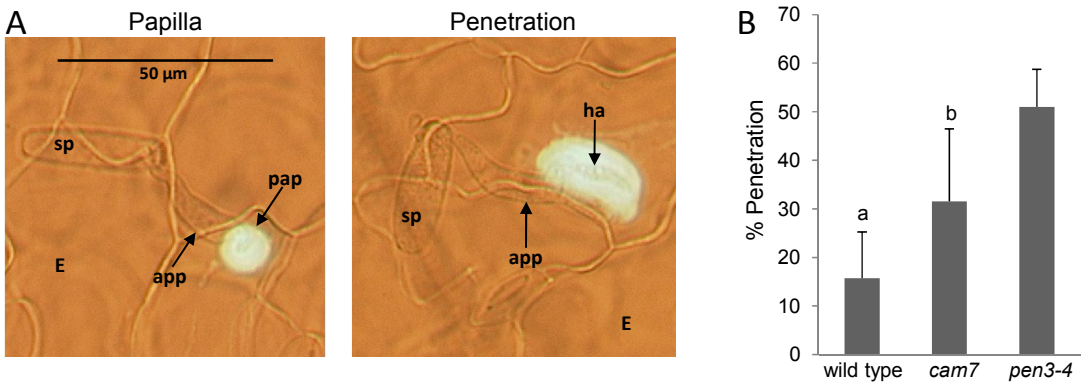

Figure 21. The interaction of Arabidopsis with *Bgh*. A. Categories in the interaction of Arabidopsis and *Bgh*. B. Quantitative microscopical analysis of the interaction of wild-type Col-0, *cam7* and *pen3-4* with *Bgh*. Three-to-four week-old Arabidopsis plants were inoculated with spores of *Bgh* and harvested at 48 hpi. Leaves were destained with chloral hydrate and stained with aniline blue prior to microscopical analysis. Leaves were analyzed by simultaneous light and fluorescence microscopy using a Leica DMR microscope. On each assessed leaf 100 interaction sites were analyzed. n=15 leaves from three biological replicates for all genotypes. Photos were taken with a digital Jvc KYF 750 camera and edited with the acquisition software DISKUS. App appressorium, E epidermal cell, ha haustorium, pap papilla, sp spore. Magnification 200 fold. Scale bar representative for both photos.

4 DISCUSSION

4.1 Can one consider *P. pachyrhizi* a „heminecrotroph“?

The plant signaling hormones SA, JA and ET emerged as key regulators of inducible defenses that are activated upon pathogen attack (Loake and Grant, 2007; Pozo et al., 2004; Leon-Reyes et al., 2009). Their signaling pathways are differentially activated depending on the type of the attacker and are highly interconnected (Thomma et al., 2001). It is well appreciated that in Arabidopsis defense against biotrophic pathogens is associated with activation of the SA–dependent signaling pathway, whereas the JA- and ET-dependent pathways are usually regulating the defense against necrotrophs (Thomma et al., 1998; Glazebrook, 2005). Therefore, the finding by Loehrer et al. (2008) revealing that the biotrophic fungus *P. pachyrhizi* induced the expression of *PDF1.2*, a marker for the induction of the JA/ET-dependent pathway, but not of *PR-1*, a marker for the induction of the SA-dependent pathway, came in somewhat unexpected. The authors speculated that *P. pachyrhizi* would mimic a necrotrophic attacker at early stages of infection to circumvent, or even suppress, appropriate SA-mediated plant defense. In line with this, I observed *PDF1.2* induction in Arabidopsis in both the wild type and *pen3-4* mutant as early as 8 hpi with *P. pachyrhizi* (Figure 1), supporting this hypothesis.

Pharmacological experiments in various plant species revealed the antagonism between the SA and JA signaling pathways. Niki et al. (1998) showed that in tobacco SA treatment inhibited the JA-dependent induction of genes encoding basic PR proteins and that methyl-JA (MeJA) application inhibited the SA-dependent induction of genes encoding acidic PR proteins. Also in tomato and Arabidopsis SA treatment was shown to directly impede the activation of JA-induced genes (Doares et al., 1995; van Wees et al., 1999). The lower expression of *PDF1.2* in *pen3-4* in comparison to the wild type at 24 hpi could thus be a direct suppression caused by SA. This conclusion is supported by the observed induction of *PR-1* at this time point (Figure 1). Spoel et al. (2003) demonstrated that SA-mediated suppression of *PDF1.2* in Arabidopsis required the immunity key protein NPR1. The *npr1* mutant is slightly compromised in NHR to *P. pachyrhizi* (Loehrer et al., 2008). However, this is unlikely to be a direct effect of the impaired SA signal transduction since *PR-1* expression was not induced upon inoculation with *P. pachyrhizi* in the wild type.

The finding that *P. pachyrhizi* rapidly induces *PDF1.2* instead of *PR-1* in Arabidopsis (Figure 1) supports the hypothesis that the pathogen mimics a necrotroph to manipulate the plant's defense response. However, it remained unclear whether this unexpected *PDF1.2* activation was due to an active manipulation of the plant by fungus-secreted chemical compounds or to the penetration and subsequent death of the epidermal cell. To address this question, I analyzed the

expression of defense marker genes in Arabidopsis leaves upon treatment with cell-free germination fluids of *P. pachyrhizi*.

Since decades cell-free culture fluids were used to investigate the influence of a given pathogen on the plant host. Early reports demonstrated that cell-free cultures of several pathogens elicit phytoalexin accumulation in their hosts. Uehara (1958) applied filtrates from *Fusarium* cultures to seed pods of soybean and observed that a fungitoxic compound accumulated in the treated bean tissue. Soybean also reacted with glyceollin synthesis to treatment with extracellular fluid of *Phytophtora sojae* cultures (Ayers et al., 1976), and a compound from *Colletotrichum lindemuthanium* elicited defense responses in bean (Anderson-Prouty and Albersheim, 1975). However, many of the substances from these early studies were identified as polysaccharides released from the fungal or oomycete cell wall and not necessarily as compounds that were actively secreted by the pathogen. The first scientists to use cell-free fluids derived from germinating spores of *P. pachyrhizi* were Deverall et al. (1977) who demonstrated that these so-called germination fluids caused browning of seed cavities inside soybean pods. Batches of collected fluids in which germination of *P. pachyrhizi* spores failed were inactive. Thus, it is unlikely that the eliciting compound was a fungal cell wall component or just spore leak-out. The early death of the penetrated cell gave rise to the idea that the germ-tubes of *P. pachyrhizi* might release a toxic compound that kills the host cells (Deverall et al., 1977).

Application of germination fluid just as the direct inoculation with *P. pachyrhizi* also led to *PDF1.2* gene activation eight hours after treatment (Figure 3). This finding clearly revealed that this induction is neither dependent on the presence of the fungus itself nor the penetration and/or cell death of the attacked cell. Therefore, there is likely a fungal compound secreted during the germination process exhibiting the *PDF1.2*-eliciting capacity. Furthermore, secretion of the *PDF1.2*-inducing compound did not require plant-derived signals, because secretion occurred during germination in water. For the same reason, secretion did not require information about whether the plant is a host or nonhost, suggesting that the observed response is not NHR-specific and that the elicitor is secreted during germination to facilitate early colonization of the host.

As mentioned, the JA- and SA-mediated signaling pathways can act antagonistically. The early induction of the JA pathway could therefore serve the pathogen by suppressing and delaying appropriate SA-dependent defenses. All tested JA/ET pathway markers, but not SA signaling marker genes, were induced in Arabidopsis at eight hours upon inoculation with *P. pachyrhizi* spores and treatment with germination fluid suggesting that the observed differential gene expression was a true induction of the JA/ET-mediated pathway rather than an unspecific response of *PDF1.2*.

To date, many pathogen effectors modulating plant defense are known which enable parasitic colonization of plant tissue (Hogenhout et al., 2009). Effectors function in a plant cellular environment although they are encoded by pathogen genes. Therefore, they could have evolved to mimic plant molecules such as phytohormones (Hogenhout et al., 2009). One prominent example of molecular mimicry is coronatine, a phytotoxin secreted by *P. syringae* that is a structural and functional mimic of the phytohormone JA-isoleucine (Weiler et al., 1994; Bender et al., 1999) and able to suppress SA-dependent defenses to promote susceptibility (Brooks et al., 2005; Uppalapati et al., 2007). Thus, the interplay between hormonal signaling pathways provides the plant with a powerful regulatory potential, but it also makes a common target for plant attackers to manipulate the host immune response (Pieterse et al., 2009; Grant and Jones, 2009). Not only bacteria but also oomycete and fungal pathogens were shown to produce effectors that target phytohormone homeostasis. Caillaud et al. (2013) demonstrated that the effector HaRxL44 from the oomycete downy mildew pathogen of Arabidopsis, *H. arabidopsidis*, was able to shift the balance of defense transcription from SA-responsive defense to JA/ET signaling and thereby enhancing susceptibility to biotrophs. The chorismate mutase 1 (Cmu1) of the biotrophic fungal pathogen *Ustilago maydis* can be taken up into the cytoplasm of maize cells where it channels chorismate into the phenylpropanoid pathway and in turn lowers the available substrate for SA biosynthesis (Djamei et al., 2011). Since the suppression of SA levels is likely to be particularly important for biotrophic pathogens it was not surprising that the authors found genes encoding secreted chorismate mutases in many genomes of eukaryotic biotrophic and several hemibiotrophic pathogens but only rarely in necrotrophs.

The abovementioned examples demonstrate that effectors are very diverse in their biochemical nature. Besides proteins and other small molecules, also small RNAs (sRNA) can act as effectors. sRNA molecules of *Botrytis cinerea* target Arabidopsis genes MPK1 and MPK2 which both participate in the plant immune response against the necrotrophic pathogen. By hijacking the plant's own silencing machinery these fungal sRNAs are able to suppress host immunity (Weiberg et al., 2013). The *PDF1.2*-eliciting compound in the *P. pachyrhizi* germination fluid was likely to be of proteinaceous nature, since autoclaved and trypsin-digested aliquots of germination fluid did not induce *PDF1.2* expression, whereas the TCA-precipitated protein fraction still exhibited its *PDF1.2*-eliciting activity (Figure 5).

Initiation of JA/ET-dependent defenses by a biotrophic pathogen suggests that *P. pachyrhizi* exploits the hormonal crosstalk to delay or suppress activation of SA-dependent defense responses of the plant at early stages of infection. In line with this, Cruz et al. (2013) showed that the severity of rust symptoms caused by *P. pachyrhizi* could be significantly reduced by pretreatment of soybean plants with the SA analog benzothiodiazole (BTH), but not by pretreat-

ment with JA. This finding indicates that the *P. pachyrhizi* effector does not only affect the hormonal crosstalk in the nonhost Arabidopsis but presumably also in the host plant soybean. It remains unknown whether the secreted protein manipulates the plant at the level of hormone biosynthesis, bioactivity or signal transduction and whether it is translocated into the plant cell or functions outside the cell by binding to a receptor or by releasing damage-associated molecular patterns (DAMPs). Translocation into the plant cell was demonstrated for several fungal proteinaceous effectors. The rust transferred protein 1 from *Uromyces fabae* (Uf-RTP1p) was not only detected in the extrahaustorial matrix, but also inside infected plant cells (Kemen et al., 2005). Also Cmu1 and the *Pyrenophora tritici-repentis* toxin ToxA were shown to translocate into the plant cytoplasm (Djamei et al., 2011; Manning and Ciuffetti, 2005). ToxA did not require the pathogen for translocation inside host cells (Manning et al., 2009). However, the mechanisms by which fungal effector proteins cross the plant membrane and accumulate in the host cytoplasm are still unknown.

Expression analysis after application of germination fluid of mutants impaired in hormone crosstalk or biosynthesis could give additional information on how the manipulation is achieved. Avoidance or delay in activation of SA-mediated defenses at early stages of plant infection could potentially represent an important evolutionary advantage for a biotrophic pathogen and might facilitate colonization of the mesophyll in soybean. This could also explain why *P. pachyrhizi* uredospores, unlike those from most other rust fungi, penetrate the epidermis directly and do not enter the plant via stomata, which seems to be an easier way to access the plant mesophyll. If death of the penetrated epidermal cell facilitates the entry into the plant and is thus actively elicited by the fungus itself, one could indeed consider *P. pachyrhizi* to be a 'heminecrotroph'.

4.2 Screening for PEN3 interaction partners

Starting with the sequencing of the Arabidopsis genome in 2000 (Arabidopsis Genome Initiative, 2000) the number of fully-sequenced genomes of higher plants, including many crops and model plants, rapidly increased. However, despite the growing genomic information, knowledge about the function of the majority of the encoded proteins remains limited. Proteins often operate in complexes. Hence, the identification and analysis of interaction partners can provide valuable information about a given protein's function.

Several methods can be applied to identify novel interaction partners of plant proteins, all having their advantages and disadvantages. The most commonly used techniques are yeast-based assays such as yeast-two-hybrid and split-ubiquitin. These are well-established, easy to handle and high throughput methods, but they are sensitive to artifacts and there is no control of equal expression levels of all proteins from the used cDNA library (Fukao, 2012; Braun et al.,

2013). With the emergence of ultrasensitive mass spectrometry (MS) the purification of protein complexes from plant tissue with subsequent MS identification of the single proteins aroused as an alternative to yeast-based assays. The main advantage is the direct purification of an endogenous plant protein. However, highly abundant proteins are often co-purified which makes transient and weak interactions hard to detect. Furthermore, purification procedures such as gel filtration, sucrose density centrifugation or ion exchange chromatography are difficult and have to be optimized for every single protein. Tandem affinity purification (TAP) is a two-step purification that thereby increases the specificity, but for the same reason loses many interactions (Fukao, 2012; Braun et al., 2013). High density PMAs emerged as a new technology for high throughput interaction screenings. The major drawback is the time-consuming production of the arrays; each single protein needs to be heterologously expressed, purified and spotted on the array. However, once the arrays are available, they provide an easy-to-handle high throughput screening procedure with the advantage of controlled experimental conditions. Still, like in every *in vitro* method, protein folding and binding properties might be compromised due to the immobilization on the array (Popescu et al., 2007b). For Arabidopsis, two different PMAs are currently available at ABRC. The ATPROTEINCHIP1 contains 5,000 proteins, which are mainly known signaling components including kinases and transcription factors. The ATPROTEINCHIP2 or 10K PMA contains 10,000 additional proteins.

Considering the advantages and disadvantages of the above mentioned methods the use of both available Arabidopsis PMAs, which together represent approximately half of the Arabidopsis proteome, was chosen for the screening for PEN3 interacting proteins. I used the AtPMA-5000 chip (Popescu et al., 2009) provided by Sorina Popescu, which has a slightly modified layout and protein content instead of the ATPROTEINCHIP1 from ABRC. Thereby, I identified a list of putative PEN3-interacting candidate proteins and gained new insights into PEN3's molecular function which is to date only poorly understood. However, during the experimental procedure several difficulties occurred which will be discussed in the following sections. First, heterologous production, purification and solubilization of a large membrane-bound protein like PEN3 was not suitable. The use of truncated protein versions for protein-protein interaction screens has been reported in literature. For example both, the intra- and extracellular domain of the flagellin receptor FLS2 were used in co-immunoprecipitation studies to show domain-specific FLS2-FLS2 association (Sun et al., 2012). I successfully used the N-terminal cytoplasmic domain (CyD1) of PEN3, which consists of approximately one third of the protein and contains the first ABC domain and the known phosphorylation sites (Figure 6), for the *in vitro* binding assays. However, as a consequence, I might have lost interactions which involve the second cytoplasmic domain, the C-terminus of the protein or an intramolecular complex formed by one or

more of these domains. Furthermore, all putative interactions have to be subsequently verified not only with the domain but also with the full-length protein.

The next step towards the binding assay was the expression and purification of CyD1. Compared to *E. coli*, expression and purification in *N. benthamiana* yielded less protein and therefore was labor-intensive. Many purifications had to be performed and pooled to obtain enough protein. The bottleneck of the procedure was the cleavage of the protein from the tag using the PreScission® protease, which turned out to be extremely inefficient (Figure 7B). Nevertheless, I consider the expression in a plant system as the best method to ensure correct folding and post-translational modification that might be important for subsequent protein-protein interactions. A different purification tag could have been chosen to improve the cleavage efficiency.

Furthermore, the choice of the affinity tag for detection of the interactions on the PMA is crucial for the outcome of the experiments. Since both, the target proteins on the arrays and the purified CyD1 contained the myc-tag, protein-protein interactions were detected using the specific α-PEN3 and secondary α-rabbit-DyLight649 antibody. Although I proved the suitability of the α-PEN3 antibody by using a self-printed test array (Figure 8), high background binding of the antibody occurred on the 10K PMA. The unspecific background signals occurred in repetitive patterns all over the array, indicating a possible carry-over of a contamination during the array printing process. Due to the high background, statistical analysis of the 10K PMA proved to be difficult and did not withstand the false discovery rate control. The use of a primary fluorophore-labeled antibody seems to produce more reliable data and should be preferred.

In conclusion, PMAs were a suitable means to detect PEN3 interaction partners. However, since only the 5K PMA produced reliable data the obtained results are biased towards signaling components present on this array.

4.2.1 Putative PEN3-interacting proteins identified on the 5K PMA

175 proteins were identified as putative PEN3 interaction partners after normalization and statistical testing. Approximately one third of these candidates were transcription factors (TFs), roughly reflecting the proportion of TFs on the 5K PMA. Since the group of TFs was overrepresented on the 5K PMA, a high number of interactions and, in turn, false positives was experienced in other PMA experiments (Sorina Popescu, personal communication). Furthermore, TFs are supposed to function in the nucleus and therefore most of them are not very likely to interact with a membrane or cytoplasmic protein. However, there are exceptions and many plant TFs have been shown to be involved in pathogen defense, mainly from the classes of ERF, bZIP, WRKY and MYB TFs (Singh et al., 2002). The tomato ERF TF PTI4 was phosphorylated in the cytoplasm by the PTO kinase upon pathogen attack. In turn, phosphorylated PTI4 was translo-

cated to the nucleus where it enhanced the expression of *PR* genes (Gu et al., 2000). Also several proteins from the bZIP family are present in the cytoplasm and move to the nucleus in response to elicitor recognition to activate transcription of defense-related genes (Alves et al., 2013). Many WRKY TFs were demonstrated to act in a complex defense response network as both positive and negative regulators (Eulgem and Somssich, 2007). To narrow down my candidate list, I first excluded all TFs, although some of them might be interesting candidates directly interacting with PEN3. The list of TFs could be analyzed in a following project. Subcellular localization studies could give a first hint on which TFs are likely to interact with PEN3.

In a second step, the candidate list was filtered using gene ontologies. All proteins involved in "any process that results in a change in state or activity of a cell as a result of a stimulus" (GO:0051716) were selected as candidates, which in connection with their interaction with PEN3 might be involved in defenses related processes upon pathogen attack. The resulting list of 28 candidates (Table 8) included several Ca^{2+} sensors, kinases, F-box, and other proteins. These groups are shortly discussed in the following sections.

4.2.1.1 Ca^{2+} sensors

With nine out of 28 candidates, Ca^{2+} sensors were the most prominent group among the putative PEN3-interacting proteins. Those included the two calmodulin isoforms CaM3 and CaM7, several calmodulin-like proteins (CML; CAL4/TCH3, CML8, CML9, CML37, CML38), the calcineurin B-like protein (CBL) CBL4/SOS3 and an additional EF-hand protein. The role of Ca^{2+} signaling in plant defenses and the interaction of PEN3 with CaM will be discussed in detail in chapter 4.2.2.

4.2.1.2 Kinases

A number of kinases were identified to putatively interact with PEN3, including MPK7, MPK10, MPK16, MAPKKK19 and WNK4. MPK cascades are signaling kinase modules that function downstream of receptors/sensors and transmit extracellular stimuli into intracellular responses by phosphorylating their targets (Herskowitz, 1995). However, it is not very likely that PEN3 gets directly phosphorylated by one of these MPKs, since the known phosphorylation sites in PEN3 do not correspond to the low or high stringency MPK phosphorylation site motifs ((pS/pT)P) or (PX(pS/pT)P), respectively (Songyang et al., 1996). Possibly, PEN3 binds to one or several of these kinases and thereby mediates interaction and phosphorylation of other proteins in a PEN3-bound complex.

4.2.1.3 F-Box proteins

The Arabidopsis genome encodes for almost 700 F-Box containing proteins (Vierstra, 2003) and several of them were found to interact with PEN3. F-Box proteins were first characterized as

components of SCF (SKP1/Cullin/F-box) ubiquitin-ligase complexes in which they bind substrates for ubiquitin-mediated proteolysis through the 26S proteasome (Kipreos and Pagano, 2000). Regulation through protein degradation is considered as important as regulation through protein biosynthesis or posttranslational modification, and F-Box proteins were found to be involved in all aspects of plant biology, including hormone signaling and disease resistance (Vierstra, 2003). The Arabidopsis F-Box protein SON1 regulates defense responses against the oomycete pathogen *Hyaloperonospora parasitica* and the bacterial pathogen *Pst* DC3000 through the ubiquitin-proteasome pathway (Kim and Delaney, 2002). Also the JA receptor COI1, which regulates defense against insects and pathogens, is a F-box protein and regulated via the stabilization or degradation through the SCF complex or the 26S proteasome, respectively (Xie et al., 1998; Yan et al., 2013). One of the putative PEN3-binding F-Box proteins is the EIN3-BINDING F BOX PROTEIN1 (EBF1), shown to be important for the regulation of EIN3-dependent plant ET signaling. EIN3 is an ET-sensitive TF that controls the transcription of defense-related genes including *FLS2* (Potuschak et al., 2003; Guo and Ecker, 2003; Boutrot et al., 2010). However, since EBF1 was shown to only localize to the nucleus (Potuschak et al., 2003), it is not very likely to directly interact with PEN3. Nevertheless, PEN3 might be regulated in a similar way by the bound F-Box proteins or mediate the degradation of other PEN3-interacting proteins.

4.2.1.4 Other proteins

Several other proteins identified by the PMAs might be interesting candidates and contribute to PEN3's molecular function. The U-box type E3 ubiquitin ligase PUB23 like the abovementioned F-Box proteins is involved in protein targeting for degradation. Together with its homologs PUB22 and PUB24 it acts as a negative regulator of PTI in response to several distinct PAMPs. The triple mutant *pub22 pub23 pub24* exhibited enhanced activation of PTI responses that also resulted in increased resistance against bacterial and oomycete pathogens, which was accompanied by increased production of ROS and cell death (Trujillo et al., 2008). The authors speculated that the PUB triplet controls the output of one or more targets that are positive regulators of immune responses. However, no targets were identified so far. An ubiquitination assay could give insights on whether PEN3 is directly targeted and regulated by PUB23.

Another putative PEN3-interacting protein is the conserved carboxylesterase/phospholipase SUPPRESSOR OF AVRBST-ELICITED RESISTANCE1 (SOBER1). AvrBsT, a type III effector of *Xanthomonas campestris* pv *vesicatoria*, is translocated into plant cells during infection where it targets intracellular host proteins (Cunnac et al., 2007). SOBER1 suppresses AvrBsT-elicited HR by regulating the levels of phosphatidic acid (PA), an important lipid second messenger that accumulates upon multiple stimuli including wounding and pathogen attack

(Kirik and Mudgett, 2009; Testerink and Munnik, 2005). In turn, lack of SOBER1 leads to accumulation of PA, HR and consequentially to resistance against bacteria. Interestingly, also PEN3 is involved not only in resistance to fungi but also against bacteria. The *pen3-1* mutant was shown to be compromised in resistance to *Pst* DC3000 and required for flg22- and BTH-induced immunity against this pathogen (Xin et al., 2013). Furthermore, upon infection with *P. pachyrhizi* *pen3-1* mutant plants accumulated high levels of transcripts of *NHL10* (NDR1/HIN1-like), a marker for tissue undergoing HR (Zheng et al., 2004), indicating that PEN3 negatively influences signals required for *NHL10* expression and consequently also negatively influences HR (Loehrer et al., 2008). It would be interesting to analyze whether PEN3-mediated resistance and negative regulation by SOBER1 are interconnected through their bimolecular interaction. Presence of PEN3 or absence of SOBER1 leads to the establishment of HR and resistance. Therefore, it could be hypothesized, that SOBER1 activity through binding to PEN3 is somehow suppressed, e.g. by simply keeping SOBER1 away from subsequent signaling components or by mediating the interaction with F-Box proteins that mark SOBER1 for subsequent degradation.

PEN3 was suggested to transport antimicrobial compounds to the site of pathogen attack (Lipka et al., 2005). Yet, the fact that PEN3 is not only important for resistance against fungi but also against bacteria indicates that PEN3 functions through a more complex mechanism, since the entry of bacteria into the plant is not restricted to a confined area or mediated by penetration. Plant ABC transporters were proposed to play a multifunctional role in a variety of processes rather than just being detoxifiers (Martinoia et al., 2002). Several transporters also act as receptor proteins, such as the glutamate receptors, which also function as cation channels and are involved in nutrient uptake, intra-plant transport and (wound) signaling (Davenport, 2002; Mousavi et al., 2013). The multifunctionality of transporters is not restricted to plants. The cellodextrin transporters CDT-1 and CDT-2 of the filamentous fungus *Neurospora crassa* may also act as transporting receptors, leading to the term “transceptor” (Znameroski et al., 2014). In this regard, PEN3 might also function as a receptor, a signaling component, or a scaffold protein mediating the formation of a multi-protein complex involved in plant defenses against pathogens.

4.2.2 PEN3 is a novel CaM-binding protein

4.2.2.1 CaM, CMLs and Ca^{2+} signaling in plant immunity

The Ca^{2+} ion is an indispensable second messenger in various plant signaling pathways, translating a plethora of external and internal stimuli into adequate cell responses. Under resting conditions, the concentration of free Ca^{2+} in the cytosol is maintained between 100 and 200 nM, whereas it ranges from 100 µM to 1 mM in the apoplast and cellular organelles (Bush, 1995). The

steep gradient provides the potential for a rapid influx of Ca^{2+} into the cytosol and explains the important role of Ca^{2+} in very early signaling events. Changes in the intracellular Ca^{2+} concentration have been reported upon numerous signals such as light, abiotic stresses, hormones and microbial elicitors (Lecourieux et al., 2006). Given the variety of stimuli that induce Ca^{2+} signaling in the cell, the necessity for a precise deciphering system becomes obvious, that transduces a certain Ca^{2+} stimulus to the appropriate cell response. There is evidence that the spatial and temporal changes in free Ca^{2+} caused by a given stimulus contribute to the specificity of the biological outcome (Ng and McAinsh, 2003). These so-called "calcium signatures" can differ in lag time, amplitude and frequency and can be differently received by the plant depending on the organ, tissue or the cell type (McAinsh and Hetherington, 1998). Ca^{2+} movements are regulated by active transport through Ca^{2+}-ATPases and Ca^{2+}-antiporters and passive fluxes through Ca^{2+}-channels (Sanders et al., 1999).

Decoding the calcium signature involves a set of Ca^{2+}-binding proteins which in turn induce a cascade of downstream effects (Sanders et al., 2002). In plants Ca^{2+} sensors are roughly divided into two groups; sensor relays such as CaM, CMLs and CBLs have no intrinsic enzyme activity. They undergo a Ca^{2+}-induced conformational change that is relayed to a downstream target by bimolecular interaction. By contrast, sensor responders such as calcium-dependent protein kinases (CDPKs) undergo a Ca^{2+}-induced conformational change which alters their own activity (Sanders et al., 2002). In contrast to the Ca^{2+} sensors CMLs, CBLs and CDPKs which are plant-specific, CaM is highly conserved between all eukaryotes (Poovaiah et al., 2013). CaM is a 149 amino acid protein with two globular domains, each consisting of two Ca^{2+}-binding EF hands connected by a long flexible helix (Strynadka and James, 1989; Meador et al., 1993). Arabidopsis has seven CaM loci encoding for three distinct CaM isoforms, which differ by not more than four amino acids. Furthermore, Arabidopsis has a family of 50 CML genes, encoding proteins that, like CaM, have no other functional domains than EF hands and share at least 16 % amino acid identity with CaM (McCormack and Braam, 2003). The function of the different CaM and CML isoforms will be discussed in a later section. The specificity of the calcium signature, the two types of decoding Ca^{2+} signals and the vast variety of Ca^{2+}-sensing proteins provide the plant with the necessary flexibility and diversity in its response to the Ca^{2+} trigger.

The rapid Ca^{2+} influx from the apoplast into the cytosol has been demonstrated in early studies to be a key event in the activation of defense responses by elicitors (Kurosaki et al., 1987; Stäb and Ebel, 1987; Atkinson et al., 1990; Conrath et al., 1991; Tavernier et al., 1995). Also Ca^{2+} sensors and their diverse targets are involved in plant immunity. Kim et al. (2002) identified the transmembrane MLO protein from barley, a negative regulator of plant defense and cell death, to interact with CaM in a Ca^{2+}-dependent manner. Barley plants carrying loss-of-function alleles of

the *Mlo* locus are resistant against the powdery mildew *Bgh* (Jorgensen, 1992). CaM binding strongly enhanced MLO activity to negatively regulate defense against *Bgh* (Kim et al., 2002b). *mlo*-mediated penetration resistance was shown to be overcome by overexpression of the membrane-localized cell death suppressor BAX inhibitor 1 (BI-1) (Hückelhoven et al., 2003). Interestingly, also BI-1 activity to suppress *Pst*-induced cell death was regulated by CaM-binding (Kawai-Yamada et al., 2009). The regulation via CaM might be a possible connection of both proteins' function. Furthermore, CaM interferes with downstream signaling such as MAPK cascades via the interaction with the MAPK phosphatase 1 (MKP1). Phosphatase activity of AtMKP1 was increased by CaM in a Ca^{2+}-dependent manner (Lee et al., 2008). AtMKP1 in turn was shown to negatively regulate MPK6-mediated PAMP responses and to repress SA biosynthesis (Anderson et al., 2011; Bartels et al., 2009). Another direct connection between Ca^{2+} signaling and SA-mediated immune responses was provided by Du et al. (2009). The CaM-binding transcription factor AtSR1/CAMTA3 bound to the promoter of EDS1, an established regulator of SA level, and repressed its expression.

4.2.2.2 The role of the CaM/CML-PEN3 interaction

Given that CaMs (and CMLs) are essentially noncatalytic regulators, the investigation of CaM-target interactions is considered crucial for our understanding how Ca^{2+} exerts downstream events. In the present study PEN3 was identified as a novel CaM-binding protein by *in vitro* binding assays. This interaction could be verified *in vitro* and *in vivo* by a CaM overlay assay, pull-down with CaM Sepharose and BIFC. In both, the overlay and pull-down experiments, the PEN3-CaM interaction was enhanced in the presence of Ca^{2+}. Hence, stress-induced Ca^{2+} influx seems to support the PEN3-CaM interaction in the cell to boost defense and cause immunity.

Furthermore, the *cam7* mutant exhibited enhanced susceptibility against two non-adapted fungal pathogens, *P. pachyrhizi* and *Bgh*. However, the enhanced susceptibility was not as pronounced as in the *pen3-4* mutant, indicating that CaM-binding is not crucial for PEN3's function, or that CaM7 functions are compensated by another CaM isoform. Conversely, CaM7 function seems to be dependent on or downstream of PEN3, since the interaction phenotype of the *pen3-4 cam7* double mutant did not differ considerably from *pen3-4*.

Besides CaM, PEN3 presumably interacts with a number of additional Ca^{2+} sensors, some of them already revealed to play a role in plant innate immunity, namely CML9, and the closely related CML37 and CML38. *CML9* is induced early during a bacterial pathogen challenge and contributes to plant innate immunity through a flagellin-dependent signaling pathway (de Torres et al., 2003; Leba et al., 2012). Gene expression analysis of *CML37* and *CML38* showed that transcript levels markedly increased in response to the avirulent *Pst* strain avrRpt. This

response was particularly pronounced for *CML37* (Vanderbeld and Snedden, 2007). To learn more about the connection of PEN3 and Ca^{2+} signaling, a PEN3/Ca^{2+} signaling network was drawn based on data retrieved from the BAR Arabidopsis interaction viewer, containing PEN3, its nine Ca^{2+}-binding interaction partners and the partner's binary interactors (Figure 10). The BAR Arabidopsis interaction viewer combines confirmed Arabidopsis protein interactions retrieved from more than 1,000 literature sources including high throughput screens using Y2H or PMAs. The resulting network contained 266 proteins represented as nodes. The size of the node was dependent on the protein's connectivity, revealing CaM6, HSP90, and MPK4 and MPK6 as major hubs of the network, the latter three known to play a role in the plant defense response. HSP90 is a conserved chaperone which was shown to modulate the function of several R proteins, including RPM1, RPS2 and RPP4 (Hubert et al., 2003; Takahashi et al., 2003; Bao et al., 2014). Furthermore, HSP90 is an essential component of NHR in *N. benthamiana* (Kanzaki et al., 2003). MPK4 was demonstrated to be required for JA-responsive gene expression (Petersen et al., 2000) and to function together with MEKK1 and MKK1/MKK2 in a signaling cascade (Gao et al., 2008) whereas MPK6 functions downstream of MKK3 (Takahashi et al., 2007). The MKK3-MPK6 cascade is induced by JA and important for the JA signal transduction pathway, indicating a role in pathogen defense. In line with this, resistances against the oomycete *H. parasitica* and both virulent and avirulent *Pseudomonas* strains were compromised in MPK6-silenced plants (Menke et al., 2004). MPK4 is connected to PEN3 via CaM3 and MPK6 via CML38, further pointing to a possible role of MPK6-dependent signaling in PEN3-mediated resistance.

In silico expression analysis of large datasets can give valuable information on which genes are most likely to be connected to the process of interest. PEN3 is a known component of a distinct regulon that includes several penetration resistance components (Humphry et al., 2010). Thus, I cross-checked the components of the PEN3-Ca^{2+} signaling network for co-regulation with PEN3. Only six genes in the network show the same regulation pattern as PEN3 (Table A3). Remarkably, two of those are direct interactors of PEN3, namely *CAL4/TCH3* and *AT2G4660*. Co-expression and interaction with PEN3 makes them likely to play a role in PEN3's function and highly interesting candidates for follow-up experiments.

Furthermore, using microarray data of *P. pachyrhizi* inoculated Arabidopsis plants (C. Langenbach, unpublished data), I analyzed which candidates were upregulated upon infection with *P. pachyrhizi*. Fourteen genes were induced in this screen (Table A3), the most interesting ones being *CML37* and *CPK10*. CPK10 is a calcium-dependent protein kinase that can phosphorylate a PEN3 peptide *in vitro* (Curran et al., 2011), thus providing a direct link to PEN3's function. CPK10 is connected with PEN3 through CML9. Since also CML9 was demonstrated to contribute to plant innate immunity through a flagellin-dependent signaling pathway (Leba et

al., 2012), it appears likely that CML9 recruits CPK10 for PEN3 phosphorylation upon a pathogen-elicited Ca^{2+} influx. This is further supported by the recent finding that besides the elicitors flg22 and xylanase also RALF leads to PEN3 phosphorylation (Benschop et al., 2007; Haruta et al., 2014), a peptide known to induce a rapid Ca^{2+} influx in Arabidopsis seedlings (Haruta et al., 2008).

Although the creation and analysis of the PEN3/Ca^{2+} signaling network gave more insights and additional hints on connections between PEN3 associated proteins, one should take in account that a network can only reflect the current state of the art. Furthermore, since several of the large scale interaction screens implemented in the BAR interaction database were performed with specific targets, including CaMs, CMLs and MPKs it is not surprising that these proteins are revealed as major hubs of the network. Nevertheless, the *in silico* expression analysis of the network components gave valuable information about which candidates are likely to be involved in PEN3's functional network and which are not.

4.2.2.3 An eliminated PEN3 CaMBD is not crucial for the PEN3-CaM interaction

The *cam7* mutant was compromised in NHR against *P. pachyrhizi* and *Bgh*, whereas susceptibility was not or only slightly enhanced in the *pen3-4 cam7* double mutant when compared to *pen3-4*. This indicates that the impaired resistance in *cam7* is connected to PEN3 function. However, for this conclusion it has to be determined whether CaM-binding is crucial for PEN3 function and which PEN3 region mediates the PEN3-CaM interaction.

The majority of CaM-binding proteins does not contain a conserved sequence motif but a structural CaM target site composed of a stretch of twelve to 30 contiguous amino acids with positively charged amphiphilic characteristics, that tend to form an α-helix upon CaM-binding (Rhoads and Friedberg, 1997; Bouché et al., 2005). The Calmodulin Target Database predicts several putative CaMBDs with different probabilities in the full-length PEN3 protein (Figure 6), three of which are located in CyD1. Since not only full-length PEN3 but also CyD1 binds to CaM, I hypothesized that one of these first three CaMBDs is important for the interaction. I cloned a CyD1ΔCaMBD construct, which did not contain the high-probability CaMBD of CyD1, to test whether this domain mediates CyD1-CaM interaction. In both, the CaM overlay assay and the pull-down with CaM Sepharose, CyD1ΔCaMBD still bound CaM (Figure 15), suggesting that this domain is not crucial for CaM-binding to CyD1. This result demonstrates the limitations of sequence-based predictions and the necessity to analyze the role of each predicted CaMBD. Whether one (or both) of the other putative CaMBDs in CyD1 or another non-predicted region mediates the PEN3-CaM interaction needs to be elucidated.

4.2.2.4 Plants evolved CaM isoforms that have overlapping and specific functions

In contrast to animals that contain only one CaM isoform encoded by three different genes (Fischer et al., 1988), plants evolved multiple CaM genes encoding for several CaM isoforms that only differ in a few amino acids (Lee et al., 1995). This discovery suggested an additional level of sophistication in the intracellular regulation of Ca^{2+} signaling in plants (Gifford et al., 2013). Yet, the question arises how plants accomplish such a high specificity in the single CaM's function, when the differences between them are so small. One of the easiest ways to differentially regulate similar genes is their spatial and temporal expression. Tissue- and stimulus-specific expression of *CaMs* was reported from several plant species. Perera and Zielinski (1992) analyzed the expression of Arabidopsis *CaM1*, *2* and *3* in different organs and upon touch-stimulus. Only *CaM1* was found to be expressed in the roots. Upon the touch stimulus all three genes were induced, but to different extent. McCormack and Braam (2003) showed differential expression of Arabidopsis CaM loci in different organs and upon stress and hormones. Organ specific expression was also shown for soybean *SCaMs* (Lee et al., 1995). Furthermore, *SCaM4* and *5* were induced by pathogen infection whereas other *CaM* loci were not (Heo et al., 1999). Tobacco contains 13 *CaM* loci that are differentially expressed during HR, wounding and SA treatment (Yamakawa et al., 2001).

CaM isoforms can also localize to different cell compartments. Generally, the small CaM protein was shown to localize to the cytoplasm, the nucleus, mitochondria and the cell wall (Li et al., 1993). In a proteomics screen with isolated membranes, the Arabidopsis CaM isoforms 4, 5 and 7 were identified to be associated with the plasma membrane, whereas the other isoforms, despite their predictions for membrane localization, were not (Alexandersson et al., 2004). In a LC/MS analysis of SA-responsive protein secretion, only CaM7 was reported to be partially secreted into the apoplast (Cheng et al., 2009) suggesting a special role for CaM7 in SA-mediated responses.

Besides their differential expression and localization some CaMs have evolved high target specificity. Popescu et al. (2007) applied a large scale *in vitro* binding assay using protein microarrays to determine target specificity of several Arabidopsis CaMs and CMLs. Multiple CaM/CML proteins bound many binding partners, but the majority of targets were specific to one or a few CaMs/CMLs. Detailed work regarding specificity and regulation of the SCaM isoforms 1 and 4 has been performed by several groups. SCaM1 is responsible for activation of NAD kinase. The divergent SCaM4 did not activate NAD kinase at all even at 500-fold higher concentration than that of SCaM1 (Lee et al., 1995). In contrast, SCaM4 activates the enzyme nitric-oxide synthase (NOS), whereas SCaM1 is incapable of activating NOS (Ishida et al., 2008). Gifford et al. (2013) analyzed the Ca^{2+}-binding properties of both SCaMs. SCaM4 has a threefold greater affinity to-

wards Ca^{2+} than SCaM1 but a significantly reduced selectivity against the chemically similar Mg^{2+} cation. The different binding affinities of the various CaM isoforms for Ca^{2+} were suggested to modulate their ability to activate specific targets. Considering the differential expression pattern, the specificity in target activation and their binding affinities for Ca^{2+}, the authors suggested different physiological roles for SCaM1 and 4. Whereas SCaM1 is probably involved in the cell's response to light, cold, heat, wounding and symbionts, SCaM4 is more likely to be involved in the response to pathogens (Gifford et al., 2013).

Interestingly, also CaM-binding proteins can distinguish between different CaM isoforms, depending on their posttranslational modifications. There is emerging evidence that CaMs are differentially regulated by methylation (Roberts et al., 1986; Oh and Roberts, 1990; Roberts et al., 1992; Banerjee et al., 2013; Hofmann, 2013). The CaM N-methyltransferase is like CaM an evolutionary conserved enzyme in eukaryotes and transfers three methyl groups to a conserved lysine at position 115. Methylation of CaM was shown to decrease its ability to activate NAD kinase (Roberts et al., 1986). Furthermore, some targets, such as the Germin-like proteins (GLP) 9 and 10, can read the methylation status of CaM and bind preferentially to the methylated protein (Banerjee et al., 2013).

PEN3 was found to interact with CaM3 and CaM7 on the array, suggesting a higher affinity for these isoforms. However, in the pull-down experiments PEN3 also bound to animal CaM, indicating that PEN3 can bind several CaM isoforms *in vitro*, when no competition between isoforms occurs. All seven CaM isoforms were strongly expressed in Arabidopsis leaves and showed no or only marginal induction upon *P. pachyrhizi* infection (C. Langenbach, unpublished data). Only CaM7 was involved in NHR of Arabidopsis. Therefore, mechanisms other than differential expression must lead to the specificity of the PEN3-CaM7 interaction. Since CaM7 was also the only isoform shown to respond to SA treatment and to be secreted (Cheng et al., 2009), it seems to play a special role in the regulation of defense responses. The specificity might also be regulated through other proteins in a PEN3-bound complex.

In this study, I provided further evidence that the ostensible biotroph *P. pachyrhizi* mimics a necrotroph to facilitate plant invasion. By use of germination fluid I showed that the induction of marker genes for JA/ET-mediated defense upon *P. pachyrhizi* infection is neither dependent on the presence of the fungus nor penetration and/or cell death of the epidermal cell but likely elicited by a secreted protein. Yet, whether this protein acts as an effector or DAMP-releasing agent still needs to be determined. Furthermore, I identified putative PEN3-binding proteins and thereby gained more insight into PEN3's molecular functions. PEN3 was confirmed as a novel CaM-binding protein and CaM7 was demonstrated to be involved in NHR of Arabidopsis. This work

thus provided a new direct link between Ca^{2+} signaling and the plant's innate immunity. However, further studies need to be conducted to fully understand the regulation of PEN3 by CaM7 and to decipher the role of the other identified PEN3-binding proteins.

5 REFERENCES

Agrios, G. (2005). Plant Pathology 5th ed. (Elsevier Academic Press: London).

Alexandersson, E., Saalbach, G., Larsson, C., and Kjellbom, P. (2004). Arabidopsis plasma membrane proteomics identifies components of transport, signal transduction and membrane trafficking. Plant Cell Physiol. **45**: 1543–56.

Alves, M.S., Dadalto, S.P., Gonçalves, A.B., De Souza, G.B., Barros, V.A., and Fietto, L.G. (2013). Plant bZIP transcription factors responsive to pathogens: A review. Int. J. Mol. Sci. **14**: 7815–28.

Anderson, J.C., Bartels, S., González Besteiro, M.A., Shahollari, B., Ulm, R., and Peck, S.C. (2011). Arabidopsis MAP Kinase Phosphatase 1 (AtMKP1) negatively regulates MPK6-mediated PAMP responses and resistance against bacteria. Plant J. **67**: 258–68.

Anderson-Prouty, A.J. and Albersheim, P. (1975). Host-pathogen interactions: VIII. Isolation of a pathogen-synthesized fraction rich in glucan that elicits a defense response in the pathogen's host. Plant Physiol. **56**: 286–91.

Arabidopsis Genome Initiative (2000). Analysis of the genome sequence of the flowering plant *Arabidopsis thaliana*. Nature **408**: 796–815.

Assaad, F.F., Qiu, J.-L., Youngs, H., Ehrhardt, D., Zimmerli, L., Kalde, M., Wanner, G., Peck, S.C., Edwards, H., Ramonell, K., Somerville, C.R., and Thordal-Christensen, H. (2004). The PEN1 syntaxin defines a novel cellular compartment upon fungal attack and is required for the timely assembly of papillae. Mol. Biol. Cell **15**: 5118–29.

Atkinson, M.M., Keppler, L.D., Orlandi, E.W., Baker, C.J., and Mischke, C.F. (1990). Involvement of plasma membrane calcium influx in bacterial induction of the k/h and hypersensitive responses in tobacco. Plant Physiol. **92**: 215–21.

Ayers, A.R., Ebel, J., Finelli, F., Berger, N., and Albersheim, P. (1976). Host-pathogen interactions: IX. Quantitative assays of elicitor activity and characterization of the elicitor present in the extracellular medium of cultures of *Phytophthora megasperma var. sojae*. Plant Physiol. **57**: 751–9.

Banerjee, J., Magnani, R., Nair, M., Lynnette, D.M., Debolt, S., Maiti, I.B., and Houtz, R.L. (2013). Calmodulin-mediated signal transduction pathways in Arabidopsis are fine-tuned by methylation. Plant Cell **25**: 4493–511.

Bao, F., Huang, X., Zhu, C., Zhang, X., Li, X., and Yang, S. (2014). Arabidopsis HSP90 protein modulates RPP4-mediated temperature-dependent cell death and defense responses. New Phytol.: epub ahead of print.

Bartels, S., Anderson, J.C., González Besteiro, M.A., Carreri, A., Hirt, H., Buchala, A., Métraux, J.-P., Peck, S.C., and Ulm, R. (2009). MAP kinase phosphatase1 and protein tyrosine phosphatase1 are repressors of salicylic acid synthesis and SNC1-mediated responses in Arabidopsis. Plant Cell **21**: 2884–97.

Beckers, G.J.M., Jaskiewicz, M., Liu, Y., Underwood, W.R., He, S.Y., Zhang, S., and Conrath, U. (2009). Mitogen-activated protein kinases 3 and 6 are required for full priming of stress responses in *Arabidopsis thaliana*. Plant Cell **21**: 944–53.

Bednarek, P., Pislewska-Bednarek, M., Svatos, A., Schneider, B., Doubsky, J., Mansurova, M., Humphry, M., Consonni, C., Panstruga, R., Sanchez-Vallet, A., Molina, A., and Schulze-Lefert, P. (2009). A glucosinolate metabolism pathway in living plant cells mediates broad-spectrum antifungal defense. Science **323**: 101–6.

Belkhadir, Y. and Nimchuk, Z. (2004). Arabidopsis RIN4 negatively regulates disease resistance mediated by RPS2 and RPM1 downstream or independent of the NDR1 signal modulator and is not required for the virulence functions of bacterial type III effectors AvrRpt2 or AvrRpm1. Plant Cell **16**: 2822–2835.

Bender, C.L., Alarcón-Chaidez, F., and Gross, D.C. (1999). *Pseudomonas syringae* phytotoxins: mode of action, regulation, and biosynthesis by peptide and polyketide synthetases. Microbiol. Mol. Biol. Rev. **63**: 266–92.

Benschop, J.J., Mohammed, S., O'Flaherty, M., Heck, A.J.R., Slijper, M., and Menke, F.L.H. (2007). Quantitative phosphoproteomics of early elicitor signaling in Arabidopsis. Mol. Cell. Proteomics **6**: 1198–214.

Bhat, R. a, Miklis, M., Schmelzer, E., Schulze-Lefert, P., and Panstruga, R. (2005). Recruitment and interaction dynamics of plant penetration resistance components in a plasma membrane microdomain. Proc. Natl. Acad. Sci. U. S. A. **102**: 3135–40.

Boller, T. (1995). Chemoperception of microbial signals in plant cells. Annu. Rev. Plant Physiol. Plant Mol. Biol. **46**: 189–214.

Boller, T. and Felix, G. (2009). A renaissance of elicitors: perception of microbe-associated molecular patterns and danger signals by pattern-recognition receptors. Annu. Rev. Plant Biol. **60**: 379–406.

Bonde, M.R., Nester, S.E., Austin, C.N., Stone, C.L., Frederick, R.D., Hartman, G.L., and Miles, M.R. (2006). Evaluation of virulence of *Phakopsora pachyrhizi* and *P. meibomiae* isolates. Plant Dis. **90**: 708–716.

Bouché, N., Yellin, A., Snedden, W. a, and Fromm, H. (2005). Plant-specific calmodulin-binding proteins. Annu. Rev. Plant Biol. **56**: 435–66.

Boutrot, F., Segonzac, C., Chang, K.N., Qiao, H., Ecker, J.R., Zipfel, C., and Rathjen, J.P. (2010). Direct transcriptional control of the Arabidopsis immune receptor FLS2 by the ethylene-dependent transcription factors EIN3 and EIL1. Proc. Natl. Acad. Sci. U. S. A. **107**: 14502–7.

Bradford, M.M. (1976). A rapid and sensitive method for the quantitation of microgram quantities of protein utilizing the principle of protein-dye binding. Anal. Biochem. **72**: 248–54.

Braun, P., Aubourg, S., Van Leene, J., De Jaeger, G., and Lurin, C. (2013). Plant protein interactomes. Annu. Rev. Plant Biol. **64**: 161–87.

Broekaert, W.F., Terras, F.R., Cammue, B.P., and Osborn, R.W. (1995). Plant defensins: novel antimicrobial peptides as components of the host defense system. Plant Physiol. **108**: 1353–8.

Bromfield, K.R. (1984). Soybean Rust American P. (St. Paul, MN).

Brooks, D.M., Bender, C.L., and Kunkel, B.N. (2005). The *Pseudomonas syringae* phytotoxin coronatine promotes virulence by overcoming salicylic-acid-dependent defences in *Arabidopsis thaliana*. Mol Plant Pathol **6**: 629–639.

Van den Brûle, S. and Smart, C.C. (2002). The plant PDR family of ABC transporters. Planta **216**: 95–106.

Bu, Q., Jiang, H., Li, C.-B., Zhai, Q., Zhang, J., Wu, X., Sun, J., Xie, Q., and Li, C. (2008). Role of the *Arabidopsis thaliana* NAC transcription factors ANAC019 and ANAC055 in regulating jasmonic acid-signaled defense responses. Cell Res. **18**: 756–67.

Bush, D.S. (1995). Calcium regulation in plant cells and its role in signaling. Annu. Rev. Plant Physiol. Plant Mol. Biol. **46**: 95–122.

Caillaud, M.-C., Asai, S., Rallapalli, G., Piquerez, S., Fabro, G., and Jones, J.D.G. (2013). A downy mildew effector attenuates salicylic acid-triggered immunity in Arabidopsis by interacting with the host mediator complex. PLoS Biol. **11**: e1001732.

Campe, R., Loehrer, M., Conrath, U., and Goellner, K. (2014). *Phakopsora pachyrhizi* induces defense marker genes to necrotrophs in *Arabidopsis thaliana*. Physiol. Mol. Plant Pathol.

Catanzariti, A.-M., Dodds, P.N., Lawrence, G.J., Ayliffe, M.A., and Ellis, J.G. (2006). Haustorially expressed secreted proteins from flax rust are highly enriched for avirulence elicitors. Plant Cell **18**: 243–56.

Chakrabarty, R., Banerjee, R., Chung, S.-M., Farman, M., Citovsky, V., Hogenhout, S.A., Tzfira, T., and Goodin, M. (2007). PSITE vectors for stable integration or transient expression of autofluorescent protein fusions in plants: probing *Nicotiana benthamiana*-virus interactions. Mol. Plant. Microbe. Interact. **20**: 740–50.

Chanda, B., Xia, Y., Mandal, M.K., Yu, K., Sekine, K.-T., Gao, Q., Selote, D., Hu, Y., Stromberg, A., Navarre, D., Kachroo, A., and Kachroo, P. (2011). Glycerol-3-phosphate is a critical mobile inducer of systemic immunity in plants. Nat. Genet. **43**: 421–7.

Cheng, F., Blackburn, K., Lin, Y., Goshe, M.B., and Williamson, J.D. (2009). Absolute protein quantification by LC/MS(E) for global analysis of salicylic acid-induced plant protein secretion responses. J. Proteome Res. **8**: 82–93.

Chevallet, M., Diemer, H., Van Dorssealer, A., Villiers, C., and Rabilloud, T. (2007). Toward a better analysis of secreted proteins: the example of the myeloid cells secretome. Proteomics **7**: 1757–70.

Chinchilla, D., Bauer, Z., and Regenass, M. (2006). The Arabidopsis receptor kinase FLS2 binds flg22 and determines the specificity of flagellin perception. Plant Cell **18**: 465–476.

Chinchilla, D., Zipfel, C., Robatzek, S., Kemmerling, B., Nürnberger, T., Jones, J.D.G., Felix, G., and Boller, T. (2007). A flagellin-induced complex of the receptor FLS2 and BAK1 initiates plant defence. Nature **448**: 497–500.

Clay, N.K., Adio, A.M., Denoux, C., Jander, G., and Ausubel, F.M. (2009). Glucosinolate metabolites required for an Arabidopsis innate immune response. Science **323**: 95–101.

Collins, N.C., Thordal-Christensen, H., Lipka, V., Bau, S., Kombrink, E., Qiu, J.-L., Hückelhoven, R., Stein, M., Freialdenhoven, A., Somerville, S.C., and Schulze-Lefert, P. (2003). SNARE-protein-mediated disease resistance at the plant cell wall. Nature **425**: 973–7.

Conrath, U. (2011). Molecular aspects of defence priming. Trends Plant Sci. **16**: 524–31.

Conrath, U. (2006). Systemic acquired resistance. Plant Signal. Behav. **1**: 179–84.

Conrath, U., Jeblick, W., and Kauss, H. (1991). The protein kinase inhibitor, K-252a, decreases elicitor-induced Ca^{2+} uptake and K^{+} release, and increases coumarin synthesis in parsley cells. FEBS Lett. **279**: 141–4.

Cornelis, G.R. and Van Gijsegem, F. (2000). Assembly and function of type III secretory systems. Annu. Rev. Microbiol. **54**: 735–74.

Crouzet, J., Trombik, T., Fraysse, Å.S., and Boutry, M. (2006). Organization and function of the plant pleiotropic drug resistance ABC transporter family. FEBS Lett. **580**: 1123–1130.

Cruz, M.F.A. da, Rodrigues, F.A., Leonora Rodriguez Polanco, C.R. da S.C., Nascimento, K.J.T., Moreira, M.A., and Barros, E.G. (2013). Inducers of resistance and silicon on the activity of defense enzymes in the soybean-*Phakopsora pachyrhizi* interaction. Bragantia **72**: 162–172.

Cunnac, S., Wilson, A., Nuwer, J., Kirik, A., Baranage, G., and Mudgett, M.B. (2007). A conserved carboxylesterase is a SUPPRESSOR OF AVRBST-ELICITED RESISTANCE in Arabidopsis. Plant Cell **19**: 688–705.

Curran, A., Chang, I.-F., Chang, C.-L., Garg, S., Miguel, R.M., Barron, Y.D., Li, Y., Romanowsky, S., Cushman, J.C., Gribskov, M., Harmon, A.C., and Harper, J.F. (2011). Calcium-dependent protein kinases from Arabidopsis show substrate specificity differences in an analysis of 103 substrates. Front. Plant Sci. **2**: 36.

D'Ovidio, R., Mattei, B., Roberti, S., and Bellincampi, D. (2004). Polygalacturonases, polygalacturonase-inhibiting proteins and pectic oligomers in plant-pathogen interactions. Biochim. Biophys. Acta **1696**: 237–44.

Dangl, J.L. and Jones, J.D.G. (2001). Plant pathogens and integrated defence responses to infection. Nature **411**: 826–33.

Davenport, R. (2002). Glutamate receptors in plants. Ann. Bot. **90**: 549–57.

Deverall, B.J., Keogh, R.C., and McLeod, S. (1977). Responses of soybean to infection by, and to germination fluids from, urediniospores of *Phakopsora pachyrhizi*. Trans. Br. Mycol. Soc. **69**: 411–415.

Djamei, A. et al. (2011). Metabolic priming by a secreted fungal effector. Nature **478**: 395–8.

Doares, S.H., Narvaez-Vasquez, J., Conconi, A., and Ryan, C.A. (1995). Salicylic acid inhibits synthesis of proteinase inhibitors in tomato leaves induced by systemin and jasmonic acid. Plant Physiol. **108**: 1741–1746.

Van der Does, D., Leon-Reyes, A., Koornneef, A., Van Verk, M.C., Rodenburg, N., Pauwels, L., Goossens, A., Körbes, A.P., Memelink, J., Ritsema, T., Van Wees, S.C.M., and Pieterse, C.M.J. (2013). Salicylic acid suppresses jasmonic acid signaling downstream of SCFCOI1-JAZ by targeting GCC promoter motifs via transcription factor ORA59. Plant Cell **25**: 744–61.

Du, L., Ali, G.S., Simons, K.A., Hou, J., Yang, T., Reddy, A.S.N., and Poovaiah, B.W. (2009). Ca^{2+}/calmodulin regulates salicylic-acid-mediated plant immunity. Nature **457**: 1154–8.

Eckardt, N.A. (2008). Chitin signaling in plants: insights into the perception of fungal pathogens and rhizobacterial symbionts. Plant Cell **20**: 241–3.

Elmore, J.M., Lin, Z.-J.D., and Coaker, G. (2011). Plant NB-LRR signaling: upstreams and downstreams. Curr. Opin. Plant Biol. **14**: 365–71.

Eulgem, T. and Somssich, I.E. (2007). Networks of WRKY transcription factors in defense signaling. Curr. Opin. Plant Biol. **10**: 366–71.

FAOSTAT (2012). Food and Agriculture Organization of the United Nations. http://faostat3.fao.org/faostat-gateway/go/to/home/E.

Felix, G. and Boller, T. (1995). Systemin induces rapid ion fluxes and ethylene biosynthesis in *Lycopersicon peruvianum* cells. Plant J. **7**: 381–389.

Felix, G., Duran, J.D., Volko, S., and Boller, T. (1999). Plants have a sensitive perception system for the most conserved domain of bacterial flagellin. Plant J. **18**: 265–76.

Felton, G.W. and Korth, K.L. (2000). Trade-offs between pathogen and herbivore resistance. Curr. Opin. Plant Biol. **3**: 309–14.

Feys, B.J. and Parker, J.E. (2000). Interplay of signaling pathways in plant disease resistance. Trends Genet. **16**: 449–55.

Feys, B.J., Wiermer, M., Bhat, R.A., Moisan, L.J., Medina-Escobar, N., Neu, C., Cabral, A., and Parker, J.E. (2005). Arabidopsis SENESCENCE-ASSOCIATED GENE101 stabilizes and signals within an ENHANCED DISEASE SUSCEPTIBILITY1 complex in plant innate immunity. Plant Cell **17**: 2601–13.

Fischer, R., Koller, M., Flura, M., Mathews, S., Strehler-Page, M.A., Krebs, J., Penniston, J.T., Carafoli, E., and Strehler, E.E. (1988). Multiple divergent mRNAs code for a single human calmodulin. J. Biol. Chem. **263**: 17055–62.

Flor, H.H. (1971). Current status of the gene-for-gene concept. Annu. Rev. Phytopathol. **9**: 275–296.

Fukao, Y. (2012). Protein-protein interactions in plants. Plant Cell Physiol. **53**: 617–25.

Gao, M., Liu, J., Bi, D., Zhang, Z., Cheng, F., Chen, S., and Zhang, Y. (2008). MEKK1, MKK1/MKK2 and MPK4 function together in a mitogen-activated protein kinase cascade to regulate innate immunity in plants. Cell Res. **18**: 1190–8.

Gehl, C., Waadt, R., Kudla, J., Mendel, R.-R., and Hänsch, R. (2009). New GATEWAY vectors for high throughput analyses of protein-protein interactions by bimolecular fluorescence complementation. Mol. Plant **2**: 1051–8.

Geisler-Lee, J., O'Toole, N., Ammar, R., Provart, N.J., Millar, A.H., and Geisler, M. (2007). A predicted interactome for Arabidopsis. Plant Physiol. **145**: 317–29.

Gifford, J.L., Jamshidiha, M., Mo, J., Ishida, H., and Vogel, H.J. (2013). Comparing the calcium binding abilities of two soybean calmodulins: towards understanding the divergent nature of plant calmodulins. Plant Cell **25**: 4512–24.

Glazebrook, J. (2005). Contrasting mechanisms of defense against biotrophic and necrotrophic pathogens. Annu. Rev. Phytopathol. **43**: 205–27.

Goellner, K., Loehrer, M., Langenbach, C., Conrath, U., Koch, E., and Schaffrath, U. (2010). *Phakopsora pachyrhizi*, the causal agent of Asian soybean rust. Mol. Plant Pathol. **11**: 169–77.

Gómez-Gómez, L. and Boller, T. (2000). FLS2: an LRR receptor-like kinase involved in the perception of the bacterial elicitor flagellin in Arabidopsis. Mol. Cell **5**: 1003–1011.

Grant, M.R. and Jones, J.D.G. (2009). Hormone (dis)harmony moulds plant health and disease. Science **324**: 750–2.

Groot, A.J., Verheesen, P., Westerlaken, E.J., Gort, E.H., van der Groep, P., Bovenschen, N., van der Wall, E., van Diest, P.J., and Shvarts, A. (2006). Identification by phage display of single-domain antibody fragments specific for the ODD domain in hypoxia-inducible factor 1alpha. Lab. Invest. **86**: 345–56.

Gu, Y.Q., Yang, C., Thara, V.K., Zhou, J., and Martin, G.B. (2000). *Pti4* is induced by ethylene and salicylic acid, and its product is phosphorylated by the Pto kinase. Plant Cell **12**: 771–86.

Guo, H. and Ecker, J.R. (2003). Plant responses to ethylene gas are mediated by SCF(EBF1/EBF2)-dependent proteolysis of EIN3 transcription factor. Cell **115**: 667–77.

Hahn, M. and Mendgen, K. (2001). Signal and nutrient exchange at biotrophic plant-fungus interfaces. Curr. Opin. Plant Biol. **4**: 322–7.

Halkier, B.A. and Gershenzon, J. (2006). Biology and biochemistry of glucosinolates. Annu. Rev. Plant Biol. **57**: 303–33.

Haruta, M., Monshausen, G., Gilroy, S., and Sussman, M.R. (2008). A cytoplasmic Ca^{2+} functional assay for identifying and purifying endogenous cell signaling peptides in Arabidopsis seedlings: identification of AtRALF1 peptide. Biochemistry **47**: 6311–21.

Haruta, M., Sabat, G., Stecker, K., Minkoff, B.B., and Sussman, M.R. (2014). A peptide hormone and its receptor protein kinase regulate plant cell expansion. Science **343**: 408–11.

Hauck, P., Thilmony, R., and He, S.Y. (2003). A *Pseudomonas syringae* type III effector suppresses cell wall-based extracellular defense in susceptible Arabidopsis plants. Proc. Natl. Acad. Sci. U. S. A. **100**: 8577–82.

Heath, M.C. (2000). Nonhost resistance and nonspecific plant defenses. Curr. Opin. Plant Biol. **3**: 315–9.

Hennings, P. (1903). Einige neue japanische Uredinales (in German). Hedwigia **IV Suppl.**: 107–108.

Heo, W.D., Lee, S.H., Kim, M.C., Kim, J.C., Chung, W.S., Chun, H.J., Lee, K.J., Park, C.Y., Park, H.C., Choi, J.Y., and Cho, M.J. (1999). Involvement of specific calmodulin isoforms in salicylic acid-independent activation of plant disease resistance responses. Proc. Natl. Acad. Sci. U. S. A. **96**: 766–71.

Herskowitz, I. (1995). MAP kinase pathways in yeast: for mating and more. Cell **80**: 187–97.

Higgins, C.F. (1992). ABC transporters: from microorganisms to man. Annu. Rev. Cell Biol. **8**: 67–113.

Hofmann, N.R. (2013). Calmodulin methylation: another layer of regulation in calcium signaling. Plant Cell **25**: 4284.

Hogenhout, S.A., Van der Hoorn, R.A.L., Terauchi, R., and Kamoun, S. (2009). Emerging concepts in effector biology of plant-associated organisms. Mol. Plant. Microbe. Interact. **22**: 115–22.

Hu, C.-D., Chinenov, Y., and Kerppola, T.K. (2002). Visualization of interactions among bZIP and Rel family proteins in living cells using bimolecular fluorescence complementation. Mol. Cell **9**: 789–98.

Hubert, D.A., Tornero, P., Belkhadir, Y., Krishna, P., Takahashi, A., Shirasu, K., and Dangl, J.L. (2003). Cytosolic HSP90 associates with and modulates the Arabidopsis RPM1 disease resistance protein. EMBO J. **22**: 5679–89.

Hückelhoven, R., Dechert, C., and Kogel, K.-H. (2003). Overexpression of barley BAX inhibitor 1 induces breakdown of mlo-mediated penetration resistance to *Blumeria graminis*. Proc. Natl. Acad. Sci. U. S. A. **100**: 5555–60.

Huffaker, A., Pearce, G., and Ryan, C.A. (2006). An endogenous peptide signal in Arabidopsis activates components of the innate immune response. Proc. Natl. Acad. Sci. U. S. A. **103**: 10098–103.

Huffaker, A. and Ryan, C.A. (2007). Endogenous peptide defense signals in Arabidopsis differentially amplify signaling for the innate immune response. Proc. Natl. Acad. Sci. U. S. A. **104**: 10732–6.

Huitema, E., Bos, J.I.B., Tian, M., Win, J., Waugh, M.E., and Kamoun, S. (2004). Linking sequence to phenotype in *Phytophthora*-plant interactions. Trends Microbiol. **12**: 193–200.

Humphry, M., Bednarek, P., Kemmerling, B., Koh, S., Stein, M., Göbel, U., Stüber, K., Pislewska-Bednarek, M., Loraine, A., Schulze-Lefert, P., Somerville, S., and Panstruga, R. (2010). A regulon conserved in monocot and dicot plants defines a functional module in antifungal plant immunity. Proc. Natl. Acad. Sci. U. S. A. **107**: 21896–901.

Ishida, H., Huang, H., Yamniuk, A.P., Takaya, Y., and Vogel, H.J. (2008). The solution structures of two soybean calmodulin isoforms provide a structural basis for their selective target activation properties. J. Biol. Chem. **283**: 14619–28.

Jones, J.D.G. and Dangl, J.L. (2006). The plant immune system. Nature **444**: 323–9.

Jorgensen, J.H. (1992). Discovery , characterization and exploitation of Mlo powdery mildew resistance in barley. Euphytica **66**: 141–152.

Kanzaki, H., Saitoh, H., Ito, A., Fujisawa, S., Kamoun, S., Katou, S., Yoshioka, H., and Terauchi, R. (2003). Cytosolic HSP90 and HSP70 are essential components of INF1-mediated hypersensitive response and non-host resistance to *Pseudomonas cichorii* in *Nicotiana benthamiana*. Mol. Plant Pathol. **4**: 383–91.

Kauss, H., Fauth, M., Merten, A., and Jeblick, W. (1999). Cucumber hypocotyls respond to cutin monomers via both an inducible and a constitutive H_2O_2-generating system. Plant Physiol. **120**: 1175–82.

Kawai-Yamada, M., Hori, Z., Ogawa, T., Ihara-Ohori, Y., Tamura, K., Nagano, M., Ishikawa, T., and Uchimiya, H. (2009). Loss of calmodulin binding to Bax inhibitor-1 affects *Pseudomonas*-mediated hypersensitive response-associated cell death in *Arabidopsis thaliana*. J. Biol. Chem. **284**: 27998–8003.

Kay, S. and Bonas, U. (2009). How *Xanthomonas* type III effectors manipulate the host plant. Curr. Opin. Microbiol. **12**: 37–43.

Kemen, E., Kemen, A.C., Rafiqi, M., Hempel, U., Mendgen, K., Hahn, M., and Voegele, R.T. (2005). Identification of a protein from rust fungi transferred from haustoria into infected plant cells. Mol. Plant. Microbe. Interact. **18**: 1130–9.

Keogh, R.C., Deverall, B.J., and McLeod, S. (1980). Comparison of histological and physiological responses to *Phakopsora pachyrhizi* in resistant and susceptible soybean. Trans. Br. Mycol. Soc.: 329–333.

Killgore, E., Heu, R., and Gardner, D.E. (1994). First report of soybean rust in Hawaii. Plant Dis. **78**: 1216–1216.

Kim, D.-Y., Bovet, L., Maeshima, M., Martinoia, E., and Lee, Y. (2007). The ABC transporter AtPDR8 is a cadmium extrusion pump conferring heavy metal resistance. Plant J. **50**: 207–18.

Kim, H.S. and Delaney, T.P. (2002). Arabidopsis SON1 is an F-box protein that regulates a novel induced defense response independent of both salicylic acid and systemic acquired resistance. Plant Cell **14**: 1469–82.

Kim, M.C. et al. (2002a). Mlo, a modulator of plant defense and cell death, is a novel calmodulin-binding protein. Isolation and characterization of a rice Mlo homologue. J. Biol. Chem. **277**: 19304–14.

Kim, M.C., Panstruga, R., Elliott, C., Müller, J., Devoto, A., Yoon, H.W., Park, H.C., Cho, M.J., and Schulze-Lefert, P. (2002b). Calmodulin interacts with MLO protein to regulate defence against mildew in barley. Nature **416**: 447–51.

Kim, M.G., da Cunha, L., McFall, A.J., Belkhadir, Y., DebRoy, S., Dangl, J.L., and Mackey, D. (2005). Two *Pseudomonas syringae* type III effectors inhibit RIN4-regulated basal defense in Arabidopsis. Cell **121**: 749–59.

Kipreos, E.T. and Pagano, M. (2000). The F-box protein family. Genome Biol. **1**: REVIEWS3002.

Kirik, A. and Mudgett, M.B. (2009). SOBER1 phospholipase activity suppresses phosphatidic acid accumulation and plant immunity in response to bacterial effector AvrBsT. Proc. Natl. Acad. Sci. U. S. A. **106**: 20532–7.

Kline, K.G., Barrett-Wilt, G. a, and Sussman, M.R. (2010). In planta changes in protein phosphorylation induced by the plant hormone abscisic acid. Proc. Natl. Acad. Sci. U. S. A. **107**: 15986–91.

Kobae, Y., Sekino, T., Yoshioka, H., Nakagawa, T., Martinoia, E., and Maeshima, M. (2006). Loss of AtPDR8, a plasma membrane ABC transporter of *Arabidopsis thaliana*, causes hypersensitive cell death upon pathogen infection. Plant Cell Physiol. **47**: 309–18.

Koch, E., Ebrahim-Nesbat, F., and Hoppe, H.H. (1983). Light and electron microscopy studies on the development of soybean rust (*Phakopsora pachyrhizi* Syd.) in susceptible soybean leaves. Phytopathology **106**: 302–320.

Krasileva, K. V, Dahlbeck, D., and Staskawicz, B.J. (2010). Activation of an Arabidopsis resistance protein is specified by the in planta association of its leucine-rich repeat domain with the cognate oomycete effector. Plant Cell **22**: 2444–58.

Kuhn, H. and Panstruga, R. (2014). Introduction to a Virtual Special Issue on phytopathogen effector proteins. New Phytol. **202**: 727–30.

Kunze, G., Zipfel, C., Robatzek, S., Niehaus, K., Boller, T., and Felix, G. (2004). The N terminus of bacterial elongation factor Tu elicits innate immunity in Arabidopsis plants. Plant Cell **16**: 3496–507.

Kurosaki, F., Tsurusawa, Y., and Nishi, A. (1987). Breakdown of phosphatidylinositol during the elicitation of phytoalexin production in cultured carrot cells. Plant Physiol. **85**: 601–4.

Laemmli, U.K. (1970). Cleavage of structural proteins during the assembly of the head of bacteriophage T4. Nature **227**: 680–5.

Lafitte, D., Heck, A.J., Hill, T.J., Jumel, K., Harding, S.E., and Derrick, P.J. (1999). Evidence of noncovalent dimerization of calmodulin. Eur. J. Biochem. **261**: 337–44.

Langenbach, C., Campe, R., Schaffrath, U., Goellner, K., and Conrath, U. (2013). UDP-glucosyltransferase UGT84A2/BRT1 is required for Arabidopsis nonhost resistance to the Asian soybean rust pathogen *Phakopsora pachyrhizi*. New Phytol. **198**: 536–45.

Leba, L.-J., Cheval, C., Ortiz-Martín, I., Ranty, B., Beuzón, C.R., Galaud, J.-P., and Aldon, D. (2012). CML9, an Arabidopsis calmodulin-like protein, contributes to plant innate immunity through a flagellin-dependent signalling pathway. Plant J. **71**: 976–89.

Lecourieux, D., Ranjeva, R., and Pugin, A. (2006). Calcium in plant defence-signalling pathways. New Phytol. **171**: 249–69.

Lee, K., Song, E.H., Kim, H.S., Yoo, J.H., Han, H.J., Jung, M.S., Lee, S.M., Kim, K.E., Kim, M.C., Cho, M.J., and Chung, W.S. (2008). Regulation of MAPK phosphatase 1 (AtMKP1) by calmodulin in Arabidopsis. J. Biol. Chem. **283**: 23581–8.

Lee, S.H., Kim, J.C., Lee, M.S., Heo, W.D., Seo, H.Y., Yoon, H.W., Hong, J.C., Lee, S.Y., Bahk, J.D., and Hwang, I. (1995). Identification of a novel divergent calmodulin isoform from soybean which has differential ability to activate calmodulin-dependent enzymes. J. Biol. Chem. **270**: 21806–12.

Leon-Reyes, A., Spoel, S.H., De Lange, E.S., Abe, H., Kobayashi, M., Tsuda, S., Millenaar, F.F., Welschen, R.A.M., Ritsema, T., and Pieterse, C.M.J. (2009). Ethylene modulates the role of NONEXPRESSOR OF PATHOGENESIS-RELATED GENES1 in cross talk between salicylate and jasmonate signaling. Plant Physiol. **149**: 1797–809.

Levy, C. (2005). Epidemiology and chemical control of soybean rust in southern Africa. Plant Dis. **89**: 669–674.

Li, J., Liu, J., and Sun, D. (1993). Immunoelectron microscopic localization of calmodulin in corn root cells. Cell Res. **3**: 11–19.

Lipka, V. et al. (2005). Pre- and postinvasion defenses both contribute to nonhost resistance in Arabidopsis. Science **310**: 1180–3.

Liu, Y., Burch-Smith, T., Schiff, M., Feng, S., and Dinesh-Kumar, S.P. (2004). Molecular chaperone Hsp90 associates with resistance protein N and its signaling proteins SGT1 and Rar1 to modulate an innate immune response in plants. J. Biol. Chem. **279**: 2101–8.

Loake, G. and Grant, M. (2007). Salicylic acid in plant defence—the players and protagonists. Curr. Opin. Plant Biol. **10**: 466–472.

Loehrer, M., Langenbach, C., Goellner, K., Conrath, U., and Schaffrath, U. (2008). Characterization of nonhost resistance of Arabidopsis to the Asian soybean rust. Mol. Plant. Microbe. Interact. **21**: 1421–30.

Van Loon, L.C., Geraats, B.P.J., and Linthorst, H.J.M. (2006). Ethylene as a modulator of disease resistance in plants. Trends Plant Sci. **11**: 184–91.

Macho, A.P. et al. (2014). A bacterial tyrosine phosphatase inhibits plant pattern recognition receptor activation. Science **343**: 1509–12.

Malamy, J., Carr, J.P., Klessig, D.F., and Raskin, I. (1990). Salicylic acid: a likely endogenous signal in the resistance response of tobacco to viral infection. Science **250**: 1002–4.

Manning, V.A., Chu, A.L., Steeves, J.E., Wolpert, T.J., and Ciuffetti, L.M. (2009). A host-selective toxin of *Pyrenophora tritici-repentis*, Ptr ToxA, induces photosystem changes and reactive oxygen species accumulation in sensitive wheat. Mol. Plant. Microbe. Interact. **22**: 665–76.

Manning, V.A. and Ciuffetti, L.M. (2005). Localization of Ptr ToxA produced by *Pyrenophora tritici-repentis* reveals protein import into wheat mesophyll cells. Plant Cell **17**: 3203–12.

Martinoia, E., Klein, M., Geisler, M., Bovet, L., Forestier, C., Kolukisaoglu, U., Müller-Röber, B., and Schulz, B. (2002). Multifunctionality of plant ABC transporters-more than just detoxifiers. Planta **214**: 345–55.

McAinsh, M.R. and Hetherington, A.M. (1998). Encoding specificity in Ca^{2+} signalling systems. Trends Plant Sci. **3**: 32–36.

McCormack, E. and Braam, J. (2003). Calmodulins and related potential calcium sensors of Arabidopsis. New Phytol. **159**: 585–598.

Meador, W.E., Means, A.R., and Quiocho, F.A. (1993). Modulation of calmodulin plasticity in molecular recognition on the basis of x-ray structures. Science **262**: 1718–21.

Mellersh, D.G. and Heath, M.C. (2003). An investigation into the involvement of defense signaling pathways in components of the nonhost resistance of *Arabidopsis thaliana* to rust fungi also reveals a model system for studying rust fungal compatibility. Mol. Plant. Microbe. Interact. **16**: 398–404.

Menke, F.L.H., van Pelt, J.A., Pieterse, C.M.J., and Klessig, D.F. (2004). Silencing of the mitogen-activated protein kinase MPK6 compromises disease resistance in Arabidopsis. Plant Cell **16**: 897–907.

Métraux, J.P., Signer, H., Ryals, J., Ward, E., Wyss-Benz, M., Gaudin, J., Raschdorf, K., Schmid, E., Blum, W., and Inverardi, B. (1990). Increase in salicylic acid at the onset of systemic acquired resistance in cucumber. Science **250**: 1004–6.

Meyer, D., Pajonk, S., Micali, C., O'Connell, R., and Schulze-Lefert, P. (2009). Extracellular transport and integration of plant secretory proteins into pathogen-induced cell wall compartments. Plant J. **57**: 986–99.

Miles, M.R., Hartman, G.L., Levy, C., Farmers, C., and Morel, W. (2003). Current status of soybean rust by fungicides. Pestic. Outlook: 197–200.

Miles, M.R., Levy, C., Morel, W., Mueller, T., Steinlage, T., van Rij, N., Frederick, R.D., and Hartman, G.L. (2007). International fungicide efficacy trials for the management of soybean rust. Plant Dis. **91**: 1450–1458.

Miya, A., Albert, P., Shinya, T., Desaki, Y., Ichimura, K., Shirasu, K., Narusaka, Y., Kawakami, N., Kaku, H., and Shibuya, N. (2007). CERK1, a LysM receptor kinase, is essential for chitin elicitor signaling in Arabidopsis. Proc. Natl. Acad. Sci. U. S. A. **104**: 19613–8.

Moreau, M., Westlake, T., Zampogna, G., Popescu, G., Tian, M., Noutsos, C., and Popescu, S. (2013). The Arabidopsis oligopeptidases TOP1 and TOP2 are salicylic acid targets that modulate SA-mediated signaling and the immune response. Plant J. **76**: 603–14.

Mousavi, S.A.R., Chauvin, A., Pascaud, F., Kellenberger, S., and Farmer, E.E. (2013). GLUTAMATE RECEPTOR-LIKE genes mediate leaf-to-leaf wound signalling. Nature **500**: 422–6.

Mur, L.A.J., Kenton, P., Atzorn, R., Miersch, O., and Wasternack, C. (2006). The outcomes of concentration-specific interactions between salicylate and jasmonate signaling include synergy, antagonism, and oxidative stress leading to cell death. Plant Physiol. **140**: 249–62.

Mysore, K.S. and Ryu, C.-M. (2004). Nonhost resistance: how much do we know? Trends Plant Sci. **9**: 97–104.

Nandi, A., Welti, R., and Shah, J. (2004). The Arabidopsis thaliana dihydroxyacetone phosphate reductase gene SUPPRESSSOR OF FATTY ACID DESATURASE DEFICIENCY1 is required for glycerolipid metabolism and for the activation of systemic acquired resistance. Plant Cell **16**: 465–77.

Návarová, H., Bernsdorff, F., Döring, A.-C., and Zeier, J. (2012). Pipecolic acid, an endogenous mediator of defense amplification and priming, is a critical regulator of inducible plant immunity. Plant Cell **24**: 5123–41.

Newman, M.-A., Dow, J.M., Molinaro, A., and Parrilli, M. (2007). Priming, induction and modulation of plant defence responses by bacterial lipopolysaccharides. J. Endotoxin Res. **13**: 69–84.

Ng, C.K.-Y. and McAinsh, M.R. (2003). Encoding specificity in plant calcium signalling: hot-spotting the ups and downs and waves. Ann. Bot. **92**: 477–85.

Niki, T., Mitsuhara, I., Seo, S., Ohtsubo, N., and Ohashi, Y. (1998). Antagonistic effect of salicylic acid and jasmonic acid on the expression of pathogenesis-related (PR) protein genes in wounded mature tobacco leaves. Plant Cell Physiol. **39**: 500–507.

Nürnberger, T., Brunner, F., Kemmerling, B., and Piater, L. (2004). Innate immunity in plants and animals: striking similarities and obvious differences. Immunol. Rev. **198**: 249–66.

Oh, S.H. and Roberts, D.M. (1990). Analysis of the state of posttranslational calmodulin methylation in developing pea plants. Plant Physiol. **93**: 880–7.

Ono, Y., Buriticá, P., and Hennen, J.F. (1992). Delimitation of *Phakopsora*, *Physopella* and *Cerotelium* and their species on Leguminosae. Mycol. Res. **96**: 825–850.

Panstruga, R. (2003). Establishing compatibility between plants and obligate biotrophic pathogens. Curr. Opin. Plant Biol. **6**: 320–326.

Panstruga, R. and Dodds, P.N. (2009). Terrific protein traffic: the mystery of effector protein delivery by filamentous plant pathogens. Science **324**: 748–50.

Park, S.-W., Kaimoyo, E., Kumar, D., Mosher, S., and Klessig, D.F. (2007). Methyl salicylate is a critical mobile signal for plant systemic acquired resistance. Science **318**: 113–6.

Pearce, G., Strydom, D., Johnson, S., and Ryan, C.A. (1991). A polypeptide from tomato leaves induces wound-inducible proteinase inhibitor proteins. Science **253**: 895–7.

Perera, I.Y. and Zielinski, R.E. (1992). Structure and expression of the Arabidopsis CaM-3 calmodulin gene. Plant Mol. Biol. **19**: 649–64.

Petersen, M. et al. (2000). Arabidopsis map kinase 4 negatively regulates systemic acquired resistance. Cell **103**: 1111–20.

Pfaffl, M.W. (2001). A new mathematical model for relative quantification in real-time RT-PCR. Nucleic Acids Res. **29**: e45.

Pieterse, C.M., van Wees, S.C., Hoffland, E., van Pelt, J.A., and van Loon, L.C. (1996). Systemic resistance in Arabidopsis induced by biocontrol bacteria is independent of salicylic acid accumulation and pathogenesis-related gene expression. Plant Cell **8**: 1225–37.

Pieterse, C.M., van Wees, S.C., van Pelt, J.A., Knoester, M., Laan, R., Gerrits, H., Weisbeek, P.J., and van Loon, L.C. (1998). A novel signaling pathway controlling induced systemic resistance in Arabidopsis. Plant Cell **10**: 1571–80.

Pieterse, C.M.J., Leon-Reyes, A., Van der Ent, S., and Van Wees, S.C.M. (2009). Networking by small-molecule hormones in plant immunity. Nat. Chem. Biol. **5**: 308–316.

Poovaiah, B.W., Du, L., Wang, H., and Yang, T. (2013). Recent advances in calcium/Calmodulin-mediated signaling with an emphasis on plant:microbe interactions. Plant Physiol. **163**: 531–42.

Popescu, S.C., Popescu, G. V, Bachan, S., Zhang, Z., Gerstein, M., Snyder, M., and Dinesh-kumar, S.P. (2009). MAPK target networks in *Arabidopsis thaliana* revealed using functional protein microarrays. Genes Dev. **23**: 80–92.

Popescu, S.C., Popescu, G. V, Bachan, S., Zhang, Z., Seay, M., Gerstein, M., Snyder, M., and Dinesh-Kumar, S.P. (2007a). Differential binding of calmodulin-related proteins to their targets revealed through high-density Arabidopsis protein microarrays. Proc. Natl. Acad. Sci. U. S. A. **104**: 4730–5.

Popescu, S.C., Snyder, M., and Dinesh-Kumar, S.P. (2007b). Arabidopsis Protein Microarrays for the High-Throughput Identification of Protein-Protein Interactions. Plant Signal. Behav. **2**: 416–420.

Potuschak, T., Lechner, E., Parmentier, Y., Yanagisawa, S., Grava, S., Koncz, C., and Genschik, P. (2003). EIN3-dependent regulation of plant ethylene hormone signaling by two arabidopsis F box proteins: EBF1 and EBF2. Cell **115**: 679–89.

Pozo, M.J., Loon, L.C., and Pieterse, C.M.J. (2004). Jasmonates—Signals in plant-microbe interactions. J. Plant Growth Regul. **23**: 211–222.

Pré, M., Atallah, M., Champion, A., De Vos, M., Pieterse, C.M.J., and Memelink, J. (2008). The AP2/ERF domain transcription factor ORA59 integrates jasmonic acid and ethylene signals in plant defense. Plant Physiol. **147**: 1347–57.

Qi, Y. and Katagiri, F. (2009). Purification of low-abundance Arabidopsis plasma-membrane protein complexes and identification of candidate components. Plant J. **57**: 932–44.

Rhoads, R. and Friedberg, F. (1997). Sequence motifs for calmodulin recognition. FASEB J. **11**: 331–340.

Roberts, D.M., Besl, L., Oh, S.H., Masterson, R. V, Schell, J., and Stacey, G. (1992). Expression of a calmodulin methylation mutant affects the growth and development of transgenic tobacco plants. Proc. Natl. Acad. Sci. U. S. A. **89**: 8394–8.

Roberts, D.M., Rowe, P.M., Siegel, F.L., Lukas, T.J., and Watterson, D.M. (1986). Trimethyllysine and protein function. Effect of methylation and mutagenesis of lysine 115 of calmodulin on NAD kinase activation. J. Biol. Chem. **261**: 1491–4.

Ross, A., Yamada, K., Hiruma, K., Yamashita-Yamada, M., Lu, X., Takano, Y., Tsuda, K., and Saijo, Y. (2014). The Arabidopsis PEPR pathway couples local and systemic plant immunity. EMBO J. **33**: 62–75.

Roux, M., Schwessinger, B., Albrecht, C., Chinchilla, D., Jones, A., Holton, N., Malinovsky, F.G., Tör, M., de Vries, S., and Zipfel, C. (2011). The Arabidopsis leucine-rich repeat receptor-like kinases BAK1/SERK3 and BKK1/SERK4 are required for innate immunity to hemibiotrophic and biotrophic pathogens. Plant Cell **23**: 2440–55.

Ryals, J.A., Neuenschwander, U.H., Willits, M.G., Molina, A., Steiner, H.Y., and Hunt, M.D. (1996). Systemic acquired resistance. Plant Cell **8**: 1809–1819.

Rytter, J.L. (1984). Additional alternative hosts of *Phakopsora pachyrhizi*, causal agent of soybean rust. Plant Dis. **68**: 818–819.

Sánchez-Fernández, R., Davies, T.G., Coleman, J.O., and Rea, P.A. (2001). The *Arabidopsis thaliana* ABC protein superfamily, a complete inventory. J. Biol. Chem. **276**: 30231–44.

Sanders, D., Brownlee, C., and Harper, J. (1999). Communicating with calcium. Plant Cell **11**: 691–706.

Sanders, D., Pelloux, J., Brownlee, C., and Harper, J.F. (2002). Calcium at the crossroads of signaling. Plant Cell **14 Suppl**: S401–17.

Schenk, P.M., Kazan, K., Wilson, I., Anderson, J.P., Richmond, T., Somerville, S.C., and Manners, J.M. (2000). Coordinated plant defense responses in Arabidopsis revealed by microarray analysis. Proc. Natl. Acad. Sci. U. S. A. **97**: 11655–60.

Schneider, R.W., Hollier, C.A., Whitam, H.K., Palm, M.E., McKemy, J.M., Hernández, J.R., Levy, L., and DeVries-Paterson, R. (2005). First report of soybean rust caused by *Phakopsora pachyrhizi* in the continental United States. Plant Dis. **89**: 774–774.

Schulze-Lefert, P. and Panstruga, R. (2011). A molecular evolutionary concept connecting nonhost resistance, pathogen host range, and pathogen speciation. Trends Plant Sci. **16**: 117–25.

Schweizer, P., Felix, G., Buchala, A., Muller, C., and Metraux, J.-P. (1996). Perception of free cutin monomers by plant cells. Plant J. **10**: 331–341.

Schwessinger, B., Roux, M., Kadota, Y., Ntoukakis, V., Sklenar, J., Jones, A., and Zipfel, C. (2011). Phosphorylation-dependent differential regulation of plant growth, cell death, and innate immunity by the regulatory receptor-like kinase BAK1. PLoS Genet. **7**: e1002046.

Schwessinger, B. and Zipfel, C. (2008). News from the frontline: recent insights into PAMP-triggered immunity in plants. Curr. Opin. Plant Biol. **11**: 389–95.

Shah, J., Chaturvedi, R., Chowdhury, Z., Venables, B., and Petros, R.A. (2014). Signaling by small metabolites in systemic acquired resistance. Plant J.: epub ahead of print.

Singh, K., Foley, R.C., and Oñate-Sánchez, L. (2002). Transcription factors in plant defense and stress responses. Curr. Opin. Plant Biol. **5**: 430–6.

Songyang, Z. et al. (1996). A structural basis for substrate specificities of protein Ser/Thr kinases: primary sequence preference of casein kinases I and II, NIMA, phosphorylase kinase, calmodulin-dependent kinase II, CDK5, and Erk1. Mol. Cell. Biol. **16**: 6486–93.

Spoel, S.H. et al. (2003). NPR1 modulates cross-talk between salicylate- and jasmonate-dependent defense pathways through a novel function in the cytosol. Plant Cell **15**: 760–770.

Stäb, M.R. and Ebel, J. (1987). Effects of Ca2+ on phytoalexin induction by fungal elicitor in soybean cells. Arch. Biochem. Biophys. **257**: 416–23.

Stein, M., Dittgen, J., Sánchez-Rodrígez, C., Hou, B.-H., Molina, A., Schulze-Lefert, P., Lipka, V., and Somerville, S. (2006). Arabidopsis PEN3/PDR8, an ATP binding cassette transporter, contributes to nonhost resistance to inappropriate pathogens that enter by direct penetration. Plant Cell **18**: 731–746.

Stokstad, E. (2004). Agriculture. Plant pathologists gear up for battle with dread fungus. Science **306**: 1672–3.

Storey, J.D. (2002). A direct approach to false discovery rates. J. R. Stat. Soc. Ser. B **64**: 479–498.

Strader, L.C. and Bartel, B. (2009). The Arabidopsis PLEIOTROPIC DRUG RESISTANCE8/ABCG36 ATP binding cassette transporter modulates sensitivity to the auxin precursor indole-3-butyric acid. Plant Cell **21**: 1992–2007.

Strynadka, N.C. and James, M.N. (1989). Crystal structures of the helix-loop-helix calcium-binding proteins. Annu. Rev. Biochem. **58**: 951–98.

Sun, W., Cao, Y., Jansen Labby, K., Bittel, P., Boller, T., and Bent, A.F. (2012). Probing the Arabidopsis flagellin receptor: FLS2-FLS2 association and the contributions of specific domains to signaling function. Plant Cell **24**: 1096–113.

Sydow, H. and Sydow, P. (1914). A contribution to knowledge of the parasitic fungi on the island of Formosa. Ann. Mycol. **12**: 105.

Takahashi, A., Casais, C., Ichimura, K., and Shirasu, K. (2003). HSP90 interacts with RAR1 and SGT1 and is essential for RPS2-mediated disease resistance in Arabidopsis. Proc. Natl. Acad. Sci. U. S. A. **100**: 11777–82.

Takahashi, F., Yoshida, R., Ichimura, K., Mizoguchi, T., Seo, S., Yonezawa, M., Maruyama, K., Yamaguchi-Shinozaki, K., and Shinozaki, K. (2007). The mitogen-activated protein kinase cascade MKK3-MPK6 is an important part of the jasmonate signal transduction pathway in Arabidopsis. Plant Cell **19**: 805–18.

Tavernier, E., Wendehenne, D., Blein, J.P., and Pugin, A. (1995). Involvement of free calcium in action of cryptogein, a proteinaceous elicitor of hypersensitive reaction in tobacco cells. Plant Physiol. **109**: 1025–1031.

Testerink, C. and Munnik, T. (2005). Phosphatidic acid: a multifunctional stress signaling lipid in plants. Trends Plant Sci. **10**: 368–75.

Thomma, B.P., Eggermont, K., Penninckx, I. a, Mauch-Mani, B., Vogelsang, R., Cammue, B.P., and Broekaert, W.F. (1998). Separate jasmonate-dependent and salicylate-dependent defense-response pathways in Arabidopsis are essential for resistance to distinct microbial pathogens. Proc. Natl. Acad. Sci. U. S. A. **95**: 15107–11.

Thomma, B.P., Penninckx, I.A., Broekaert, W.F., and Cammue, B.P. (2001). The complexity of disease signaling in Arabidopsis. Curr. Opin. Immunol. **13**: 63–8.

Thomma, B.P.H.J., Nürnberger, T., and Joosten, M.H.A.J. (2011). Of PAMPs and effectors: the blurred PTI-ETI dichotomy. Plant Cell **23**: 4–15.

Tierens, K.F., Thomma, B.P., Brouwer, M., Schmidt, J., Kistner, K., Porzel, A., Mauch-Mani, B., Cammue, B.P., and Broekaert, W.F. (2001). Study of the role of antimicrobial glucosinolate-derived isothiocyanates in resistance of Arabidopsis to microbial pathogens. Plant Physiol. **125**: 1688–99.

De Torres, M., Sanchez, P., Fernandez-Delmond, I., and Grant, M. (2003). Expression profiling of the host response to bacterial infection: the transition from basal to induced defence responses in RPM1-mediated resistance. Plant J. **33**: 665–76.

Tremblay, A. (2009). Soybean rust : five years of research. In Soybean - Molecular Aspects of Breeding, pp. 293–334.

Trewavas, A.J. and Malhó, R. (1998). Ca^{2+} signalling in plant cells: the big network! Curr. Opin. Plant Biol. **1**: 428–33.

Trujillo, M., Ichimura, K., Casais, C., and Shirasu, K. (2008). Negative regulation of PAMP-triggered immunity by an E3 ubiquitin ligase triplet in Arabidopsis. Curr. Biol. **18**: 1396–401.

Tsuda, K. and Katagiri, F. (2010). Comparing signaling mechanisms engaged in pattern-triggered and effector-triggered immunity. Curr. Opin. Plant Biol. **13**: 459–65.

Udvardi, M.K., Czechowski, T., and Scheible, W.-R. (2008). Eleven golden rules of quantitative RT-PCR. Plant Cell **20**: 1736–7.

Uehara, E. (1958). On the phytoalexin production of the soybean pod in reaction to *Fusarium* sp., the casual fungus of pod blight. I. Some experiments on the phytoalexin production as affected by host plant conditions and on the nature of the phytoalexin produced. Ann. Phytopathol. Soc. Japan: 225–229.

Underwood, W. and Somerville, S.C. (2013). Perception of conserved pathogen elicitors at the plasma membrane leads to relocalization of the Arabidopsis PEN3 transporter. Proc. Natl. Acad. Sci. U. S. A. **110**: 12492–7.

Uppalapati, S.R., Ishiga, Y., Wangdi, T., Kunkel, B.N., Anand, A., Mysore, K.S., and Bender, C.L. (2007). The phytotoxin coronatine contributes to pathogen fitness and is required for suppression of salicylic acid accumulation in tomato inoculated with *Pseudomonas syringae pv. tomato* DC3000. Mol. Plant. Microbe. Interact. **20**: 955–65.

Vadassery, J. and Oelmüller, R. (2009). Calcium signaling in pathogenic and beneficial plant microbe interactions: what can we learn from the interaction between *Piriformospora indica* and *Arabidopsis thaliana*. Plant Signal. Behav. **4**: 1024–7.

Vakili, N.G. and Bromfield, K.R. (1976). *Phakopsora* rust on soybean and other legumes in Puerto-Rico. Plant Dis. Reports **60**: 995–999.

Vanderbeld, B. and Snedden, W. a (2007). Developmental and stimulus-induced expression patterns of Arabidopsis calmodulin-like genes *CML37*, *CML38* and *CML39*. Plant Mol. Biol. **64**: 683–97.

Vierstra, R.D. (2003). The ubiquitin/26S proteasome pathway, the complex last chapter in the life of many plant proteins. Trends Plant Sci. **8**: 135–42.

Voinnet, O., Rivas, S., Mestre, P., and Baulcombe, D. (2003). An enhanced transient expression system in plants based on suppression of gene silencing by the p19 protein of tomato bushy stunt virus. Plant J. **33**: 949–56.

Walker, R.G. and Hudspeth, A.J. (1996). Calmodulin controls adaptation of mechanoelectrical transduction by hair cells of the bullfrog's sacculus. Proc. Natl. Acad. Sci. U. S. A. **93**: 2203–7.

Wan, J., Zhang, X.-C., Neece, D., Ramonell, K.M., Clough, S., Kim, S.-Y., Stacey, M.G., and Stacey, G. (2008). A LysM receptor-like kinase plays a critical role in chitin signaling and fungal resistance in Arabidopsis. Plant Cell **20**: 471–81.

Van Wees, S.C., Luijendijk, M., Smoorenburg, I., van Loon, L.C., and Pieterse, C.M. (1999). Rhizobacteria-mediated induced systemic resistance (ISR) in Arabidopsis is not associated with a

direct effect on expression of known defense-related genes but stimulates the expression of the jasmonate-inducible gene Atvsp upon challenge. Plant Mol. Biol. **41**: 537–49.

Van Wees, S.C., de Swart, E.A., van Pelt, J.A., van Loon, L.C., and Pieterse, C.M. (2000). Enhancement of induced disease resistance by simultaneous activation of salicylate- and jasmonate-dependent defense pathways in *Arabidopsis thaliana*. Proc. Natl. Acad. Sci. U. S. A. **97**: 8711–6.

Weiberg, A., Wang, M., Lin, F.-M., Zhao, H., Zhang, Z., Kaloshian, I., Huang, H.-D., and Jin, H. (2013). Fungal small RNAs suppress plant immunity by hijacking host RNA interference pathways. Science **342**: 118–23.

Weiler, E.W., Kutchan, T.M., Gorba, T., Brodschelm, W., Niesel, U., and Bublitz, F. (1994). The *Pseudomonas* phytotoxin coronatine mimics octadecanoid signalling molecules of higher plants. FEBS Lett. **345**: 9–13.

Whisson, S.C. et al. (2007). A translocation signal for delivery of oomycete effector proteins into host plant cells. Nature **450**: 115–8.

Xie, D.X., Feys, B.F., James, S., Nieto-Rostro, M., and Turner, J.G. (1998). COI1: an Arabidopsis gene required for jasmonate-regulated defense and fertility. Science **280**: 1091–4.

Xin, X.-F., Nomura, K., Underwood, W., and He, S.Y. (2013). Induction and suppression of PEN3 focal accumulation during *Pseudomonas syringae pv. tomato* DC3000 infection of Arabidopsis. Mol. Plant. Microbe. Interact. **26**: 861–7.

Yamaguchi, Y., Barona, G., Ryan, C. a, and Pearce, G. (2011). GmPep914, an eight-amino acid peptide isolated from soybean leaves, activates defense-related genes. Plant Physiol. **156**: 932–42.

Yamakawa, H., Mitsuhara, I., Ito, N., Seo, S., Kamada, H., and Ohashi, Y. (2001). Transcriptionally and post-transcriptionally regulated response of 13 calmodulin genes to tobacco mosaic virus-induced cell death and wounding in tobacco plant. Eur. J. Biochem. **268**: 3916–29.

Yan, J., Li, H., Li, S., Yao, R., Deng, H., Xie, Q., and Xie, D. (2013). The Arabidopsis F-box protein CORONATINE INSENSITIVE1 is stabilized by SCFCOI1 and degraded via the 26*S* proteasome pathway. Plant Cell **25**: 486–98.

Zheng, M.S., Takahashi, H., Miyazaki, A., Hamamoto, H., Shah, J., Yamaguchi, I., and Kusano, T. (2004). Up-regulation of *Arabidopsis thaliana NHL10* in the hypersensitive response to Cucumber mosaic virus infection and in senescing leaves is controlled by signalling pathways that differ in salicylate involvement. Planta **218**: 740–50.

Zipfel, C., Kunze, G., Chinchilla, D., Caniard, A., Jones, J.D.G., Boller, T., and Felix, G. (2006). Perception of the bacterial PAMP EF-Tu by the receptor EFR restricts *Agrobacterium*-mediated transformation. Cell **125**: 749–60.

Zipfel, C., Robatzek, S., Navarro, L., Oakeley, E.J., Jones, J.D.G., Felix, G., and Boller, T. (2004). Bacterial disease resistance in Arabidopsis through flagellin perception. Nature **428**: 764–7.

Znameroski, E.A., Li, X., Tsai, J.C., Galazka, J.M., Glass, N.L., and Cate, J.H.D. (2014). Evidence for transceptor function of cellodextrin transporters in *Neurospora crassa*. J. Biol. Chem. **289**: 2610–9.

6 APPENDIX

6.1 Abbreviations

Abbreviation	Meaning
° C	Degree Celsius
A	Absorbance
ABC	ATP binding cassette
ABRC	Arabidopsis resource center
ANAC	ARABIDOPSIS NAC DOMAIN CONTAINING
APS	Ammonium persulfate
ASR	Asian soybean rust
ATP	Adenosine triphosphate
ATR1	ARABIDOPSIS THALIANA RECOGNIZED 1
att	Attachment
avr	Avirulence
BAK1	BRI1-ASSOCIATED RECEPTOR KINASE 1
BAR	The Bio-Analytic Resource for Plant Biology
Bgh	*Blumeria graminis f. sp. hordei*
BI-1	BAX inhibitor 1
BIFC	Bimolecular fluorescence complementation
BRT1	BRIGHT TRICHOMES 1
BSA	Bovine serum albumin
BTH	Benzothiodiazole
bZIP	BASIC LEUCINE-ZIPPER
CaM	Calmodulin
CaMBD	Calmodulin-binding domain
CBL	Calcineurin-like protein
cDNA	Complementary DNA
CDPK/CPK	Calcium-dependent protein kinase
CDT	Cellodextrin transporter
CERK1	CHITIN ELICITOR RECEPTOR KINASE 1
cLSM	Confocal laser scanning microscopy
CML	Calmodulin-like
Cmu1	Chorismate mutase 1
COI1	CORONATINE INSENSITIVE 1
Co-IP	Co-immunoprecipitation
Col-0	Columbia-0
Cy3	Cyanine 3
CyD1	Cytoplasmic domain 1
Da	Dalton
DAMPs	Damage-associated molecular patterns
DNA	Desoxyribonucleic acid

continued

Abbreviation	Meaning
ddH_2O	Bidistilled water
dH_2O	Distilled water
dNTP	Deoxyribonucleotide
dpi	Days post inoculation
DTT	Dithiothreitol
EBF1	EIN3-BINDING F BOX PROTEIN1
EDS1	ENHANCED DISEASE SUSCEPTIBILITY 1
EDTA	Ethylenediaminetetraacetic acid
EFR	EF-TU RECEPTOR
ERF	ETHYLENE RESPONSE FACTOR
ET	Ethylene
EtBr	Ethidium bromide
ETI	Effector-triggered immunity
ETS	Effector-triggered susceptibility
f. sp.	Forma specialis
FLS2	FLAGELLIN SENSITIVE 2
g	gramm
g	Gravitational acceleration
GFP	Green fluorescent protein
GO	Gene ontology
GST	GLUTATHIONE S-TRANSFERASE
GUS	β-glucuronidase
h	hour
HA	Hemagglutinin
HEPES	4-(2-hydroxyethyl)-1-piperazineethanesulfonic acid
hpi	hours post inoculation
HR	Hypersensitive response
HRP	Horseradish peroxidase
HSP	Heat shock protein
IgG	Immunoglobulin G
IPTG	Isopropyl β-D-1-thiogalactopyranoside
ISR	Induced systemic resistance
JA	Jasmonic acid
JAR1	JA RESPONSE 1
kb	kilobase
l	liter
LB	Lysogeny broth
LRR	Leucine rich repeat
m	meter
M	Mol
MAMP	Microbe-associated molecular pattern
MAPK/MPK	Mitogen-activated protein kinase
MAPKK/MKK	MAPK kinase

continued

Abbreviation	Meaning
MAPKKK/MEKK	MAPK kinase kinase
MES	2-(*N*-morpholino)ethanesulfonic acid
min	minute
MKP	MAPK phosphatase
MLO	MILDEW RESISTANCE LOCUS O
mRNA	Messenger RNA
MS	Mass spectrometry
MYB	MYB DOMAIN PROTEIN
NAD	Nicotinamide adenine dinucleotide
NCBI	National Center for Biotechnology information
NHR	Nonhost resistance
OD	Optical density
ORA59	OCTADECANOID-RESPONSIVE ARABIDOPSIS AP2/ERF 59
ORF	Open reading frame
PAD4	PHYTOALEXIN-DEFICIENT 4
PAMP	Pathogen-associated molecular pattern
PCR	Polymerase chain reaction
PDF1.2	PLANT DEFENSIN 1.2
PDR	Pleiotropic drug resistance
PEN	Penetration
PMA	Protein microarray
PMSF	Phenylmethylsulfonyl fluoride
PR	Pathogenesis-related
PRR	Pathogen recognition receptor
Pst	*Pseudomonas syringae* pv *tomato*
PTI	Pathogen-triggered immunity
PUB23	PLANT U-BOX 23
PVPP	Polyvinylpolypyrrolidone
R	Resistance
RALF	Rapid alkalinization factor
RFP	Red fluorescent protein
RIN4	RPM1 INTERACTING PROTEIN 4
RNA	Ribonucleic acid
ROS	Reactive oxygen species
rpm	Rounds per minute
RPM1	RESISTANCE TO *P. SYRINGAE PV MACULICOLA* 1
RPP1	RECOGNITION OF *PERONOSPORA PARASITICA* 1
RPP4	RECOGNITION OF *PERONOSPORA PARASITICA* 4
RPS2	RESISTANT TO *P. SYRINGAE* 2
RT	Room temperature
RT-qPCR	Real time quantitative polymerase chain reaction
s	second
SA	Salicylic acid

continued

Abbreviation	Meaning
SAG101	SENESCENCE-ASSOCIATED GENE 101
SAR	Systemic acquired resistance
SCF	SKP1/Cullin/F-box
SD	Standard deviation
S-DOC	Sodium deoxycholate
SDS	Sodium dodecyl sulfate
SDS-PAGE	Sodium dodecyl sulfate polyacrylamide gel electrophoresis
SID2	SA-DEFICIENT 2
SOBER1	SUPPRESSOR OF AVRBST-ELICITED RESISTANCE 1
SOS	SALT OVERLY SENSITIVE
sRNA	Small RNA
TAIR	The Arabidopsis information resource
TAP	Tandem affinity purification
TCA	Trichloroacetic acid
TCEP	*Tris*(2-carboxyethyl)phosphine
TCH	TOUCH
T-DNA	Transfer DNA
TEMED	Tetramethylethylenediamine
TF	Transcription factor
T_m	Annealing temperature
TMS	Transmembrane-spanning domain
Tris	Tris(hydroxymethyl)aminomethane
T3SS	Type three secretion system
UV	Ultraviolet
V	Volt
v/v	Volume per volume
vir	Virulence
w/v	Weight per volume
WB	Western blot
WRKY	WRKY DNA-BINDING PROTEIN
x-Gluc	5-Bromo-4-chloro-1*H*-indol-3-yl β-D-glucopyranosiduronic acid
Y2H	Yeast two-hybrid system
YEB	Yeast extract broth

6.3 Supplemental material

Table A1. Putative PEN3-binding proteins identified on protein microarrays

Locus	qValue	Description
AT4G14480	0.0009	Protein kinase superfamily protein
AT4G20360	0.0039	RAB GTPase homolog E1B (RABE1b)
AT4G22310	0.0039	Uncharacterised protein family (UPF0041)
AT2G41070	0.0047	Transcription factor homologous to ABI5
AT1G09710	0.0050	Homeodomain-like superfamily protein
AT3G58760	0.0050	Integrin-linked protein kinase family
AT2G01430	0.0074	Homeobox-leucine zipper protein 17 (HB17)
AT3G18980	0.0074	EIN2 targeting protein1 (ETP1)
AT5G52880	0.0074	F-box family protein
AT5G61810	0.0126	ATP/PHOSPHATE CARRIER 1 (APC1)
AT1G21550	0.0149	Calcium-binding EF-hand family protein
AT1G75950	0.0149	S PHASE KINASE-ASSOCIATED PROTEIN 1 (SKP1)
AT3G06240	0.0149	F-box family protein
AT5G23650	0.0149	Homeodomain-like transcriptional regulator
AT5G61430	0.0149	NAC domain containing protein 100 (NAC100)
AT1G75460	0.0184	ATP-dependent protease La (LON) domain protein
AT2G13960	0.0184	Homeodomain-like superfamily protein
AT2G16910	0.0184	Basic helix-loop helix transcription factor
AT5G52470	0.0184	Encodes a fibrillarin
AT2G13570	0.0209	"nuclear factor Y, subunit B7" (NF-YB7)
AT2G35640	0.0209	Homeodomain-like superfamily protein
AT2G18170	0.0213	MAP kinase 7 (MPK7)
AT2G24540	0.0213	ATTENUATED FAR-RED RESPONSE (AFR)
AT1G26690	0.0230	emp24/gp25L/p24 family/GOLD family protein
AT2G06010	0.0230	Protein coding
AT3G56800	0.0230	Calmodulin 3
AT3G15320	0.0246	Transposable element gene
AT4G39550	0.0246	Galactose oxidase/kelch repeat superfamily protein
AT5G64430	0.0246	Octicosapeptide/Phox/Bem1p family protein
AT1G02660	0.0247	alpha/beta-Hydrolases superfamily protein
AT1G17460	0.0250	Myb family transcription factor
AT1G78540	0.0250	Encodes a protein that contains an SH2 domain
AT2G17770	0.0250	Paralog of bZIP transcription factor FD
AT3G05860	0.0250	MADS-box transcription factor family protein
AT3G10760	0.0250	Homeodomain-like superfamily protein
AT3G44460	0.0250	Basic leucine zipper transcription factor (BZIP67)
AT3G57390	0.0250	MADS-box containing protein
AT4G33190	0.0250	OBSOLETE GENE
AT5G05130	0.0250	DNA/RNA helicase protein
AT5G11260	0.0250	Basic leucine zipper (bZIP) transcription factor
AT5G16380	0.0250	Protein of unknown function (DUF538)
AT5G46010	0.0250	Homeodomain-like superfamily protein
AT5G67370	0.0250	Protein of unknown function (DUF1230)
AT1G12860	0.0251	ICE2 (Inducer of CBF Expression 2)
AT1G52695	0.0251	alpha/beta-Hydrolases superfamily protein
AT1G57750	0.0251	CYP96A15
AT1G69810	0.0251	WRKY Transcription Factor (WRKY36)
AT1G74080	0.0251	Member of the R2R3 factor gene family (MYB122)
AT2G27040	0.0251	ARGONAUTE 4 (AGO4)
AT3G10000	0.0251	Embryo sac development arrest 31 (EDA31)

continued

Locus	qValue	Description
AT4G03190	0.0251	F box protein belonging to the TIR1 subfamily (GRH1)
AT5G46590	0.0253	NAC domain containing protein 96 (NAC096)
AT4G24210	0.0261	SLEEPY1 (SLY1)
AT2G06020	0.0264	Homeodomain-like superfamily protein
AT1G51380	0.0265	DEA(D/H)-box RNA helicase family protein
AT2G33550	0.0268	Homeodomain-like superfamily protein
AT2G40340	0.0268	Member of the DREB subfamily A-2 of ERF/AP2 transcription factor family
AT3G09980	0.0268	Family of unknown function (DUF662)
AT3G10585	0.0268	Homeodomain-like superfamily protein
AT3G10590	0.0268	Duplicated homeodomain-like superfamily protein
AT3G12145	0.0268	FLORAL TRANSITION AT THE MERISTEM 4 (FLOR1, FTM4)
AT3G18550	0.0268	TCP transcription factor (BRC1)
AT3G18650	0.0268	AGAMOUS-like 103 (AGL103)
AT3G46930	0.0268	Protein kinase superfamily protein
AT3G59940	0.0268	KISS ME DEADLY 4 (KMD4)
AT4G00990	0.0268	Transcription factor jumonji (jmjC) domain-containing protein
AT4G05170	0.0268	Basic helix-loop-helix (bHLH) DNA-binding superfamily protein
AT5G27130	0.0268	AGAMOUS-like 39 (AGL39)
AT5G47420	0.0268	Tryptophan RNA-binding attenuator protein-like
AT5G58350	0.0268	WNK family of protein kinases (WNK4)
AT1G76920	0.0270	F-box family protein
AT2G25490	0.0270	EIN3-BINDING F BOX PROTEIN 1 (EBF1)
AT2G31800	0.0270	Integrin-linked protein kinase family
AT4G15475	0.0270	F-box/RNI-like superfamily protein
AT1G19800	0.0273	Permease-like protein
AT5G21040	0.0274	F-BOX PROTEIN 2 (FBX2)
AT1G19490	0.0286	Basic-leucine zipper (bZIP) transcription factor family protein
AT1G45249	0.0286	Leucine zipper transcription factor
AT1G63910	0.0286	MYB103
AT2G05260	0.0286	alpha/beta-Hydrolases superfamily protein
AT2G17700	0.0286	ACT-like protein tyrosine kinase family protein
AT2G41100	0.0286	Calmodulin-like 4
AT2G46600	0.0286	Calcium-binding EF-hand family protein
AT3G50720	0.0286	Protein kinase superfamily protein
AT4G33250	0.0286	Initiation factor 3k (EIF3k)
AT5G03415	0.0286	Homolog of the animal DP protein
AT5G48990	0.0286	F-box protein
AT1G49840	0.0296	Protein of unknown function (DUF620)
AT3G15270	0.0296	Member of the SPL gene family
AT3G16640	0.0296	Homologous to translationally controlled tumor protein (TCTP) from Drosophila
AT1G51170	0.0308	Protein kinase superfamily protein
AT5G07100	0.0321	WRKY26
AT1G34670	0.0324	MYB93
AT1G66380	0.0324	Member of the MYB family of transcription factors
AT3G43810	0.0324	Calmodulin 7
AT5G42360	0.0324	Galactose oxidase/kelch repeat superfamily protein
AT1G14600	0.0331	Homeodomain-like superfamily protein
AT1G71450	0.0331	Member of the DREB subfamily A-4 of ERF/AP2 transcription factor family
AT1G79840	0.0331	Glabra 2
AT2G12900	0.0331	Basic-leucine zipper (bZIP) transcription factor family protein
AT2G20180	0.0331	Myc-related bHLH transcription factor
AT2G21950	0.0331	SKP1 interacting partner (SKIP6)
AT2G35930	0.0331	PLANT U-BOX 23 (PUB23)
AT2G40620	0.0331	Basic-leucine zipper (bZIP) transcription factor family protein

continued

Locus	qValue	Description
AT2G44840	0.0331	Member of the ERF subfamily B-3 of ERF/AP2 transcription factor family
AT3G04420	0.0331	NAC domain containing protein 48 (NAC048)
AT3G16370	0.0331	GDSL-like Lipase/Acylhydrolase superfamily protein
AT3G48880	0.0331	RNI-like superfamily protein
AT4G22300	0.0331	SUPPRESSOR OF AVRBST-ELICITED RESISTANCE 1 (SOBER1)
AT5G50000	0.0331	Protein kinase superfamily protein
AT5G58700	0.0331	Phosphatidylinositol-speciwc phospholipase C4 (PLC4)
AT1G60300	0.0339	NAC domain transcriptional regulator superfamily protein
AT5G24270	0.0339	Calcium sensor SALT OVERLY SENSITIVE 3 (SOS3)
AT2G17950	0.0343	Homeobox gene
AT3G51920	0.0352	Calmodulin-like 9
AT1G12710	0.0364	PHLOEM PROTEIN 2-A12
AT1G13450	0.0364	transcription factor GT-1
AT2G12980	0.0364	Transposable element gene
AT2G30250	0.0364	WRKY25
AT3G07550	0.0364	RNI-like superfamily protein
AT3G49410	0.0364	Transcription factor IIIC, subunit 5
AT1G76650	0.0365	Calmodulin-like 38
AT3G52060	0.0369	Core-2/I-branching beta-1,6-N-acetylglucosaminyltransferase family protein
AT4G26340	0.0369	F-box/RNI-like/FBD-like domains-containing protein
AT3G57290	0.0373	EUKARYOTIC TRANSLATION INITIATION FACTOR 3E (EIF3E)
AT1G22590	0.0376	AGAMOUS-like 87 (AGL87)
AT2G32510	0.0376	MAPKKK17
AT5G54130	0.0376	Calcium-binding endonuclease/exonuclease/phosphatase family
AT4G10925	0.0387	Nuclear transport factor 2 (NTF2) family protein
AT5G27580	0.0387	AGAMOUS-like 89 (AGL89)
AT5G56580	0.0387	MKK6
AT2G24060	0.0397	Translation initiation factor 3 protein
AT3G09600	0.0397	MYB-like transcription factor (LCL5)
AT3G12350	0.0397	F-box family protein
AT5G13180	0.0397	NAC DOMAIN CONTAINING PROTEIN 83 (NAC083)
AT5G19010	0.0397	MPK16
AT1G74300	0.0399	alpha/beta-Hydrolases superfamily protein
AT1G67360	0.0406	Rubber elongation factor protein (REF)
AT1G52630	0.0406	O-fucosyltransferase family protein
AT3G05500	0.0406	Rubber elongation factor protein (REF)
AT4G04800	0.0406	Methionine sulfoxide reductase B3 (MSRB3)
AT5G42380	0.0406	Calmodulin-like 37
AT1G53570	0.0410	MAPKKK3
AT1G28390	0.0412	Protein kinase superfamily protein
AT3G24310	0.0412	MYB DOMAIN PROTEIN 305 (MYB305)
AT4G04840	0.0412	Methionine sulfoxide reductase B6 (MSRB6)
AT4G27280	0.0412	Calcium-binding EF-hand family protein
AT5G07670	0.0412	RNI-like superfamily protein
AT3G54620	0.0412	BASIC LEUCINE ZIPPER 25 (BZIP25)
AT3G14075	0.0423	Mono-/di-acylglycerol lipase
AT1G32320	0.0427	MKK10
AT1G53320	0.0427	TUBBY LIKE PROTEIN 7 (TLP7)
AT2G41410	0.0427	Calcium-binding EF-hand family protein
AT2G47070	0.0427	SQUAMOSA PROMOTER BINDING PROTEIN-LIKE 1 (SPL1)
AT3G01490	0.0427	Protein kinase superfamily protein
AT3G18100	0.0427	MYB DOMAIN PROTEIN 4R1 (MYB4R1)
AT3G19760	0.0427	EUKARYOTIC INITIATION FACTOR 4A-III
AT3G49850	0.0427	TELOMERE REPEAT BINDING FACTOR 3 (TRB3)

continued

Locus	qValue	Description
AT3G14210	0.0441	EPITHIOSPECIFIER MODIFIER 1 (ESM1)
AT4G10680	0.0441	Transcription factor IIB (TFIIB) family protein
AT1G71930	0.0445	NAC-domain transcription factor
AT5G28900	0.0445	Calcium-binding EF-hand family protein
AT5G49490	0.0445	AGAMOUS-like 83 (AGL83)
AT5G06560	0.0449	Protein of unknown function (DUF593)
AT1G30090	0.0453	Galactose oxidase/kelch repeat superfamily protein
AT5G67080	0.0453	MAPKKK19
AT3G59790	0.0461	MPK10
AT1G53885	0.0461	Protein of unknown function (DUF581)
AT2G35670	0.0461	FERTILIZATION INDEPENDENT SEED 2 (FIS2)
AT2G40290	0.0461	eIF2alpha homolog
AT4G28780	0.0463	GDSL-like Lipase/Acylhydrolase superfamily protein
AT5G45430	0.0495	Protein kinase superfamily protein
AT1G80440	0.0497	KISS ME DEADLY 1 (KMD1)
AT2G31180	0.0497	MYB DOMAIN PROTEIN 14 (MYB14)
AT4G14640	0.0497	Calmodulin-like 8
Total		175

Table A2. Detailed GO analysis of the 28 putative PEN3 binding proteins with GO involved in cellular response to stimulus

Locus	Description	GO molecular function	GO biological process
AT3G56800	Calmodulin 3	calcium ion binding	calcium-mediated signaling, Golgi vesicle transport, cellular membrane fusion
AT3G43810	Calmodulin 7	calcium ion binding, protein binding	calcium-mediated signaling, detection of calcium ion, response to mechanical stimulus, acetyl-CoA metabolic process,second-messenger-mediated signaling, regulation of photomorphogenesis
AT2G41100	Calmodulin-like 4/CAL4/TOUCH3	calcium ion binding, protein binding	calcium-mediated signaling, regulation of plant-type hypersensitive response, negative regulation of programmed cell death, response to chitin, response to mechanical stimulus, cellular membrane fusion, protein targeting to membrane, response to wounding, response to absence of light, thigmotropism
AT4G14640	Calmodulin-like 8	calcium ion binding	calcium-mediated signaling, detection of calcium ion, actin filament-based movement, peroxisome localization, response to mechanical stimulus
AT3G51920	Calmodulin-like 9	calcium ion binding, protein binding	calcium-mediated signaling, detection of calcium ion, regulation of defense response, systemic acquired resistance, cellular cation homeostasis, divalent metal ion transport, response to abscisic acid stimulus, response to salt stress, response to mechanical stimulus, response to cold (and others)
AT5G42380	Calmodulin-like 37	calcium ion binding	defense response by callose deposition, ethylene biosynthetic process, response to ozone, heat acclimation, endoplasmic reticulum unfolded protein response
AT1G76650	Calmodulin-like 38	calcium ion binding	intracellular signal transduction, response to fungus, response to chitin, response to wounding, response to jasmonic acid stimulus, response to ethylene stimulus, response to wounding, abscisic acid mediated signaling pathway, jasmonic acid biosynthetic process, ethylene mediated signaling pathway
AT5G24270	SALT OVERLY SENSITIVE 3 (SOS3)	calcium ion binding, protein binding, calcium-dependent protein serine/threonine phosphatase activity	calcium-mediated signaling, detection of calcium ion, N-terminal protein myristoylation, stomatal movement, cellular potassium ion homeostasis, hypotonic salinity response
AT2G46600	Calcium-binding EF-hand family protein	calcium ion binding, protein binding	hydrogen peroxide catabolic process, trichome branching
AT2G18170	MPK7	protein binding, MAP kinase activity, protein tyrosine kinase activity protein, serine/threonine kinase activity	signal transduction, protein phosphorylation, circadian rhythm, response to hydrogen peroxide
AT3G59790	MPK10	protein binding, MAP kinase activity, ATP binding, protein serine/threonine kinase activity	signal transduction, protein phosphorylation
AT5G19010	MPK16	MAP kinase activity	protein phosphorylation, signal transduction, regulation of meristem growth
AT5G67080	MAPKKK19	protein kinase activity, protein serine/threonine kinase activity	protein phosphorylation, abscisic acid mediated signaling pathway, response to water deprivation, hyperosmotic salinity response, response to abscisic acid stimulus, response to ethylene stimulus
AT5G58350	WNK family of protein kinases (WNK4)	protein serine/threonine kinase activity	protein phosphorylation, protein autophosphorylation, galactolipid biosynthetic process, organ senescence, cellular response to phosphate starvation, cellular response to water deprivation
AT1G75460	ATP-dependent protease La (LON) domain protein	ATP-dependent peptidase activity	negative regulation of defense response, regulation of plant-type hypersensitive response, response to bacterium, systemic acquired resistance, regulation of protein dephosphorylation, protein targeting to membrane, salicylic acid mediated signaling pathway, jasmonic acid mediated signaling pathway, regulation of hydrogen peroxide metabolic process, MAPK cascade (and others)
AT2G24540	ATTENUATED FAR-RED RESPONSE (AFR)	protein binding	response to UV-B, red or far-red light signaling pathway, myo-inositol hexakisphosphate biosynthetic process, flavonoid biosynthetic process, response to sucrose stimulus, red, far-red light phototransduction

continued

Locus	Description	GO molecular function	GO biological process
AT4G24210	SLY1	protein binding	seed dormancy process, response to ethylene stimulus, seed germination, positive regulation of gibberellic acid mediated signaling pathway, hyperosmotic salinity response, jasmonic acid mediated signaling pathway, floral organ morphogenesis, salicylic acid mediated signaling pathway, response to abscisic acid stimulus, raffinose family oligosaccharide biosynthetic process
AT1G80440	KMD1	unknown	unknown
AT3G59940	KMD4	unknown	unknown
AT5G47420	Tryptophan RNA-binding attenuator protein-like	unknown	cellular response to biotic stimulus, ER-nucleus signaling pathway, response to endoplasmic reticulum stress
AT2G35930	PLANT U-BOX 23 (PUB23)	ubiquitin-protein ligase activity	negative regulation of defense response, regulation of plant-type hypersensitive response, systemic acquired resistance, defense response to bacterium, defense response to fungus, response to chitin, protein targeting to membrane, respiratory burst involved in defense response, jasmonic acid mediated signaling pathway, salicylic acid mediated signaling pathway (and others)
AT5G58700	Phosphatidylinositol-speciwc phospholipase C4 (PLC4)	phosphatidylinositol phospholipase C activity, phosphoric diester hydrolase activity	intracellular signal transduction, D-xylose metabolic process, lipid metabolic process, actin filament-based movement
AT3G57290	EUKARYOTIC TRANSLATION INITIATION FACTOR 3E (EIF3E)	protein binding, translation initiation factor activity	post-translational protein modification, flower development, DNA-dependent positive regulation of transcription, response to freezing, sugar mediated signaling pathway, seed dormancy process, embryo development ending in seed dormancy, ubiquitin-dependent protein catabolic process, photorespiration, response to salt stress (and others)
AT2G25490	EIN3-BINDING F BOX PROTEIN 1 (EBF1)	protein binding	negative regulation of ethylene mediated signaling pathway, response to ethylene stimulus, ubiquitin-dependent protein catabolic process, regulation of circadian rhythm, ubiquitin-protein ligase activity
AT4G03190	F box protein belonging to the TIR1 subfamily (GRH1)	protein binding, ubiquitin-protein ligase activity, auxin binding	response to molecule of bacterial origin, regulation of hormone levels, signal transduction, stomatal complex morphogenesis, ubiquitin-dependent protein catabolic process, root hair elongation, anthocyanin accumulation in tissues in response to UV light, polysaccharide biosynthetic process, multidimensional cell growth, stamen development (and others)
AT5G21040	FBX2	unknown	cellular response to phosphate starvation
AT4G04800	Methionine sulfoxide reductase B3 (MSRB3)	peptide-methionine (S)-S-oxide reductase activity,methionine-R-sulfoxide reductase activity	galactolipid biosynthetic process, cold acclimation, cellular response to water deprivation, cellular response to oxidative stress, cellular response to phosphate starvation, oxidation-reduction process
AT4G22300	SUPPRESSOR OF AVRBST-ELICITED RESISTANCE 1 (SOBER1)	carboxylesterase activity, hydrolase activity	regulation of plant-type hypersensitive response, defense response, incompatible interaction

Table A3. The PEN3-Ca^{2+} signaling network

Locus	Description	Co-regulated with *PEN3*	Induced by ASR
AT1G25420	Protein of unknown function (DUF292)		
AT3G19100	Calcium-dependent protein kinase (CDPK) family protein		
AT1G80120	Protein of unknown function (DUF567)		
AT1G11330	S-locus lectin protein kinase family protein		
AT3G49910	Translation protein SH3-like family protein		
AT5G49760	Leucine-rich repeat protein kinase family protein	x	
AT5G06560	Protein of unknown function (DUF593)		
AT4G02010	Protein kinase superfamily protein		
AT1G56145	Leucine-rich repeat transmembrane protein kinase		
AT1G21630	Calcium-binding EF hand family protein		
AT4G18650	A maternally expressed imprinted gene		
AT4G30600	Signal recognition particle receptor alpha subunit family protein		
AT3G15010	RNA-binding (RRM/RBD/RNP motifs) family protein		
AT3G22750	Protein kinase superfamily protein		
AT1G68400	Leucine-rich repeat transmembrane protein kinase family protein		
AT1G11270	F-box and associated interaction domains-containing protein		
AT1G48150	MADS-box transcription factor family protein		
AT5G24080	S-locus lectin protein kinase family protein		
AT3G20790	NAD(P)-binding Rossmann-fold superfamily protein		
AT4G16410	unknown protein		
AT5G41920	GRAS family transcription factor		
AT1G26665	Mediator complex, subunit Med10		
AT4G18950	Integrin-linked protein kinase family		
AT1G27690	Protein of unknown function (DUF620)		
AT3G12350	F-box family protein		
AT5G23540	Mov34/MPN/PAD-1 family protein		
AT1G54610	Protein kinase superfamily protein		
AT2G23070	Protein kinase superfamily protein		
AT1G20950	Phosphofructokinase family protein		
AT4G17080	Histone H3 K4-specific methyltransferase SET7/9 family protein		
AT4G02410	Concanavalin A-like lectin protein kinase family protein	x	x
AT3G59150	F-box/RNI-like superfamily protein		
AT1G27190	Leucine-rich repeat protein kinase family protein		
AT3G56270	Plant protein of unknown function (DUF827)		
AT4G17140	Calcium-dependent lipid-binding family protein		
AT4G10320	tRNA synthetase class I (I, L, M and V) family protein		
AT5G10390	Histone superfamily protein		
AT5G64400	Cox19-like CHCH family protein		
AT4G21820	Calmodulin binding protein		
AT1G76270	O-fucosyltransferase family protein		
AT5G11620	SWIM zinc finger family protein / MAPKKK-related		
AT1G68380	Core-2/I-branching beta-1,6-N-acetylglucosaminyltransferase family protein		
AT3G05520	Subunits of heterodimeric actin filament capping protein Capz superfamily		
AT5G20810	SAUR-like auxin-responsive protein family		
AT5G56890	Protein kinase superfamily protein		
AT2G20110	Tesmin/TSO1-like CXC domain-containing protein		
AT1G74490	Protein kinase superfamily protein		
AT5G55690	MADS-box transcription factor family protein		
AT3G61160	Protein kinase superfamily protein		
AT5G01890	Leucine-rich receptor-like protein kinase family protein		
AT4G18905	Transducin/WD40 repeat-like superfamily protein		
AT4G37240	unknown protein		
AT3G28450	Leucine-rich repeat protein kinase family protein	x	
AT3G11250	Ribosomal protein L10 family protein		
AT4G28706	pfkB-like carbohydrate kinase family protein		
AT4G15770	RNA binding		

continued

Locus	Description	Co-regulated with *PEN3*	Induced by ASR
AT5G56040	Leucine-rich receptor-like protein kinase family protein		
AT4G27435	Protein of unknown function (DUF1218)		
AT1G51170	Protein kinase superfamily protein		
AT4G23900	Nucleoside diphosphate kinase family protein		
AT4G28800	Basic helix-loop-helix (bHLH) DNA-binding superfamily protein		
AT3G23310	AGC kinase family protein		
AT1G34300	Lectin protein kinase family protein		
AT1G58110	Basic-leucine zipper (bZIP) transcription factor family protein		
AT2G43850	Integrin-linked protein kinase family		
AT3G18430	Calcium-binding EF-hand family protein		
AT3G05050	Protein kinase superfamily protein		
AT3G02880	Leucine-rich repeat protein kinase family protein		
AT1G48090	Calcium-dependent lipid-binding family protein		
AT4G34380	Transducin/WD40 repeat-like superfamily protein		
AT5G24260	Prolyl oligopeptidase family protein		
AT5G40540	Protein kinase superfamily protein		
AT2G26730	Leucine-rich repeat protein kinase family protein		
AT2G46600	Calcium-binding EF-hand family protein	x	
AT4G23050	PAS domain-containing protein tyrosine kinase family protein		
AT4G18630	Protein of unknown function (DUF688)		x
AT5G39670	Calcium-binding EF-hand family protein		x
AT5G66790	Protein kinase superfamily protein		
AT5G64780	Uncharacterised conserved protein UCP009193		x
AT1G77145	Protein of unknown function (DUF506)		
AT5G66770	GRAS family transcription factor		
AT1G28390	Protein kinase superfamily protein		
AT3G58120	Encodes a member of the BZIP family of transcription factors		
AT4G02640	Encodes a basic leucine zipper (bZIP) transcription factor AtbZIP10		
AT4G23170	Induced in response to Salicylic acid		
AT4G13020	Encodes a member of the cdc2+ family of protein kinases MHK		
AT2G15430	Non-catalytic subunit of nuclear DNA-dependent RNA polymerases II, IV and V		
ATMG00870	hypothetical protein		
AT1G66740	Located on the SSL2 region		
AT5G54770	Thiamine biosynthetic gene		
AT4G23810	Member of WRKY Transcription Factor; Group III		x
AT3G20080	Member of CYP705A		
AT3G20110	Member of CYP705A		
AT3G26170	Putative cytochrome P450		
AT4G39950	Belongs to cytochrome P450		x
AT4G31950	Member of CYP82C		
AT1G56170	Protein coding		
AT1G53850	Encodes alpha5 subunit of 20s proteosome		
AT3G14290	Encodes 20S proteasome subunit PAE2		
AT3G19290	bZIP transcription factor		
AT4G35830	Encodes an aconitase		
AT2G31200	Encodes actin depolymerizing factor 6 (ADF6)		
AT3G12110	Encodes an actin		
AT5G27050	AGAMOUS-like 101 (AGL101)		
AT5G13790	AGAMOUS-Like 15 (AGL15)		
AT4G37940	Encodes a MADS box protein		
AT1G65300	PHERES2		
AT1G60040	AGAMOUS-like 49 (AGL49)		
AT5G27070	AGAMOUS-like 53 (AGL53)		
AT1G60920	AGAMOUS-like 55 (AGL55)		
AT3G04100	AGAMOUS-like 57 (AGL57)		
AT2G24840	Member of the Agamous-like family of transcription factors		
AT5G41200	AGAMOUS-like 75 (AGL75)		

continued

Locus	Description	Co-regulated with *PEN3*	Induced by ASR
AT5G40120	AGAMOUS-like 76 (AGL76)		
AT5G38740	AGAMOUS-like 77 (AGL77)		
AT3G30260	AGAMOUS-like 79 (AGL79)		
AT5G60910	MADS box gene negatively regulated by APETALA1		
AT5G48670	AGAMOUS-like 80 (AGL80)		
AT5G49490	AGAMOUS-like 83 (AGL83)		
AT5G26950	AGAMOUS-like 93 (AGL93)		
AT5G06500	AGAMOUS-like 96 (AGL96)		
AT5G39810	AGAMOUS-like 98 (AGL98)		
AT4G36250	Encodes a putative aldehyde dehydrogenase		
AT2G24540	ATTENUATED FAR-RED RESPONSE (AFR)		
AT4G24390	RNI-like superfamily protein		
AT5G24800	Encodes bZIP protein BZO2H2		
AT5G49450	Encodes a transcription activator		
AT5G15830	basic leucine-zipper 3 (bZIP3)		
AT1G59530	basic leucine-zipper 4 (bZIP4)		
AT3G30530	basic leucine-zipper 42 (bZIP42)		
AT5G38800	basic leucine-zipper 43 (bZIP43)		
AT5G08141	basic leucine-zipper 75 (bZIP75)		
AT3G62420	Encodes a group-S bZIP transcription factor		
AT5G47120	Encodes BI-1, a homolog of mammalian Bax inhibitor 1		
AT2G46240	Member of Arabidopsis BAG (Bcl-2-associated athanogene) proteins		
AT2G39660	BIK1		
AT1G18890	CPK10		x
AT1G61950	CPK19		
AT2G38910	CPK20		
AT2G35890	CPK25		
AT1G74740	CPK30		
AT3G57530	CPK32		
AT4G23650	CPK3		
AT3G56800	CaM3		
AT5G21274	CaM6		
AT3G43810	CaM7		
AT4G14640	CML8		
AT3G51920	CML9		
AT5G42380	CML37		x
AT5G12480	CPK7		
AT1G76650	CML38		x
AT4G04870	Cardiolipin Synthase		
AT4G14340	Casein Kinase I		
AT2G44680	Encodes casein kinase II beta chain		
AT2G23080	Encodes casein kinase II alpha chain		
AT4G35600	Encodes a receptor-like cytoplasmic kinase		x
AT3G13320	Low affinity calcium antiporter CAX2		
AT3G17510	Encodes a CBL-interacting protein kinase		
AT5G01810	Encodes a CBL-interacting serine/threonine protein kinase		
AT3G23000	Encodes a serine/threonine protein kinase		
AT1G01140	Encodes a CBL-interacting protein kinase		
AT3G50360	Centrin2 (CEN2)		
AT2G28190	Encodes a chloroplastic copper/zinc superoxide dismutase CSD2		
AT1G20930	Cyclin-dependent kinase		
AT4G04570	Encodes a cysteine-rich receptor-like protein kinase CRK40		
AT3G61880	Encodes a cytochrome p450 monooxygenase		
AT5G63770	Member of the diacylglycerol kinase gene family		
AT1G13180	Actin-related protein 3		
AT1G30825	Actin-related protein C2A		
AT2G28380	Encodes a cytoplasmic dsRNA-binding protein DRB2		

continued

Locus	Description	Co-regulated with *PEN3*	Induced by ASR
AT3G18980	EIN2 targeting protein1 (ETP1)		
AT4G08980	Encodes an F-box gene that is a novel negative regulator of AGO1		
AT5G23980	Encodes a ferric chelate reductase		
AT3G61650	Gamma-tubulin		
AT1G78300	G-box binding factor GF14 omega encoding a 14-3-3 protein		
AT5G17330	Encodes one of two isoforms of glutamate decarboxylase.		
AT2G29100	Member of putative ligand-gated ion channel subunit family		x
AT1G02920	Encodes glutathione transferase belonging to the phi class of GSTs		
AT5G02500	Encodes a member of heat shock protein 70 family		
AT5G56030	Member of heat shock protein 90 (HSP90) gene family		
AT5G52640	Encodes a cytosolic heat shock protein AtHSP90.1		
AT1G24180	Pyruvate dehydrogenase E1a-like subunit		
AT3G17600	Member of the Aux/IAA family of proteins (IAA31)		
AT1G17140	Encodes a ROP/RAC effector (ICR1)		
AT5G03080	Encodes a phosphatidic acid phosphatase		
AT3G17240	Lipoamide dehydrogenase precursor		
AT5G23450	Encodes a sphingosine kinase		
AT5G50850	MACCI-BOU (MAB1)		
AT3G59790	MPK10		
AT4G01370	MPK4		
AT4G11330	MPK5		
AT2G43790	MPK6		
AT5G56580	MKK6		
AT4G26070	MKK1		
AT2G07690	Member of the minichromosome maintenance complex		
AT4G25200	AtHSP23.6-mito mRNA		
AT1G10210	MPK1		
AT1G53510	MPK18		
AT1G59580	MPK2		
AT3G50310	MAPKKK20		
AT3G58680	Multiprotein bridging factor 1		
AT4G17380	Meiosis-specific member of the MutS-homolog family		
AT2G31180	MYB14		
AT3G12720	MYB67		
AT2G23290	MYB70		
AT5G43900	Myosin 2		
AT1G04160	Myosin VI B		
AT2G33240	Myosin VI D		
AT3G04430	NAC domain containing protein 49 (NAC049)		
AT3G12200	NEK7		
AT2G34390	Aquaporin NIP2.1		
AT5G53450	OBP3-responsive gene 1 (ORG1)		
AT3G09920	Phosphatidyl inositol monophosphate 5 kinase (PIP5K9)		
AT5G64070	Phosphatidylinositol 4-OH kinase (PI-4Kbeta1)		
AT4G37870	Encodes a phosphoenolpyruvate carboxykinase		
AT1G12680	Phosphoenolpyruvate carboxylase-related kinase 2 (PEPKR2)		
AT5G47810	Phosphofructokinase 2 (PFK2)		
AT4G26270	Phosphofructokinase 3 (PFK3)		
AT2G22480	Phosphofructokinase 5 (PFK5)		
AT5G51820	Phosphoglucomutase 1		
AT1G70730	Phosphoglucomutase 2		
ATCG00020	Photosystem II reaction center protein A		
AT2G34650	Encodes a protein serine/threonine kinase		
AT1G29340	PUB17		
AT1G14370	Encodes protein kinase APK2a		x
AT2G02800	Encodes protein kinase APK2b		
AT5G09650	Pyrophosphorylase 6		

continued

Locus	Description	Co-regulated with *PEN3*	Induced by ASR
AT5G14800	Delta 1-pyrroline-5-carboxylate reductase		
AT5G63840	Encodes the alpha-subunit of a glucosidase II enzyme		
AT5G38470	RADIATION SENSITIVE23 D (RAD23D)		
AT2G48010	Receptor-like serine/threonine kinase (RKF3)		
AT4G21470	Riboflavin kinase		
AT5G10520	ROP binding protein kinases 1 (RBK1)		x
AT3G56070	Rotamase cyclophilin 2 (ROC2)		
AT4G38740	Encodes cytosolic cyclophilin ROC1		
AT5G35410	Encodes a member of the CBL-interacting protein kinase family		
AT5G24270	SOS3		
AT2G04890	Encodes a scarecrow-like protein (SCL21)		
AT2G03710	This gene belongs to the family of SEP genes		
AT5G01820	Encodes a CBL-interacting serine/threonine protein kinase (CIPK14)		x
AT1G09840	Shaggy-like protein kinase 41 (SK41)		
AT2G30980	Encodes a GSK3-like protein kinase		
AT3G58780	AGAMOUS-like 1 (AGL1)		
AT4G39540	Shikimate kinase 2 (SK2)		
AT3G12800	Short-chain dehydrogenase-reductase B (SDRB)		
AT5G58380	CIPK10		
AT4G30960	CIPK6		
AT2G30360	CIPK11		
AT3G47620	Transcription factor AtTCP14		
AT1G22070	TGA3	x	
AT1G08320	BZIP21		
AT2G41100	Calmodulin-like 4, ATCAL4, TCH3	x	
AT2G38560	Encodes RNA polymerase II transcript elongation factor TFIIS		
AT5G23260	AGAMOUS-like 32 (AGL32)		
AT4G24040	Encodes a trehalase, member of Glycoside Hydrolase Family 37		
AT1G06910	Myb family transcription factor		
AT1G14610	Required for proper proliferation of basal cells		
AT2G39840	Encodes the catalytic subunit of a Type 1 phosphoprotein Ser/Thr phosphatase		
AT2G30110	Encodes a ubiquitin-activating enzyme (E1)		
AT3G08690	Ubiquitin-conjugating enzyme 11 (UBC11)		
AT5G56150	Ubiquitin-conjugating enzyme 30 (UBC30)		
AT3G53090	Ubiquitin-protein ligase 7		
AT2G30590	WRKY21		
AT2G46130	WRKY43		
AT3G01970	WRKY45		

Co-regulation data from Humphry at al., (2010);
Microarray data upon *P. pachyrhizi* (ASR) inoculation from C. Langenbach, unpublished

6.4 Vector maps

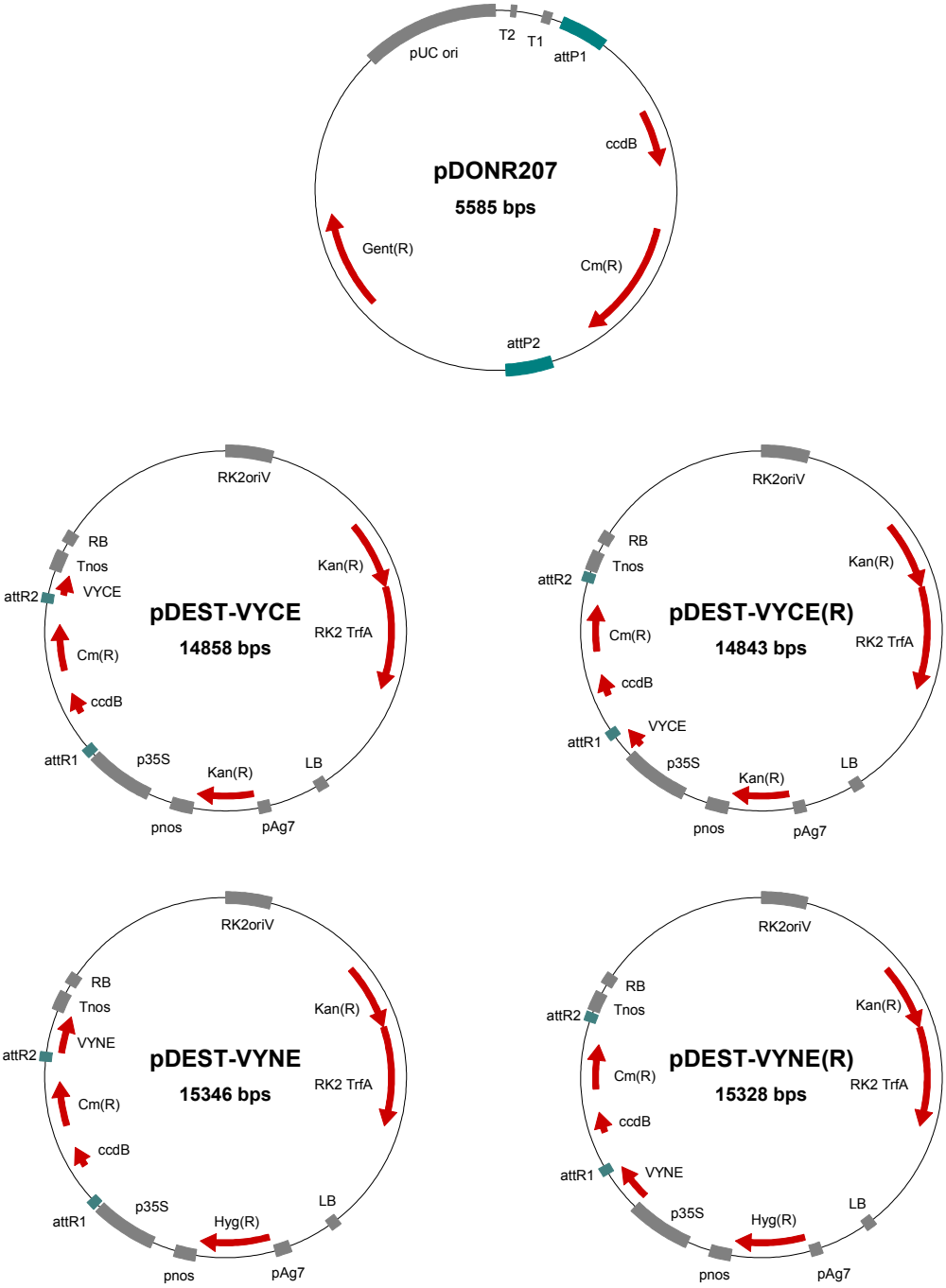

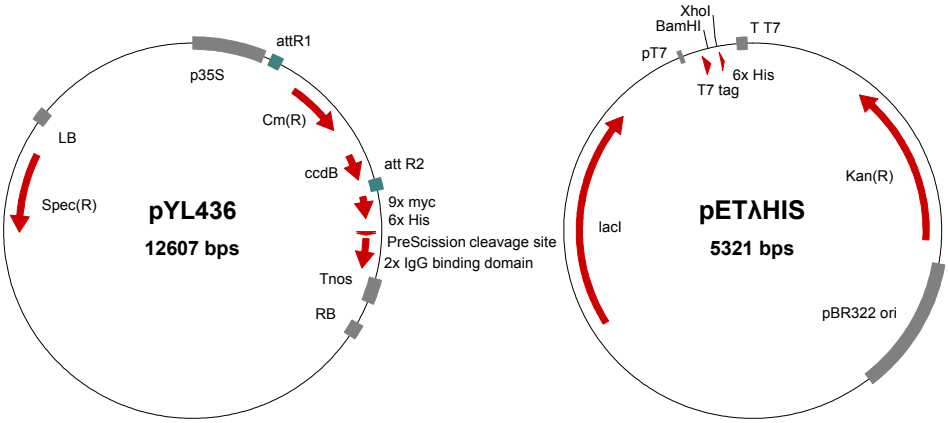

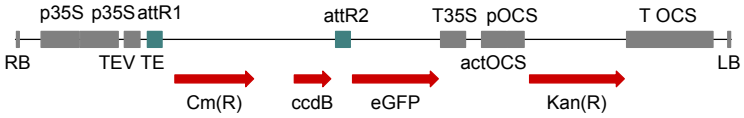

pSITE-2NB

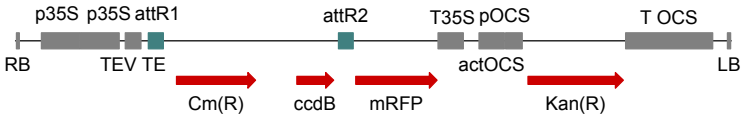

pSITE-4NB

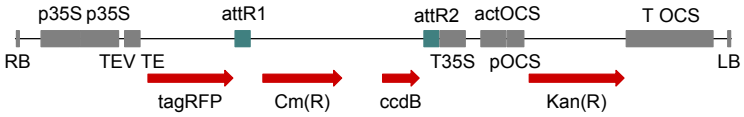

pSITE-6C1

6.5 Acknowledgments/Danksagung

Viele Menschen haben mich auf dem Weg vom Anfang meines Studiums bis hin zur Abgabe dieser Arbeit begleitet, motiviert und unterstützt. Dafür möchte ich mich bei euch allen ganz herzlich bedanken!

Großer Dank gebührt Uwe, der sich seit meinem ersten Tag in seinem Labor unglaublich viel Zeit genommen hat, um mich in jeder Hinsicht zu fördern, der großes Vertrauen in mich gesetzt hat und der auch mal bei plötzlichem Unwohlsein ein „Heilmittel" parat hatte.

Auch bei Katharina bedanke ich mich für ihr Vertrauen, für die Freiheit, meine eigenen Entscheidungen treffen zu dürfen und für die Möglichkeit schon früh an so vielen wissenschaftlichen Tagungen teilnehmen zu dürfen. All das hat sicherlich zu meiner Entwicklung zu einer selbstständigen Wissenschaftlerin beigetragen.

Bei Ralph Panstruga und Jan Schirawski bedanke ich mich für die Übernahme des Drittprüfers bzw. des Vorsitzes der Prüfungskommission und für den regelmäßigen wissenschaftlichen Input im Institutsseminar.

Gerold und Caspar, was ich euch schon immer mal sagen wollte: ihr seid wirklich supergeile Kollegen! ;) Vielen Dank dafür!

I greatly appreciate the opportunity given by Sorina Popescu to spend three months in her lab at the Boyce Thompson Institute for Plant Research, what led to the breakthrough in my PhD project. Many thanks also to her team: George, Mauricio, Liz, Dharmendra and Tim who helped me to find my way in the lab and to combat the cold Ithaca winter.

Ich bedanke mich bei der gesamten Sojarostgruppe mit Uli, Marco und Renate für ständige Unterstützung und wissenschaftliche Diskussion.

Martin N. und auch Michal danke ich für die Geduld bei der Behebung jeglichen Computerproblems und der riesen Hilfe beim Formatieren!

Dank gilt auch allen meinen Forschungspraktikanten, Bachelor-, Master-Studenten und Hiwis: Kylene, Heike, Quintana, Tin, Frauke, Anne, Sebi und Franz. Es hat Spaß gemacht eure Arbeiten zu betreuen und euch ein stückweit während eures Studiums zu begleiten. Besonderer Dank gilt

dabei Franz, Anne und Sebi, die mich im letzten Jahr meiner Arbeit unterstützt haben und so maßgeblich zu deren Gelingen beigetragen haben.

Ich danke außerdem allen Kollegen der AG Conrath/Göllner: Gerold, Caspar, meiner Banknachbarin Stephi, den ehemaligen Mitgliedern Dennis und Martin N., Michal, Martin T., Nicola, Britta, Irina, Deiziane, Franz, Sebi und Ramona und der gesamten Mannschaft der Bio3 für ständige Hilfsbereitschaft, Ideen und Kritik im Labmeeting, Blumen gießen, gute Stimmung, Aufmunterung nach frustrierenden Experimenten, Kaffeepausen und (Freitags)biergesprächen.

Ich bedanke mich bei meiner Familie, die mich schon immer in allen meinen Entscheidungen unterstützt und an mich geglaubt hat.

Mädels (und Jungs), für euch auch ein großes Danke für Ablenkung, Aufmunterung, Motivation und den Glauben an „die Wissenschaftlerin in mir“! ;)

Al final, muchas gracias a ti, Hugo, por siempre creer en mi y darme las fuerzas de levantarme todas las mañanas!

Für finanzielle Unterstützung bedanke ich mich bei der RWTH Graduiertenförderung, dem DAAD und IS-MPMI.

6.6 Curriculum vitae

Name	Campe
Surname	Ruth Maria
Address	Oppenhoffallee 26
	52066 Aachen, Germany
Email	campe@bio3.rwth-aachen.de
Date of birth	February 4th 1984
Place of birth	Siegburg
Nationality	German

Education/ University training

09/2014	Receipt of Doctorate Degree (Dr. rer. nat.)
11/2012 - 01/2013	Visiting scholar with Sorina Popescu, Boyce Thompson Institute for Plant Research, Ithaca, USA
From 04/2010	PhD Thesis with Katharina Goellner/ Uwe Conrath; Thesis entitled "Molecular aspects in Arabidopsis nonhost resistance to *Phakopsora pachyrhizi*"
	Molecular Phytopathology Group, Department of Plant Physiology (Bio3), RWTH Aachen University, Germany.
02/2010	Diploma in Biology
04/2009 – 02/2010	Diploma thesis with Katharina Goellner/ Uwe Conrath; Thesis entitled "Analysis of differentially regulated Arabidopsis genes in response to attack by Asian soybean rust"
	Molecular Phytopathology Group, Department of Plant Physiology (Bio3), RWTH Aachen University, Germany.
09/2006 – 06/2007	Stay abroad in the Master Program "Master professionnel de Chimie et Biologie Végétales", Université Claude Bernard, Lyon 1, France
From 10/2003	Studies of Biology at RWTH Aachen University, Germany
06/2003	High School Final (Abitur)

6.7 List of publications

6.7.1 Primary research papers

Campe, R., Loehrer, M., Conrath, U., Goellner, K. (2014). *Phakopsora pachyrhizi* induces marker genes to necrotrophs in *Arabidopsis thaliana*. Physiological and Molecular Plant Pathology (2014), doi: 10.1016/j.pmpp.2014.04.005

Langenbach, C., Campe, R., Schaffrath, U., Goellner, K. and Conrath, U. (2013). UDP glucosyltransferase UGT84A2/BRT1 is required for Arabidopsis nonhost resistance to the Asian soybean rust pathogen *Phakopsora pachyrhizi*. New Phytologist 198: 536-545

6.7.2 Short publications/abstracts

Campe, R., Leissing, F., Langenbach, C., Beckers, G., Popescu, S., Conrath, U., Göllner, K. (2014). Calmodulin interacts with the ABC transporter PEN3 and is involved in Arabidopsis nonhost resistance. Journal of Plant Diseases and Protection

Campe, R., Langenbach, C., Beckers, G., Popescu, S., Conrath, U., Göllner, K. (2013). Screening for PEN3 interaction partners by Protein Microarrays. Journal of Plant Diseases and Protection 1/2014; 121: 41-49

Campe, R., Schaffrath, U., Conrath, U., Göllner, K. (2010). The role of differentially regulated Arabidopsis genes in response to attack by Asian soybean rust. Journal of Plant Diseases and Protection 3/2010; 117:138

6.7.3 Posters

Campe, R., Leissing, F., Beckers, G., Popescu, G., Langenbach, C., Popescu, S., Conrath, U., Göllner, K. (2014). Calmodulin interacts with the ABC transporter PEN3 and is involved in nonhost resistance of Arabidopsis (XVI International Congress of Molecular Plant-Microbe Interactions, Rhodes/ Greece, July 2014)

Campe, R., Leissing, F., Langenbach, C., Beckers, G., Popescu, S., Conrath, U., Göllner, K. (2014). Calmodulin interacts with the ABC transporter PEN3 and is involved in nonhost resistance of Arabidopsis (Conference “Current Findings in Plant Pathology, Aachen / Germany, June 2014)

Campe, R., Leissing, F., Langenbach, C., Beckers, G., Popescu, S., Conrath, U., Göllner, K. (2013). The ABC-transporter PEN3 interacts with calmodulin (32nd NPS Symposium, Buenos Aires/ Argentina, November 2013)

Campe, R., Löhrer, M., Langenbach, C., Beckers, G., Schaffrath, U., Conrath, U., Göllner, K. (2012). The biotroph *Phakopsora pachyrhizi* pretends a necrotrophic pest (XV International Congress of Molecular Plant-Microbe Interactions, Kyoto/ Japan, July 2012)

Campe, R., Langenbach, C., Baum, S., Klasen, C., Conrath, U., Göllner, K. (2011). Silencing of an Arabidopsis transcription factor leads to enhanced proliferation of *Phakopsora pachyrhizi* in the plant (Conference „Molecular Biology of Plants" of the German Botanical Society, Dabringhausen/ Germany, February 2011)

6.7.4 Patent

Conrath, U., Göllner, K., Campe, R., Schultheiss, H., Tresch, N.: Genes to enhance the defense against pathogens in plants. WO2013092275

6.8 Scholarships, grants and awards

2014	IS-MPMI travel award to the MPMI meeting in Rhodes, Greece
2013	Runners-Up Poster Prize at the 32nd New Phytologist Symposium "Plant interactions with other organisms: molecules, ecology and evolution" in Buenos Aires, Argentina
2010-2013	RWTH Aachen University PhD program, graduate student scholarship
2012	DAAD travel award to the MPMI meeting in Kyoto, Japan
2009	RWTH Aachen University undergraduate fund for attending the Tri National Arabidopsis Meeting in Cologne, Germany
2006/2007	Erasmus fellowship